BASIS FOR THE DISCRIMINATION OF SUPERCOIL HANDEDNESS DURING DNA CLEAVAGE BY HUMAN AND BACTERIAL TYPE II TOPOISOMERASES

By

Jeffrey Jian

Dissertation

Submitted to the Faculty of the

Graduate School of Vanderbilt University

in partial fulfillment of the requirements

for the degree of

DOCTOR OF PHILOSOPHY

in

Biochemistry

May 12, 2023

Nashville, Tennessee

Approved:

Neil Osheroff, Ph.D.

Charles R. Sanders, Ph.D.

James M. Dewar, Ph.D.

Katherine L. Friedman, Ph.D.

Martin Egli, Ph.D.

"You don't raise heroes, you raise sons. And if you treat them like sons, they'll turn out to be heroes, even if it's just in your own eyes."

– Walter Schirra

To Meredith, Salem, and Spooky

ACKNOWLEDGEMENTS

Well. Where to begin. First and foremost, my biggest thanks and gratitude go out to my Ph.D. advisor, Dr. Neil Osheroff, for giving me a chance in his research team. This doctoral experience was not easy by any means, not the least of which was a global pandemic that set everything back. Thank you, Neil, for being a fantastic mentor and guide as I navigated the ins and outs of my project. You've built your lab to be an outstandingly educational and motivating place for all of us, with the shoulders of topoisomerase giants to stand on. Your dedication and enthusiasm to your research has certainly not been unnoticed by me, with the consistent abstract/manuscript/poster/review/proposal draft edits at wee ungodly hours in the morning and Zooming in from who-knows-where-in-the-world-this-time to make sure I understand what I'm doing. I will attempt to draw inspiration from your unflagging work ethic, but you will have to forgive me if I can't fully keep up. And of course, thank you for demonstrating to me the qualities to look for in a mentor: wit, patience, confidence, sarcasm-with-an-unreadable-expression, and an endless stream of personal life lessons and anecdotes. I'll try to remember to bring/send you a bottle of Dr. Konstantin Frank white wine the next time I'm up at the Finger Lakes area.

Up next: my dissertation committee–Dr. Chuck Sanders, Dr. James Dewar, Dr. Kathy Friedman, and Dr. Martin Egli. Thank you all for your guidance, advice, and support throughout these years. While you have all held me to high standards that were tough to achieve, I am now a better scientist and researcher for it and I will always be grateful. James, thank you for the work that you do to assist the wellbeing of graduate students and postdocs; the increased awareness and activism of graduate students supporting each other is because of you. Chuck, thank you for

sticking it out with me through the toughest of times. You have seen it all, and I am relieved to have been able to show you a happy ending to my graduate school career.

My lab mates (including former ones)! To Jo Ann Byl: simply put, you are the backbone of our lab. You make sure that everything runs smoothly and you've been consistently reliable in pushing us to be the best scientists we can be. Thank you for your continued guidance and for your help as I navigated the toughest parts of my project. My levels of precision and detail towards experimental design and execution have substantially improved over the years because of you.

Esha Dalvie, Alexandria Oviatt, Jessica Collins, Jill Armenia, Samika Joshi, and Soziema Dauda: it has been a wild rollercoaster of surviving graduate school in the middle of a global pandemic. These were indeed interesting times that we've lived through. I will attempt to keep up the tradition of playing Christmas music early (starting in November). A special thanks to Esha and Alexandria for their training and guidance during my early transition months into the Osheroff Lab. I am grateful to have (had) you as (older) lab sisters, and you have created a welcoming environment that the rest of us will certainly pass down to newer grad students in the years to come. To Katie Rothamel, Sarah Arcos, and Byungil Kim: I am grateful to have had your support and training during the first few years of my graduate school career. Katie, I am certain that we will make time to get bubble tea, fried popcorn chicken, and long afternoon walks again.

To my research collaborators–Dr. Keir Neuman, Dr. Ian Morgan, Dr. Fred Guengerich, and Kevin McCarty: thank you all for your guidance, training, advice, and support during the final stretches of my Ph.D. I have learned a lot from each of you, and I am grateful to have had you as work companions as my project grew and evolved. To Dr. Beth Bowman: you have been a never-ending source of inspiration and motivation through your unbridled enthusiasm towards and energy for looking after all students. Your demonstratively incredible resilience will be something

that I aspire to emulate throughout the rest of my career. To Dr. Ashley Brady and Kate Stuart: thank you both (and the rest of the BRET ASPIRE team) for your encouragement and for making sure that I am on top of my career development. I promise that my LinkedIn profile will be complete at some point.

To my undergraduate research advisor, Dr. Kenneth Simpson, and my supervisors and colleagues: Dr. Belgin Dogan and Dr. Shiying Zhang. Thank you for granting me the training necessary to begin my graduate school journey. I look forward to returning to campus and catching up with you all.

And, of course, to my friends and support people in New York City area and Nashville. David, Payam, Dana, Hannah, Greg, Iris, Esco, Jaclyn, Dysart, Natalie, Gabriel, Manuel, Mollie, Callan, Peter, George, Sabrina, Balthazar, and far, far too many others to be listed here. None of this would have been possible without any of you, and thank you for putting up with my graduate school journey in Nashville during this last half-decade. I look forward to being able to visit you all again soon; easing my ramen and dim sum withdrawals depend on it. To my Vanderbilt Magic group, my fellow D&D Doorknockers, my fellow giraffe competitive PTCG testers, and my Climb Nashville friends: thank you all for enriching my time here in Nashville and in Tennessee. Dr. Janice Aber: it's been a long journey and you've seen it all at this point. I'm grateful to have badgered you over the last decade and then some. Two out of three and I'll probably hold at this point.

Phew, final stretch! To my current family: 谢谢妈妈, 老爸, 和弟弟的帮助这几年. 我希望我可以尽快帮助我们的家. 终于完成了我的博士研究. 更上一层楼.

To my family-to-be: Renee, Stephen, Sam(wise), Charles, and Jennifer. I am immensely grateful to have been welcomed so readily into your family, and I thank all of you for your warmth and support these last few years. I look forward to having all of our family together soon, and for many more years to come. A special thanks to Renee for physically bringing a specific person into my life, and speaking of which…

…to my fiancée Meredith: you cannot imagine how much love and kindness you have brought into my life. You have constantly demonstrated unparalleled and unwavering confidence and support in me and my work, and I would not be here today without you. Suffice to say that I have an inkling of suspicious that my lab prefers you over me, but I'll take whatever brownie points I can get. Beyond my research, you have made me a better person and a better (assuming heteronormativity) man, and I am extremely fortunate that you took a chance on me to see what we could become together. I am incredibly proud of how much you have grown as a researcher and person, and I look forward to spending the rest of my life with you. And last but certainly not least, our kitties with arguably the biggest personalities of this whole Acknowledgements section: Salem the evil genius, and Spooky the adorable dumdum. The two of you are the sources of unaware curiosity, unbridled joy, insatiable appetites, and meowing chaos, but I wouldn't have it any other way. We'll work on building a social media presence for the two of you yet.

TABLE OF CONTENTS

Page

LIST OF FIGURES

Figure Page

Chapter 1:

Chapter 2:

LIST OF TABLES

Table Page

Chapter 2:

LIST OF ABBREVIATIONS

(-)SC	negatively supercoiled
(+)SC	positively supercoiled
ATP	adenosine triphosphate
bp	base pair
DTT	dithiothreitol
EDTA	ethylenediaminetetraacetic acid
kb	kilobase
L	linear
Lk	linking number
N	nicked
R	relaxed
SC	supercoiled
SDS	sodium dodecyl sulfate
Tw	twist
Wr	writhe
ΔLk	change in linking number

CHAPTER ONE

INTRODUCTION

DNA

All living organisms, ranging from bacteria to plants to humans, have their genetic information encoded in the form of deoxyribonucleic acids (DNA) (Watson and Crick 1953, Watson and Crick 1953A, Voet and Voet 2004). As the hereditary material, DNA is composed of monomeric units known as nucleotides. Each nucleotide consists of one nitrogenous base (adenine [A], cytosine [C], thymine [T], and guanine [G]), a deoxyribose moiety, and a phosphate group (Watson and Crick 1953, Watson and Crick 1953A). The nucleotide bases on one strand of the DNA double helix are connected to each other by phosphodiester linkages and form hydrogen bonds with their complementary bases of the second strand, thus forming the rungs of a ladder with a sugar-phosphate backbone (A with T; C with G). This complementary duplex stores the biological information encoded by the sequences of nucleotide base pairs and can take the shape of two braided linear (free ends, like a ladder) or circular (like a circle) chains. The sequence of nucleotide base pairs that form the DNA polynucleotide duplex contains the biological information necessary for the development, reproduction, growth, and function of all known bacteria, animals, and plants. The determination of the DNA double helix by Watson and Crick laid the groundwork for decades of additional research into the genetic material.

In their seminal publication in 1953, Watson and Crick put forth the structure of the DNA double helix, later known as B-form DNA (Watson and Crick 1953). Watson and Crick later followed up in their second paper by recognizing the importance of accessing the genetic material

for nucleic acid processes that required access and manipulation of DNA itself, such as replication, transcription, and chromosomal segregation (Watson and Crick 1953A). Subsequent studies demonstrated that the structural nature of the double helix itself, coupled with the necessary separation of the two strands of DNA, could led to foreseeable problems with the spatial relationships of the DNA duplex that needed to be resolved for proper biological function of occur. Although DNA can be visualized as a ladder, the way that the nucleotide base pairs stack upon each other introduces a slight twist in the structure, such that the ladder is converted into a double-stranded helix. This plectonemic coiling leads to a number of topological problems with DNA (Bates and Maxwell 2005, Deweese, Osheroff et al. 2008, Pommier, Sun et al. 2016, Ashley and Osheroff 2019). Consequently, questions about the topological, or three-dimensional, properties of the genetic material began to gain scientific attention in the 1970s.

DNA Topology

Topological properties of DNA are defined as those that cannot be changed without breaking one or both strands of the DNA double helix (Bates and Maxwell 2005, Deweese, Osheroff et al. 2008, Deweese and Osheroff 2009, Pommier, Sun et al. 2016, Ashley and Osheroff 2019). These properties become extremely important upon consideration of the sheer amount of DNA that exists in eukaryotic species, such as humans, and bacteria, such as *Escherichia coli*. In humans, the diploid genome is encoded in ~6 billion base pairs across 46 chromosomes. When the DNA from a single human cell is laid out end-to-end, there is ~2 m in length of genetic material that needs to be compressed and properly stored in a nucleus of ~10 μm in diameter (Kornberg and Baker 1992, Voet, Voet et al. 2002). Given that the human body is comprised of ~30 trillion cells, there are ~180 sextillion base pairs of DNA that would stretch ~60 billion km in length if

laid end-to-end. Putting this into geographical context, it would be the equivalent of traveling from the Earth to the Sun and back more than 200 times! In addition, each molecule of DNA in human cells experiences extreme compaction and high friction associated with a two-braid of such length, as well as anchorage to scaffolding proteins that "fix" or prevent free rotation of the ends of DNA (Deweese, Osheroff et al. 2008, Deweese and Osheroff 2009). In most bacterial cells, DNA exists as a circular molecule (and therefore has no ends) and is tethered to membrane structures. These properties, together with the interwound nature and restricted rotational movement of the double helix, create a number of topological issues that profoundly affect all functions of DNA (Deweese, Osheroff et al. 2008, Deweese and Osheroff 2009). As such, although the genetic information is organized in a linear sequence of nucleotide bases, it is the topological state of DNA that facilitates or restricts access to this information (Bates and Maxwell 2005, Deweese, Osheroff et al. 2008, Deweese and Osheroff 2009, Liu, Deibler et al. 2009, Finzi and Olson 2016).

DNA topology can be defined mathematically by three concepts: twist (Tw), writhe (Wr), and linking number (Lk; Figure 1.1) (Bauer, Crick et al. 1980, White and Cozzarelli 1984, Bates and Maxwell 2005, Deweese, Osheroff et al. 2008, Pommier, Sun et al. 2016, Ashley and Osheroff 2019). Twist is the total number of double helical turns in a defined DNA segment and represents the torsional or rotational stress that the double helix undergoes at any given point in time. By convention, positive twist (right-handed twist) is observed in the normal Watson-Crick DNA structure (Figure 1.1). Writhe is defined as the number of times the double helix crosses itself if the DNA segment is projected in two dimensions and represents axial stress in the molecule. Writhe is a spatial property of the DNA molecule and is defined as the number of times the double helix crosses itself. Writhe is assigned a value of -1 (negative) or +1 (positive), depending on the handedness or directionality of the crossover to "reset" the DNA molecule. If

the resetting directionality must be rotated clockwise, then the writhe is negative (i.e., right-handed). If the directionality must be rotated counterclockwise, then the writhe is positive (i.e., left-handed). Linking number represents the sum of twist and writhe, and is expressed as the sum thereof:

$$Lk = Tw + Wr$$

Assuming the ends of DNA strands are "fixed" in cellular environments and the double helix is not broken, the linking number is invariant. In biological systems, each of these properties of DNA is extremely relevant. In an environment absent of external stress, DNA duplexes that are not undergoing torsional strain, as observed in the canonical Watson-Crick structure, are known as "relaxed" molecules, with the two strands twisting around the helical axis once every ~10.5 base pairs (Bauer, Crick et al. 1980, Deweese, Osheroff et al. 2008). One important consideration is that the Lk for a right-handed plectonemically coiled structure is always positive; the Lk for a left-handed structure is negative. Having a Lk = 0 would mean that the DNA double helix is melted (i.e., paranemic) with no crossings between the two strands. Thus, DNA topology is expressed as the change in linking number, ΔLk, which is defined as the difference between the actual Lk of the molecule and the Lk if the molecule was fully relaxed. It is the addition or removal of twist strain that imposes torsional stress upon the molecule.

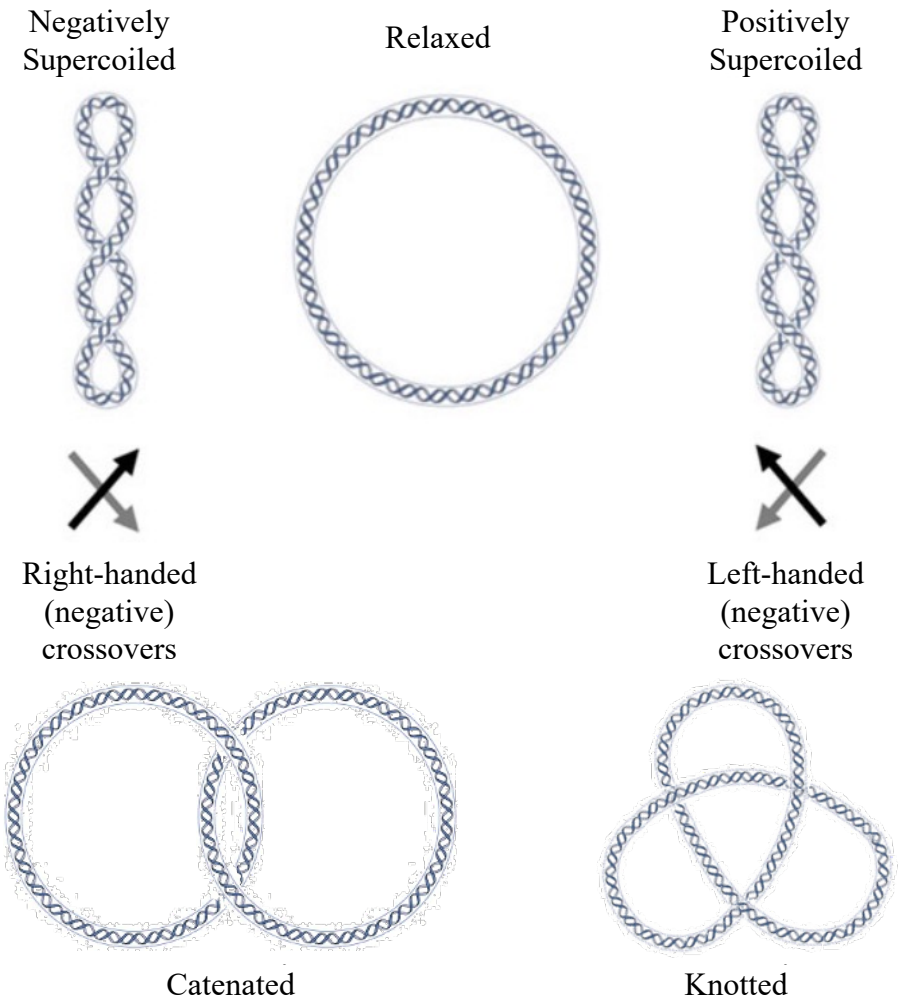

Figure 1.1: Topological states of DNA. Top: DNA that contains no torsional stress is considered "relaxed" (top middle). Underwinding or overwinding the DNA results in negatively supercoiled [(-)SC, top left] or positively supercoiled [(+)SC, top right] DNA. Here, DNA supercoiling is depicted as writhe (Wr) for visual clarity but twist (Tw) and Wr are interconvertible within these molecules. Bottom: Intermolecular catenanes (bottom left) and intramolecular knots (bottom right) can also form in DNA. In these cases, Tw and Wr are not interconvertible. Artwork from Ashley *et al.*, 2019.

As a mathematical example, the *Escherichia coli* pBR322 circular plasmid, which is a plasmid commonly used in DNA topology assays, has a linking number of ~ +415. This value is determined based on the number of base pairs in a single pBR322 plasmid (4361) and the average number base pairs it takes to form one helical turn along the DNA backbone (10.5). If the pBR322 plasmid molecule is linearized and the ends are constrained, the linking number will not change (White and Bauer 1986, Deweese, Osheroff et al. 2008, Dorman and Dorman 2016, Ashley and Osheroff 2019). However, when one end of the linear molecule is rotated 360° in a right-handed direction (overwinding), the linking number will increase by +1, generating a positive twist or supercoil [(+)SC] in the segment ($\Delta Lk = +1$). Conversely, a rotation by 360° in a left-handed direction (underwinding) will decrease the linking number by -1, generating a negative twist or supercoil [(-)SC, $\Delta Lk = -1$]. If the linear plasmid were to be continuously rotated in a given direction and the ends were allowed to move closer to each other, eventually the twist (positive or negative) would be converted to writhe and the double helix would begin to wrap around itself, forming supercoils.

Nucleic acid processes such as recombination and replication also generate knots and tangles (i.e., catenanes; Figure 1.1) in the cell (Liu, Deibler et al. 2009). Knots are formed within a DNA molecule during processes such as DNA recombination (Bates and Maxwell 2005, Falaschi, Abdurashidova et al. 2007, McClendon and Osheroff 2007, Deweese, Osheroff et al. 2008, Ashley and Osheroff 2019). In contrast, catenanes form between multiple DNA molecules as a result of genome replication (Fortune and Osheroff 2000, Bates and Maxwell 2005, McClendon and Osheroff 2007, Deweese, Osheroff et al. 2008, Ashley and Osheroff 2019). Catenanes must be removed to enable separation of sister chromatids during mitosis. If knots accumulate in the genome, DNA tracking systems will be unable to properly separate the two

strands of the double helix. If tangles are left unresolved prior to cell division, cells will die of mitotic failure (Holm, Goto et al. 1985, Uemura, Ohkura et al. 1987, Baxter and Diffley 2008, Baxter, Sen et al. 2011, Bauer, Marie et al. 2012, Sen, Leonard et al. 2016).

Taken together, there are biological implications of DNA supercoiling, as well as the formation of structures such as knots and tangles. DNA supercoiling is extremely relevant during essential nucleic acid processes that require DNA strand separation, such as DNA replication, and transcription (Espeli and Marians 2004, Bates and Maxwell 2005, Falaschi, Abdurashidova et al. 2007, Travers and Muskhelishvili 2007, Deweese, Osheroff et al. 2008, Ashley and Osheroff 2019). Globally, the DNA double helix exists in a slightly (~6%) underwound [i.e., (-)SC] state (Bates and Maxwell 2005, Deweese, Osheroff et al. 2008, Ashley and Osheroff 2019). This has important ramifications because the two strands of the DNA duplex must be separated to access the genetic information. The globally underwound nature of the genome imparts increased single-stranded character to the double helix and reduces the energy needed to melt (i.e., break) the hydrogen bonds between complementary bases, facilitating ease of strand separation (Liu and Wang 1987, Wang 1996, Wang 2002, Schvartzman and Stasiak 2004). However, once movement of DNA tracking machinery begins, the deleterious effects of DNA topology manifest (Figure 1.2). Since helicases and polymerases separate, but do not unwind, the two strands of DNA, they do not remove any of the turns of the double helix. Consequently, there is an imparted increase of torsional stress that needs to be resolved. An acute overwinding [i.e., (+)SC] subsequently begins ahead of DNA tracking machinery (Postow, Crisona et al. 2001). If not resolved, the accumulation of (+)SCs will present a block to replication and transcription, and these processes will stall rapidly (Brill, DiNardo et al. 1987, Kim and Wang 1989, Wang 1996, Peter, Ullsperger et al. 1998, Wang 2002).

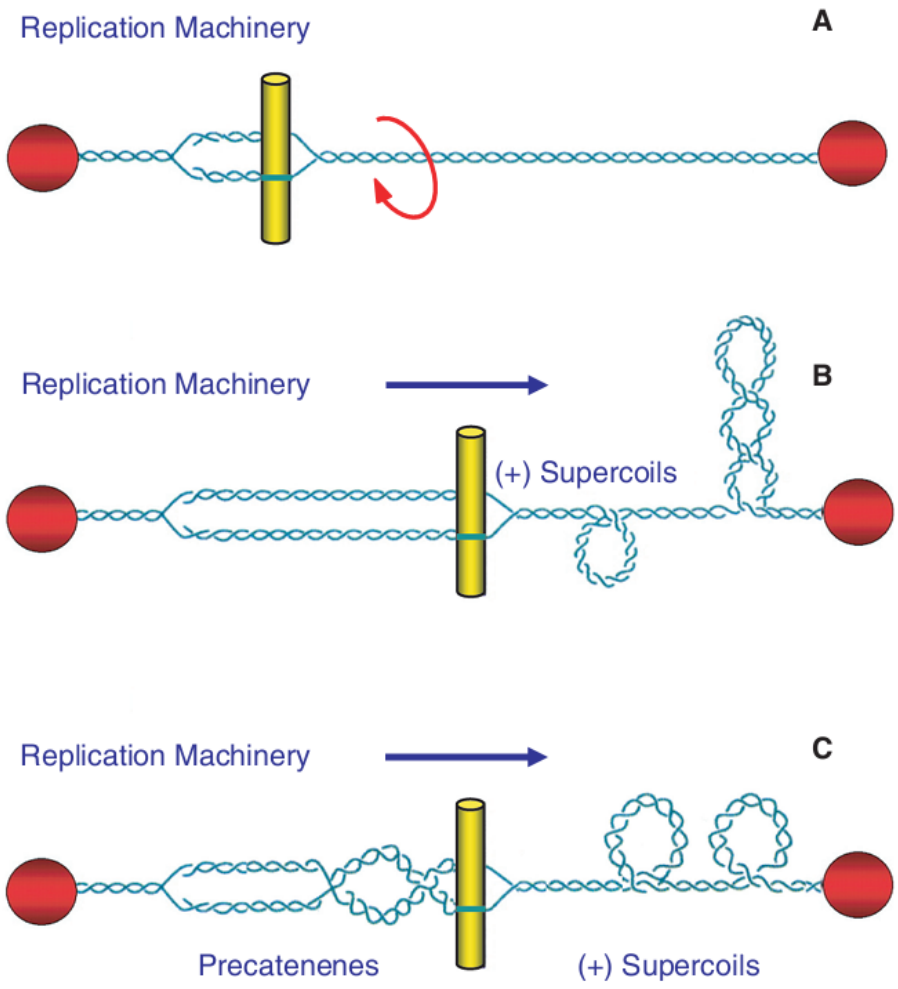

Figure 1.2: Movement of DNA tracking machinery causes topological problems. As DNA tracking systems move through the DNA, twists are pushed ahead of replication forks and transcription complexes, resulting in DNA overwinding that is converted into (+)SCs (A). In the case of replication, precatenanes form behind the fork (B); during transcription, (-)SCs form behind the moving DNA tracking machinery (C).

Topoisomerases

To maintain the appropriate levels of DNA supercoiling and remove knots and tangles in the genome, cells encode enzymes known as topoisomerases (Deweese, Osheroff et al. 2008, Deweese and Osheroff 2009, Vos, Tretter et al. 2011, Chen, Chan et al. 2013, Pommier, Sun et al. 2016, Austin, Lee et al. 2018, Ashley and Osheroff 2019). These enzymes are ubiquitous to all domains of life and are necessary for cellular survival. All topoisomerases modulate the levels of supercoiling in the genome through the creation of a transient break in the DNA helical backbone. Broadly, there are two types of topoisomerases, classified by the number of DNA strands cleaved per enzyme reaction cycle (Bates and Maxwell 2005, Deweese, Osheroff et al. 2008, Deweese and Osheroff 2009, Chen, Chan et al. 2013, Ashley and Osheroff 2019). Type I topoisomerases generate a single-stranded break, or "nick," in the genetic material (Deweese, Osheroff et al. 2008, Chen, Chan et al. 2013, Ashley and Osheroff 2019, McKie, Neuman et al. 2021). In contrast, type II topoisomerases create a double-stranded break in the DNA double helix (Deweese, Osheroff et al. 2008, Deweese and Osheroff 2009, Vos, Tretter et al. 2011, Chen, Chan et al. 2013, Ashley and Osheroff 2019, McKie, Neuman et al. 2021). All topoisomerases require the use of active site tyrosine residues for catalysis and the process of cutting their DNA substrate results in the formation of covalent bonds between the tyrosine residues and the phosphate backbone of the cleaved DNA substrate. The transiently-cleaved, covalently-linked enzyme-DNA structure that is formed is known as the "cleavage complex" (Deweese, Osheroff et al. 2008, Deweese and Osheroff 2009, Liu, Deibler et al. 2009, Vos, Tretter et al. 2011, Chen, Chan et al. 2013, Ashley and Osheroff 2019, McKie, Neuman et al. 2021, Vann, Oviatt et al. 2021). Formation of the cleavage complex during enzyme catalysis is thus tightly coordinated to prevent formation of permanent DNA breaks or disruption to genomic integrity (Deweese, Osheroff et al. 2008,

Deweese and Osheroff 2009, Forterre and Gadelle 2009, Vos, Tretter et al. 2011, Chen, Chan et al. 2013, Pommier, Sun et al. 2016, Austin, Lee et al. 2018, Ashley and Osheroff 2019).

Type I Topoisomerases

Type I topoisomerases are primarily monomeric enzymes (with the exception of reverse gyrase, which is tetrameric), most of which do not require a high-energy cofactor, such as ATP, to function (McClendon and Osheroff 2007, Chen, Chan et al. 2013, Seol and Neuman 2016, Ashley and Osheroff 2019). There are three subclasses of type I enzymes: IA, IB, and IC (Wang 1971, Champoux and Dulbecco 1972, Slesarev, Stetter et al. 1993, Deweese, Osheroff et al. 2008, Vos, Tretter et al. 2011).

Type IA topoisomerase was the first topoisomerase discovered and biochemically characterized (i.e., bacterial ω protein) (Wang 1971). Type IA topoisomerases function by creating a transient cut in one strand of the DNA double helix and then passing the opposite intact strand through the break, otherwise known as a "single-strand passage" event (Schvartzman and Stasiak 2004, Deweese, Osheroff et al. 2008, Vos, Tretter et al. 2011, Ashley and Osheroff 2019). All type IA topoisomerases require the coordination of divalent cations, such as Mg^{2+}, for DNA scission. Upon catalytic cleavage of the sugar-phosphate DNA backbone, the bond energy is conserved via formation of a new covalent bond between a tyrosine residue of the enzyme active site and the newly generated 5'-terminal phosphate of the cleaved DNA. This single-stranded DNA passage mechanism changes value of the linking number by 1. As such, type IA enzymes are able to relax the supercoiled molecule but cannot remove knots and tangles. Type IA topoisomerases mainly function on (-)SCs, preventing the accumulation of hypernegatively supercoiled DNA and formation of R-loops (a DNA:RNA hybrid) during transcription (Drolet, Broccoli et al. 2003, Tan,

Zhou et al. 2015). However, a few type IA enzymes, such as the reverse gyrase enzyme that is only found in thermophilic bacterial species and archaea, are able to introduce (+)SCs into DNA substrates, but only in the presence of ATP (Kikuchi and Asai 1984, Confalonieri, Elie et al. 1993).

Type IB topoisomerases, in contrast to type IA enzymes, do not utilize a strand passage mechanism to regulate DNA supercoiling. Instead, type IB enzymes cut one strand of the DNA substrate and then perform a controlled rotation of the cleaved end around the opposite intact strand (Champoux and Dulbecco 1972, Stivers, Harris et al. 1997, Deweese, Osheroff et al. 2008, Ashley and Osheroff 2019). This "swivel" mechanism occurs when the enzyme is covalently attached to the 3'-terminal phosphate of the cleaved end, allowing the 5'-DNA terminus to freely rotate. This rotation is controlled by the level of torque contained in the DNA molecule (Koster, Croquette et al. 2005). As such, the greater the level of supercoiling in the DNA substrate, the more supercoils are relaxed by the enzyme in one rotation cycle. Similar to the type IA enzymes, the linking number is changed by 1 for every 360º rotation. Type IB enzymes can function on both underwound and overwound DNA substrates but cannot function to decatenate substrates (Vos, Tretter et al. 2011).

Lastly, type IC topoisomerases have been identified only in a single hyperthermophilic methanogenic bacterial species. The only known member of this class is topoisomerase V (Slesarev, Stetter et al. 1993, Ashley and Osheroff 2019). Topoisomerase V activity is independent of ATP and divalent cations, and also behaves similarly to type IB enzymes in its controlled rotation mechanism (Taneja, Patel et al. 2006). The linking number is also changed by 1 for every rotation of the DNA double helix. There is little structural similarity between the type IB and type IC enzymes.

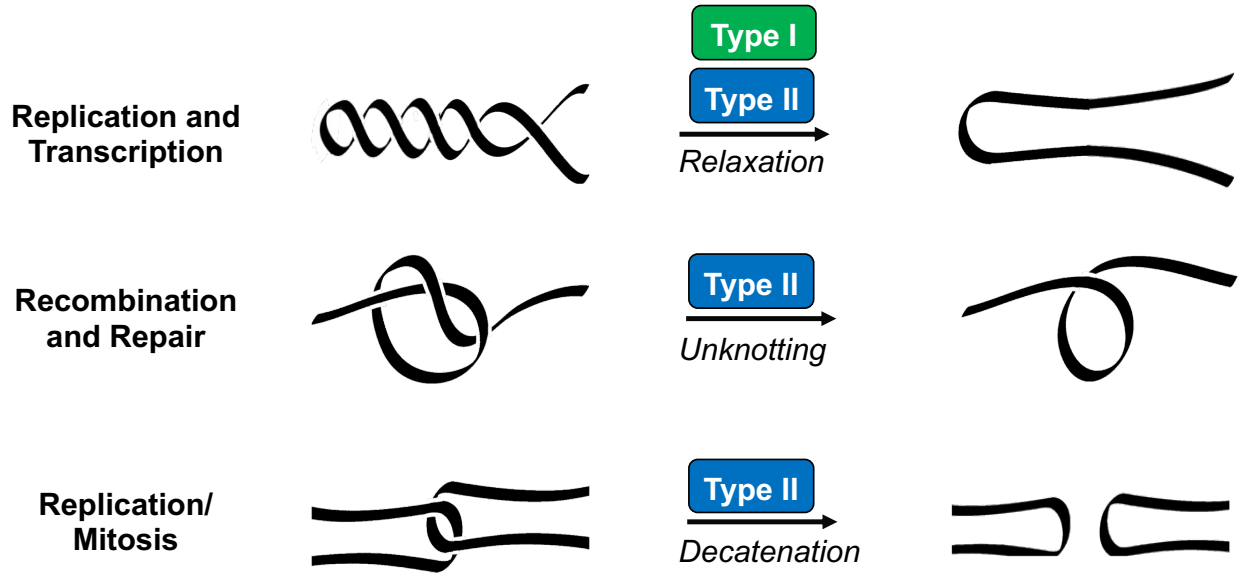

Figure 1.3: Functions of type I and type II topoisomerases. The different functions of type I and type II topoisomerases from human and bacterial species allow them to work on DNA substrates of different topological states. Because type I enzymes only cut one strand of DNA, they are only able to work on Tw. Because type II enzymes cut both strands of the DNA double helix, they are able to work on Wr.

Bacteria encode primarily type IA topoisomerases, topoisomerase I and topoisomerase III. Historically, bacterial topoisomerase I has been referred to as the ω protein (Wang 1971, Ashley and Osheroff 2019). Despite the similar numerical designation, bacterial topoisomerase I is unrelated to human topoisomerase I (i.e., bacterial topoisomerase I is a type IA enzyme, whereas human topoisomerase I is a type IB enzyme). ω protein functions in tandem with bacterial gyrase (a type II topoisomerase that will be discussed later) to regulate the overall level of DNA supercoiling in the bacterial genome (Nöllmann, Crisona et al. 2007). Bacterial topoisomerase III is related to human topoisomerase IIIα and IIIβ and is involved in maintaining genomic stability. Although the specific cellular activities of bacterial topoisomerase III are less clear, it has been shown to be more efficient at resolving knots and tangles over relaxing supercoils (Terekhova, Gunn et al. 2012). Bacterial species from genera such as *Mycobacterium* also encode type IB topoisomerases (Tse-Dinh 1998, Krogh and Shuman 2002, Forterre, Gribaldo et al. 2007, Forterre and Gadelle 2009, Sandhaus, Chapagain et al. 2018). These bacterial type IB enzymes do not structurally resemble those of archaeal or eukaryotic species, but instead are similar to those of poxviruses (Krogh and Shuman 2002, Forterre and Gadelle 2009).

Humans encode both type IA (topoisomerase IIIα and IIIβ) and IB (topoisomerase I) enzymes (Deweese, Osheroff et al. 2008, Vos, Tretter et al. 2011, Ashley and Osheroff 2019). Human topoisomerase III is believed to function to relax hypernegatively supercoiled DNA and prevent inappropriate recombination, as well as resolve recombination intermediates and stalled replication forks (Vos, Tretter et al. 2011). The IIIα isoform can resolve single-stranded DNA tangles (i.e., hemicatenanes) that can arise during replication, repair, and recombination processes; deletion of the IIIα isoform is lethal in mice (Hiasa, DiGate et al. 1994, Harmon, DiGate et al. 1999). The human IIIβ isoform can act as a dual DNA and ribonucleic acid (RNA) topoisomerase,

performing both cleavage and strand passage on RNA (Ahmad, Shen et al. 2017, Goto-Ito, Yamagata et al. 2017). In humans, deletion or mutation of topoisomerase IIIβ has been linked to schizophrenia and neurodevelopmental disorders (Stoll, Pietilainen et al. 2013, Ahmad, Shen et al. 2017). In mice, deletion of the IIIβ isoform is known to shorten life span and can negatively affect neurodevelopment (Stoll, Pietilainen et al. 2013, Xu, Shen et al. 2013). Human topoisomerase I mainly functions to relax (+)SCs and remove torsional stress ahead of replication and transcription machinery. Topoisomerase I has been implicated in maintaining genomic stability and gene-specific transcription. Topoisomerase I is dispensable at the cellular level but appears to be necessary for proper development in multicellular organisms (Lee, Brown et al. 1993, Morham, Kluckman et al. 1996, Nitiss 1998, Miao, Player et al. 2007).

Given the focus of my dissertation, the remainder of the Introduction will focus solely on type II topoisomerases and type I enzymes will not be further discussed.

Type II Topoisomerases

Type II topoisomerases can be classified into two subgroups, IIA and IIB, based on sequence and structural homology (Bates and Maxwell 2005, Deweese, Osheroff et al. 2009, Ashley and Osheroff 2019). The first type IIA topoisomerase (bacterial DNA gyrase) was discovered in 1972 (Gellert, Mizuuchi et al. 1976), and the first type IIB enzyme (topoisomerase VI) was identified in 1997 (Levine, Hiasa et al. 1998, Corbett and Berger 2004, Sissi and Palumbo 2010). All of these type II enzymes can relax DNA supercoils and resolve knots and tangles, and undergo similar catalytic cycles, but can differ in their sequences and structural domains. In contrast to the type I enzymes, type II topoisomerases function via a double-stranded passage reaction, whereby the DNA double helix is cut on both strands (Deweese, Osheroff et al. 2008,

Deweese, Osheroff et al. 2009, Ashley and Osheroff 2019). As such, during reactions, the linking number of their DNA substrates is changed in steps of 2. Lower eukaryotes, such as yeast, and invertebrates encode only one type IIA enzyme, topoisomerase II. Vertebrates such as humans express two closely related forms of the IIA enzyme, topoisomerase IIα and topoisomerase IIβ (Deweese, Osheroff et al. 2008, Deweese and Osheroff 2009, Liu, Deibler et al. 2009, Nitiss 2009, Chen, Chan et al. 2013, Pommier, Sun et al. 2016, Austin, Lee et al. 2018, Ashley and Osheroff 2019, McKie, Neuman et al. 2021, Vann, Oviatt et al. 2021). Most bacterial species, such as the Gram-negative *E. coli* and the Gram-positive *Bacillus anthracis,* encode two type IIA enzymes, gyrase and topoisomerase IV. A few bacterial species, such as *Mycobacterium tuberculosis,* which is classified as neither Gram-positive nor Gram-negative, encode only a single type IIA topoisomerase, gyrase (Austin and Marsh 1998, Deweese, Osheroff et al. 2008, Deweese and Osheroff 2009, Forterre and Gadelle 2009, Vos, Tretter et al. 2011, Chen, Chan et al. 2013, Pommier, Sun et al. 2016, Austin, Lee et al. 2018, Ashley and Osheroff 2019). The only known type IIB topoisomerase, topoisomerase VI, exists only in plants and archaeal species (Bergerat, Gadelle et al. 1994, Sugimoto-Shirasu, Stacey et al. 2002). Type IIB enzymes are heterotetramers (similar to bacterial type IIA enzymes) but differ from type IIA enzymes in that the TOPRIM domain (to be discussed later) exists in the A subunit of gyrase (instead of in the B subunit, as with bacterial species) (Bergerat, de Massy et al. 1997, Gadelle, Krupovic et al. 2014). The A subunits of type IIA and type IIB topoisomerases do not share sequence or structural identity (Gadelle, Krupovic et al. 2014).

Given the focus of my dissertation, type IIA topoisomerases will often be collectively referred to as type II topoisomerases and type IIB enzymes will not be further discussed.

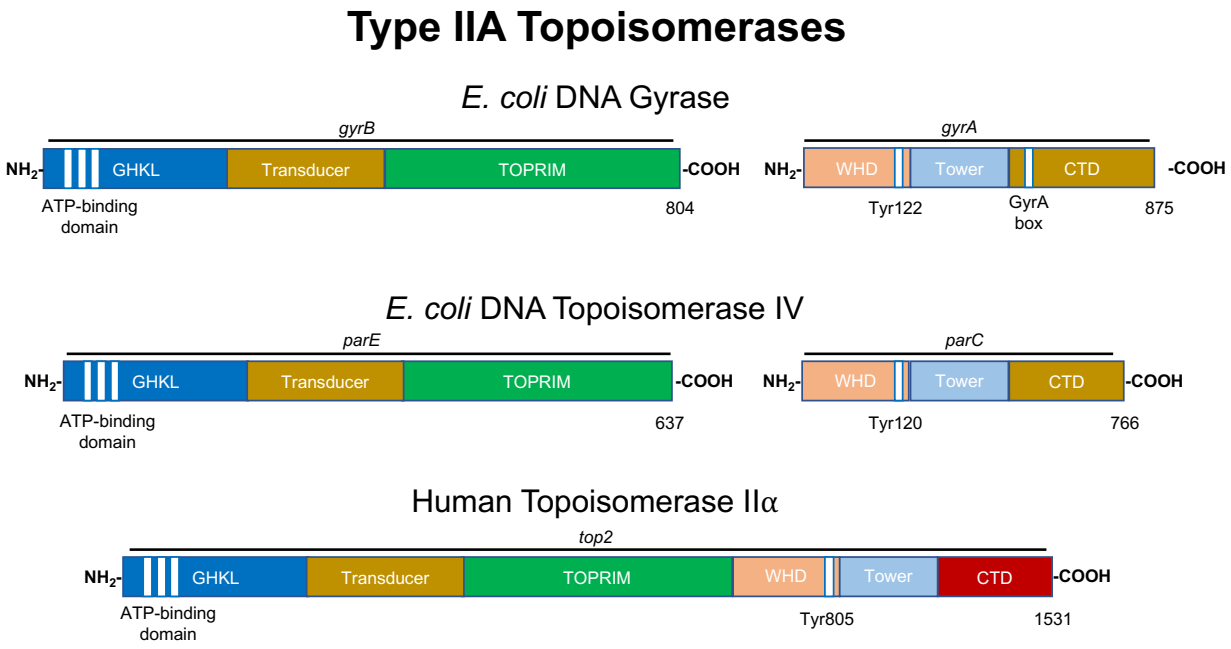

Figure 1.4: Structures of type IIA topoisomerases. The domain structures of three type IIA topoisomerases, bacterial (*Escherichia coli*) DNA gyrase and topoisomerase IV, and human topoisomerase IIα are shown. Regions of homology among the enzymes are indicated by colors. The N-terminal (*i.e.*, GyrB) homology domains contain the regions responsible for ATP binding and hydrolysis (GHKL). The vertical white stripes represent the three conserved motifs that define the ATP-binding domain. The N-terminal domain also contains the binding site for divalent metal ions (TOPRIM). The central (*i.e.*, GyrA) region (WHD) contains the active site tyrosyl residue that forms the covalent bond with DNA during scission. For bacterial gyrase, the variable C-terminal domain contains the "GyrA box" that is necessary for the wrapping mechanism. For human topoisomerase IIα, the CTD contains nuclear localization sequences (NLS) and phosphorylation sites (PO_4). The active site tyrosine residue is indicated for each enzyme.

Type II Topoisomerase Structure Overview

Whereas most bacterial type II topoisomerases are comprised of two heterotetramer units (A_2B_2), the human type II topoisomerases are formed by two fused heterotetramer units, forming homodimers (A_2). All known type IIA topoisomerases in humans and bacteria share a number of common structural features across three regions: the N-terminus, the catalytic core, and the C-terminus (Figure 1.4) (Deweese, Osheroff et al. 2008, Deweese and Osheroff 2009, Vos, Tretter et al. 2011, Chen, Chan et al. 2013, Ashley and Osheroff 2019, Dalvie and Osheroff 2021, McKie, Neuman et al. 2021). The N-terminal region, where the DNA double helical segment enters the enzyme (i.e., the DNA-gate), includes the ATPase, also known as the GHKL (DNA gyrase, Hsp90, bacterial CheA-family histidine kinases, and MutL), domain, and the transducer domain that relays hydrolysis information to the catalytic core (Nitiss 2009, Wendorff, Schmidt et al. 2012). The catalytic core contains the topoisomerase/primase (TOPRIM) domain that coordinates the active site divalent cations, the winged-helix domain (WHD) that contains the active site tyrosine residue, and the tower domain that maintains polar and electrostatic interactions with the DNA substrate (Wendorff, Schmidt et al. 2012, Chang, Wang et al. 2013). The two domains fundamental to the Mg^{2+}-dependent double-stranded DNA cleavage reaction are the WHD domain and the TOPRIM domain. The C-terminal domain is an intrinsically disordered region (IDR) that contains nuclear localization signals, sites for posttranscriptional modification, and is critical to the recognition of DNA topology (McClendon and Osheroff 2007, Deweese and Osheroff 2009, Nitiss 2009, Lindsey, Pendleton et al. 2014).

First, the WHD contains a helix-turn-helix fold, which a characteristic of all WHD proteins but is commonly found in proteins with DNA-binding function (Harrison and Aggarwal 1990, McKie, Neuman et al. 2021). In addition to its ability to bind DNA, the WHD also contains the

active site tyrosine residue, which is necessary for the nucleophilic attack on the scissile phosphate of the DNA double helical backbone and the formation of the transient reversible topoisomerase-DNA covalent bind (Nitiss 2009, Wendorff, Schmidt et al. 2012, Lindsey, Pendleton et al. 2014).

Second, the TOPRIM domain is formed from an α/β/α Rossman-like fold (an extended beta sheet that is sandwiched by alpha helices) (Chang, Wang et al. 2013, McKie, Neuman et al. 2021). The TOPRIM domain is necessary for the transesterification reaction between the scissile phosphate of the DNA backbone and active site tyrosine residue. The active site divalent cation is held by an aspartate-any residue-aspartate (DxD) motif and a glutamate residue that can act as a general acid-base moiety (Aravind, Leipe et al. 1998, Sissi and Palumbo 2009). Collectively, the DxD motif and its coordinate divalent cation in the TOPRIM domain, with the active site tyrosine of the WHD, enable the formation of the two transient cuts of the DNA backbone.

Third, the tower domain functions in DNA bending. The tower domain contains a beta sheet that can interact with one of the captured DNA double helices (the gate or G-segment, to be discussed later), bending the DNA segment to promote cleavage (Dong and Berger 2007, Lee, Jung et al. 2012, Jang, Son et al. 2019, McKie, Neuman et al. 2021). The presence of a conserved, invariant isoleucine residue (across eukaryotic and bacterial species) has been found to intercalate between two base pairs of the G-segment, inducing a ~150º bend. Deletion or mutation of this isoleucine has been found to interfere with proper DNA bending and subsequent relaxation of (+)SC or (-)SC substrates (Dong and Berger 2007, Lee, Dong et al. 2013).

Fourth, the GHKL domain contains an ATP-binding region that is formed from an 8-stranded antiparallel beta sheet surrounded by alpha helices (Corbett and Berger 2004, McKie, Neuman et al. 2021). Binding of ATP induces dimerization and shifting the N-gate into a closed conformation. The bound ATP interacts with a lysine residue in the transducer domain, and

subsequently facilitates rotation (11–18º) between the GHKL and transducer domains (Corbett and Berger 2003, Corbett and Berger 2005, McKie, Neuman et al. 2021). Despite these similarities in enzyme structure among human and bacterial type II topoisomerases, there are substantial differences, which will be discussed below.

Human Type II Topoisomerase Structure

Overall, eukaryotic type II topoisomerases are homologous to bacterial enzymes (described above) (Deweese, Osheroff et al. 2008, Deweese and Osheroff 2009, Vos, Tretter et al. 2011, Chen, Chan et al. 2013, Ashley and Osheroff 2019, Dalvie and Osheroff 2021, McKie, Neuman et al. 2021). There is an N-terminus, followed by a catalytic core region, and then a C-terminus. However, in contrast to the bacterial enzymes, eukaryotic type II topoisomerases consist of a fusion of the two subunits into a single polypeptide sequence with protomer masses ~160-180 kDa (Deweese, Osheroff et al. 2008, Deweese and Osheroff 2009, Chen, Chan et al. 2013, Ashley and Osheroff 2019). In humans, there are two isoforms of type II topoisomerases: topoisomerase IIα and topoisomerase IIβ (Austin and Marsh 1998, Deweese, Osheroff et al. 2008, Deweese and Osheroff 2009, Forterre and Gadelle 2009, Vos, Tretter et al. 2011, Chen, Chan et al. 2013, Gentry and Osheroff 2013, Ashley and Osheroff 2019). These isoforms are related in amino acid sequence (~70%) and enzyme structure, but they are encoded by different genes (TOP2A and TOP2B, located at chromosomal bands 17q21–22 and 3p24, respectively) and differ in molecular mass. Whereas human topoisomerase IIα is 170 kDa in protomer mass, topoisomerase IIβ is 180 kDa (Deweese, Osheroff et al. 2008, Deweese and Osheroff 2009, Chen, Chan et al. 2013, Ashley and Osheroff 2019). On the basis of amino acid sequence comparisons with *E. coli* gyrase, the N-terminus of eukaryotic type II enzymes is homologous to GyrB and the central domain is

homologous to GyrA (McClendon and Osheroff 2007, Vos, Tretter et al. 2011, Ashley and Osheroff 2019, McKie, Neuman et al. 2021). Crystal structures of the N-terminus and catalytic core in humans have been solved (Schmidt, Osheroff et al. 2012, Wendorff, Schmidt et al. 2012). The C-termini of eukaryotic topoisomerase IIα and IIβ do not share homology with the corresponding C-terminal domain of gyrase or topoisomerase IV. Eukaryotic C-terminus contains nuclear localization sequences and sites for posttranslational modifications such as phosphorylation and SUMOylation (McClendon and Osheroff 2007, Ashley and Osheroff 2019, McKie, Neuman et al. 2021). For the IIα isoform, these modifications can allow the enzyme to be concentrated at centromeres during mitosis (Linka, Porter et al. 2007, Antoniou-Kourounioti, Mimmack et al. 2019). Like *E. coli* gyrase, it is the C-terminus of human type II topoisomerases that allow it to recognize supercoil handedness during relaxation, preferentially relaxing (+)SC faster than (-)SC DNA (McClendon and Osheroff 2006, McClendon, Gentry et al. 2008, Ashley and Osheroff 2019). To date, the structure of the eukaryotic C-terminal region has not yet been solved (McClendon, Gentry et al. 2008).

Bacterial Type II Topoisomerase Structure

The founding type II enzyme, gyrase, is comprised of two distinct subunits, GyrA (~96 kDa) and GyrB (~88 kDa). Gyrase was first discovered in 1972 during *E. coli* sedimentation analyses of DNA that showed the presence of negative supercoiling (Worcel and Burgi 1972, Gellert, Mizuuchi et al. 1976). The enzyme was later purified in 1976 (Gellert, Mizuuchi et al. 1976). Structurally, the GyrA portion of the enzyme (WHD, Tower, CTD; Figure 1.4) contains the active site tyrosine residue that forms the covalent bond with DNA during the cleavage reaction, as well as the C-terminal domain (Corbett and Berger 2004, Vos, Tretter et al. 2011, Gentry and

Osheroff 2013, McKie, Neuman et al. 2021). The GyrB portion contains motifs that allow ATP and divalent cation binding as part of the N-terminal domain (GHKL, Transducer, TOPRIM; Figure 1.4) (Corbett and Berger 2004, Vos, Tretter et al. 2011, Gentry and Osheroff 2013, McKie, Neuman et al. 2021). As such, one can envision that GyrB "comes before" GyrA when visualizing the linear polypeptide sequences from left to right. The main function of gyrase in bacteria is to maintain the proper supercoil density of the bacterial genome; gyrase can relax (+)SCs that accumulate ahead of DNA tracking machinery during processes such as replication and transcription, but it is also able to, to a lesser efficiency, decatenate (i.e., unlink) DNA in the presence of divalent cations (Marians 1987, Ullsperger and Cozzarelli 1996, Deweese, Osheroff et al. 2008, Deweese and Osheroff 2009, Vos, Tretter et al. 2011, Chen, Chan et al. 2013, Ashley and Osheroff 2019, Dalvie and Osheroff 2021).

One major distinguishing feature of gyrase is a seven-amino acid motif in the C-terminal domain of the GyrA subunit (Figure 1.4) (Kramlinger and Hiasa 2006, Sissi and Palumbo 2010, Vos, Tretter et al. 2011, Lanz and Klostermeier 2012, McKie, Neuman et al. 2021). This structure is known as the GyrA box, and it uniquely allows for the wrapping of the DNA substrate to introduce (-)SCs and rapidly relax (+)SC DNA in the presence of ATP (Deweese, Osheroff et al. 2008, Sissi and Palumbo 2010, Aldred, Kerns et al. 2014, Gibson, Ashley et al. 2018, Ashley and Osheroff 2019, McKie, Neuman et al. 2021). The GyrA box is found within a loop between strands 1 and 6 of a six-stranded beta pinwheel structure in the C-terminal region (Corbett, Shultzaberger et al. 2004, McKie, Neuman et al. 2021). Previous studies have demonstrated that the GyrA box (sequence QRRGGKG), when mutated via deletions or alanine substitutions, abrogate the ability of the enzyme to introduce (-)SCs (Kampranis and Maxwell 1996, Kramlinger and Hiasa 2006, Ashley, Dittmore et al. 2017, Ashley and Osheroff 2019, McKie, Neuman et al. 2021). Mutations

within the GyrA box affect the ability of gyrase to rapidly relax (+)SC DNA and relax (-)SC in the presence of ATP (Kramlinger and Hiasa 2006, Ashley, Dittmore et al. 2017, Ashley and Osheroff 2019, McKie, Neuman et al. 2021). It thus appears that the GyrA box is the defining feature of gyrase that enables it to freely supercoil DNA. Negative supercoils are introduced into the DNA substrate when the G-segment, being bound to the DNA-gate of the N-terminus, is chirally wrapped around one of the GyrA C-terminal domains to form a constrained (+)SC (Nöllmann, Crisona et al. 2007, Deweese, Osheroff et al. 2008, Ashley and Osheroff 2019, McKie, Neuman et al. 2021). This positive supercoil is then converted into a negative supercoil following strand passage, where the G-segment is translocated at a 60° angle, introducing negative writhe to the molecule (Deweese, Osheroff et al. 2008, Ashley and Osheroff 2019, McKie, Neuman et al. 2021).

Like gyrase, topoisomerase IV is also a heterotetramer that contains two subunits. The nomenclature of topoisomerase IV stemmed from their first identification in 1990 as gyrase homologs required for chromosomal segregation and cellular partitioning (Kato, Nishimura et al. 1990, Deweese, Osheroff et al. 2008, Deweese and Osheroff 2009, Forterre and Gadelle 2009, Vos, Tretter et al. 2011, Chen, Chan et al. 2013, Ashley and Osheroff 2019). In Gram-negative species such as *E. coli,* the topoisomerase IV subunits are designated as ParC (~88 kDa, homologous to GyrA) and ParE (~70 kDa, homologous to GyrB) (Kato, Nishimura et al. 1990, Kato, Suzuki et al. 1992). In Gram-positive species such as *B. anthracis,* the subunits of topoisomerase IV are named GrlA (Gyrase-like gene A) and GrlB (Gyrase-like gene B) (Levine, Hiasa et al. 1998, Gentry and Osheroff 2013, Ashley, Dittmore et al. 2017). “Reading” from left to right, the enzyme “order” would thus be ParE/GrlB and ParC/GrlA. Like gyrase, topoisomerase IV is also able to relax (+)SC DNA. However, topoisomerase IV differs from gyrase because of the inability to supercoil DNA (Hiasa and Marians 1994, Crisona, Strick et al. 2000, Zechiedrich,

Khodursky et al. 2000). In comparison to gyrase, the ParC C-terminal domain does not contain the necessary structure to supercoil DNA, instead having a "broken" five (not six) beta pinwheel, and the absence of a GyrA box (Corbett, Shultzaberger et al. 2004, Corbett, Schoeffler et al. 2005, Tretter, Lerman et al. 2010, Vos, Lee et al. 2013). Remnants of the canonical GyrA motif have been found in each of its pinwheel "blades" (Tretter, Lerman et al. 2010, Vos, Lee et al. 2013). Nonetheless, the ParC C-terminal domain contains positively charged moieties on its outer surface, suggesting a role in binding DNA (Corbett and Berger 2004). The loss of the ParC C-terminal domain has been found to impede the ability of *E. coli* topoisomerase IV to distinguish between topologically distinct substrates when relaxing and decatenating DNA substrates of different supercoil handedness (Corbett, Schoeffler et al. 2005, Vos, Lee et al. 2013).

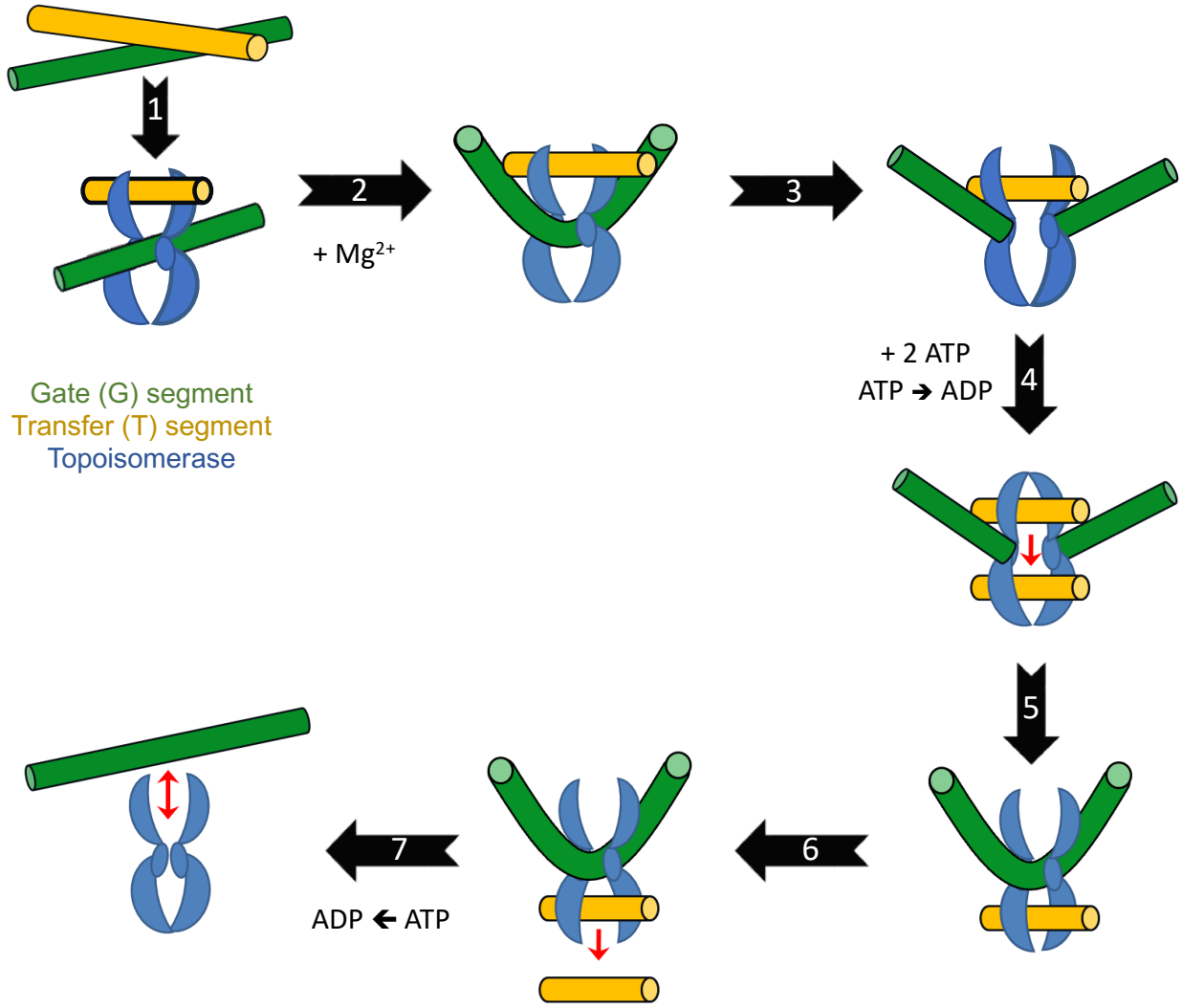

Figure 1.5: The catalytic cycle of type II topoisomerases. The double-stranded DNA passage reaction of topoisomerase II can be separated into seven discrete steps. 1) Type II enzyme (blue) binding to two segments of DNA: the gate segment (green) and transport segment (yellow). 2) Bending of the gate segment, which requires the presence of Mg^{2+} or other divalent metal ions. These metal ions are required for all subsequent steps. 3) Double-stranded DNA cleavage of the gate segment (*i.e.*, formation of the cleavage complex). 4) Passage of the transport segment through the DNA gate generated by cleavage. This reaction requires the binding of 2 ATP molecules, and strand passage proceeds more rapidly if one of the two ATP molecules is hydrolyzed. 5) Ligation of the cleaved DNA gate segment. 6) Hydrolysis of the second ATP molecule, which allows release of the gate segment through a C-terminal gate in the protein. 7) Enzyme turnover and closing of the protein gate, which regenerates the enzyme to initiate a new round of catalysis. Artwork from Ashley *et al.*, 2019.

Type II Topoisomerase Function Overview

All type II topoisomerases function by forming transient double-stranded DNA breaks and modulate the topological state of DNA by a double-stranded passage reaction (Figure 1.5) (Deweese, Osheroff et al. 2008, Deweese and Osheroff 2009, Vos, Tretter et al. 2011, Ashley and Osheroff 2019, McKie, Neuman et al. 2021, Vann, Oviatt et al. 2021). The enzyme begins its catalytic cycle by first capturing a segment of DNA through the opening of the N-terminal region of the enzyme (Figure 5, step 1). This first segment will be cut by the enzyme and is known as the "gate" or G-segment. In contrast, the segment that will be secondly captured and eventually transported through the transiently cleaved G-segment is known as the "transport" or T-segment. In the presence of a divalent cation such as Mg^{2+} and in coordination with the TOPRIM domain, the G-segment is assessed for bendability (Jang, Son et al. 2019). DNA sequences that can be bent are distorted to an angle of ~150° and can be used as the site for scission (Dong and Berger 2007, Lee, Dong et al. 2013).

The bent G-segment is then cleaved via a nucleophilic attack by the two active site tyrosine residues on the phosphate backbone of the double helix (Figure 1.5, step 2). Cleavage is initiated when a general base, which is believed to be a conserved histidine residue, deprotonates the hydroxyl group of the active site tyrosine, allowing the oxyanion to attack the scissile phosphate (Figure 1.5, step 3). Two cofactors are needed by the enzyme to carry out this and the subsequent double-stranded DNA passage reactions (Deweese, Osheroff et al. 2008, Deweese and Osheroff 2009, Vos, Tretter et al. 2011, Chen, Chan et al. 2013, Ashley and Osheroff 2019). The first cofactor is a divalent cation, such as magnesium (i.e., Mg^{2+}), for all steps beyond enzyme-DNA binding. The enzyme uses a non-canonical two-metal ion mechanism at each cut site (Noble and Maxwell 2002, Deweese and Osheroff 2009, Schmidt, Burgin et al. 2010, Pommier, Sun et al.

2016). The presence of one divalent cation enables interaction with the bridging 5'-oxygen molecule of the scissile bond and speeds up rates of enzyme-mediated cleavage at the first cut site. A second divalent cation is believed to make critical contacts with and help deprotonate the active site tyrosine, thereby stabilizing the DNA transition state. Once the first DNA strand is cut, the second strand is cleaved ~20-fold faster (Deweese, Guengerich et al. 2009). The resulting transiently-cleaved cleavage complex has the enzyme covalently bound to the scissile 5'-phosphate of the double helical backbone. The second cofactor is ATP, which drives the strand passage reaction. ATP is not necessary for either the DNA cleavage or religation of the DNA substrate (Deweese, Osheroff et al. 2008, Deweese and Osheroff 2009, Vos, Tretter et al. 2011, Chen, Chan et al. 2013, Ashley and Osheroff 2019, McKie, Neuman et al. 2021, Vann, Oviatt et al. 2021).

In greater detail, the cleavage complex is a transient enzyme-DNA structure connected by two staggered 4-base single-stranded cohesive overhangs in the 5'-end of one DNA sequence, a 3'-hydroxyl moiety on the opposite terminus of the cleaved strand, and a gap in the double helix (Deweese and Osheroff 2009, Nitiss 2009, Pommier, Leo et al. 2010, Vos, Tretter et al. 2011, Ashley and Osheroff 2019, McKie, Neuman et al. 2021, Vann, Oviatt et al. 2021). To maintain the bond energy of the sugar-phosphate backbone as well as genomic integrity during the cleavage process, the type II enzyme forms covalent bonds between the active site tyrosine and the 5'-phosphate group of the DNA backbone, generating a phosphotyrosyl linkage (Deweese and Osheroff 2009, Nitiss 2009, Pommier, Leo et al. 2010, Vos, Tretter et al. 2011, Ashley and Osheroff 2019, McKie, Neuman et al. 2021, Vann, Oviatt et al. 2021). Upon the binding of two ATP molecules, the N-terminal gate is closed. Closing of the N-terminal gate triggers a conformational change in the enzyme that helps translocate the T-segment through the transient

opening in the enzyme active site, performing strand passage (Figure 1.5, step 4). Although hydrolysis of the high-energy cofactor is not necessarily a prerequisite for strand passage to occur, it appears that this step occurs faster if one of the two bound ATP molecules is hydrolyzed (Lindsley and Wang 1993).

After strand passage, a second, post-strand passage, cleavage complex is formed (Figure 1.5, step 5). The type II enzyme then religates the cleaved DNA to regenerate the intact DNA double helix. DNA religation is initiated when a general acid removes the hydrogen from the 3'-terminal hydroxyl group (Deweese and Osheroff 2009, Wendorff, Schmidt et al. 2012). Another nucleophilic attack is then initiated on the phosphotyrosyl bond, regenerating the intact DNA double helical backbone and the enzyme active site. The T-segment is then released from the protein (Figure 1.5, step 6). Hydrolysis of a second ATP molecule then occurs, and the enzyme releases the G-segment. Lastly, the type II enzyme conformation is reset, allowing for the next cycle of catalysis (Figure 1.5, step 7) (Osheroff 1986, Roca and Wang 1992, Wang 1998, Wilstermann and Osheroff 2001, Deweese and Osheroff 2009, Vos, Tretter et al. 2011, Vann, Oviatt et al. 2021).

Human Type II Topoisomerase Function

In humans, type II topoisomerases play a role in virtually every major nucleic acid process (Deweese, Osheroff et al. 2008, Deweese and Osheroff 2009, Forterre and Gadelle 2009, Vos, Tretter et al. 2011, Chen, Chan et al. 2013, Pommier, Sun et al. 2016, Ashley and Osheroff 2019). These functions include untangling daughter chromosomes that form during replication, resolving knots formed during recombination, removing (+)SC DNA generated ahead of replication forks and transcription complexes, and maintaining proper chromosome organization and structure as

the major non-histone protein of the mitotic chromosome scaffold and the interphase nuclear matrix (Earnshaw, Halligan et al. 1985, Gasser, Laroche et al. 1986, Deweese and Osheroff 2009, Vos, Tretter et al. 2011). Lower eukaryotes and non-vertebrate species such as yeast encode only a single type II enzyme, topoisomerase II (Wyckoff and Hsieh 1988, McClendon, Rodriguez et al. 2005). In vertebrates and humans, however, both topoisomerase IIα and topoisomerase IIβ are expressed; it remains unclear why two distinct isoforms are encoded (Deweese, Osheroff et al. 2008, Deweese and Osheroff 2009, Forterre and Gadelle 2009, Vos, Tretter et al. 2011, Chen, Chan et al. 2013, Pommier, Sun et al. 2016, Ashley and Osheroff 2019). Despite their broad similarities, there are several crucial differences in expression and function between these two isoforms that will be discussed.

Human topoisomerase IIα and topoisomerase IIβ are distinct in their expression patterns (Heck and Earnshaw 1986, Heck, Hittelman et al. 1988, Woessner, Mattern et al. 1991, McClendon and Osheroff 2007, Vos, Tretter et al. 2011). Topoisomerase IIα is required for the survival of proliferating cells (Heck and Earnshaw 1986, Heck, Hittelman et al. 1988, Hsiang, Wu et al. 1988, McClendon and Osheroff 2007, Ketron and Osheroff 2014). Levels of topoisomerase IIα expression increase throughout S-phase of the cell cycle, beginning at lower levels during G_1 and rising through S, eventually peaking at the G2/M phase boundary (Heck, Hittelman et al. 1988, Woessner, Mattern et al. 1991, Kimura, Saijo et al. 1994). Topoisomerase IIα is found almost exclusively in actively proliferating tissues, localizes predominantly in the nucleus, is associated with replication forks and transcription machinery, and has been found to be tightly bound to chromosomes and sister chromatids throughout mitosis (Uemura, Ohkura et al. 1987, Woessner, Mattern et al. 1991, Kimura, Saijo et al. 1994, Mirski, Gerlach et al. 1997, Grue, Grasser et al. 1998, Mirski, Gerlach et al. 1999, McClendon and Osheroff 2007, Lee and Berger 2019). As such,

the type IIα enzyme is believed to be the main isoform that functions in growth-related processes such as replication and chromosomal segregation (Grue, Grasser et al. 1998, Nitiss 2009, Pommier, Sun et al. 2016, McKie, Neuman et al. 2021, Vann, Oviatt et al. 2021). While there is evidence that topoisomerase IIα can act ahead of replication forks, it is believed to primarily act behind them (Heintzman, Campos et al. 2019).

In contrast to topoisomerase IIα, the IIβ isoform is not required for survival at the cellular level, and IIβ activity cannot replace that of IIα (Dereuddre, Delaporte et al. 1997, Grue, Grasser et al. 1998, Bakshi, Galande et al. 2001, Nitiss 2009, Ketron and Osheroff 2014, Austin, Lee et al. 2018). The concentration of topoisomerase IIβ expressed in cells is independent of the stage of the cell cycle and this isoform is found at generally consistent levels in most cell types regardless of cell proliferation status (Austin and Marsh 1998, Christensen, Larsen et al. 2002, Cowell, Sondka et al. 2012, McKie, Neuman et al. 2021). Unlike its IIα counterpart, the IIβ enzyme dissociates from chromosomes during mitosis (Austin and Marsh 1998, Isaacs, Davies et al. 1998, Linka, Porter et al. 2007). Although the precise cellular functions of topoisomerase IIβ have yet to be fully understood, it has been shown to be involved in the regulation of hormonally-related genes at the transcriptional level (Yang, Li et al. 2000, Ju, Lunyak et al. 2006, Deweese and Osheroff 2009, Ketron and Osheroff 2014, Austin, Lee et al. 2018, McKie, Neuman et al. 2021, Vann, Oviatt et al. 2021). Topoisomerase IIβ is necessary for proper neural development in mouse embryos (Yang, Li et al. 2000, Lyu and Wang 2003). Conditional knockouts have implicated topoisomerase IIβ activity in proper retinal development and ovulation (Zhang, Yu et al. 2013, Li, Hao et al. 2014). More recently, NGS studies using chromatin immunoprecipitation sequencing (ChIP-seq) have mapped IIβ activity at borders of chromosomal domains and at conserved transcription factor binding sites (Uuskula-Reimand, Hou et al. 2016, Martínez-Garcia, García-Torres et al. 2021,

McKie, Neuman et al. 2021). Taken together, there may be functions of topoisomerase IIβ in proper hormonal development and cellular differentiation via interactions with transcription machinery (Yang, Li et al. 2000, Ju, Lunyak et al. 2006, McClendon and Osheroff 2007, Liu, Deibler et al. 2009, Nitiss 2009, Pommier, Sun et al. 2016, Bollimpelli, Dholaniya et al. 2017, Austin, Lee et al. 2018).

Gyrase and Topoisomerase IV Function

Despite their similarities in structure, gyrase and topoisomerase IV play different roles in cellular environments. In addition to its unique ability to introduce (-)SCs into DNA, the strand wrapping mechanism of gyrase allows it to remove (+)SCs substantially faster than it introduces (-)SCs into DNA (Ashley, Blower et al. 2017, Ashley, Dittmore et al. 2017). Because of its ability to wrap DNA during catalysis, gyrase functions primarily to relax or generate supercoils (Levine, Hiasa et al. 1998, Khodursky, Peter et al. 2000, Hsu, Chung et al. 2006, Tadesse and Graumann 2006, Deweese, Osheroff et al. 2008, Aldred, Kerns et al. 2014, Gibson, Ashley et al. 2018, Ashley and Osheroff 2019). To put this into the context of biological function, DNA gyrase plays an important role in removing the (+)SCs that can form ahead of DNA tracking machinery (i.e., polymerases and helicases) during essential nucleic acid processes such as replication and transcription (Levine, Hiasa et al. 1998, Khodursky, Peter et al. 2000, Hsu, Chung et al. 2006, Tadesse and Graumann 2006, Deweese, Osheroff et al. 2008, Aldred, Kerns et al. 2014, Gibson, Ashley et al. 2018). Its strong ability to rapidly and preferentially relax (+)SCs versus introduce (-)SCs would make it a suitable enzyme to function ahead of replication forks and transcription complexes to alleviate torsional stress induced by DNA overwinding. Additionally, gyrase works

in conjunction with ω protein (a type I topoisomerase) to maintain the global negative superhelicity of DNA (Mirkin, Zaitsev et al. 1984, Tse-Dinh 1998, Ashley and Osheroff 2019).

In contrast to gyrase, topoisomerase IV is the enzyme primarily responsible for resolving knots and tangles that form during nucleic acid processes (Levine, Hiasa et al. 1998, Tadesse and Graumann 2006, Deweese, Osheroff et al. 2008, Wang, Reyes-Lamothe et al. 2008, Liu, Deibler et al. 2009, Sissi and Palumbo 2010, Aldred, Kerns et al. 2014, Zawadzki, Stracy et al. 2015, Gibson, Ashley et al. 2018, Ashley and Osheroff 2019). As such, topoisomerase IV mainly resolves precatenanes that form behind replication forks and removes DNA knots that form during recombination. Nonetheless, topoisomerase IV has been found to remove (+)SCs from DNA substrates more efficiently than it does (-)SCs (Ashley, Dittmore et al. 2017). Topoisomerase IV may also play a role ahead of DNA tracking systems, but the precise nature of this process is less understood (Vos, Lee et al. 2013, Ashley, Dittmore et al. 2017).

Type II Topoisomerases in Cellular Environments: When Good Enzymes Go Bad

All type II topoisomerases generate a transiently-cleaved, covalently-linked enzyme-DNA complex during the strand passage reaction, which is necessary for maintaining the proper topological state of DNA in cellular systems. However, the formation of the cleavage complex itself poses a potential danger to the cell (Figure 1.6) (Anderson and Osheroff 2001, Deweese and Osheroff 2009, Nitiss 2009, Aldred, Kerns et al. 2014, Ketron and Osheroff 2014, Pendleton, Lindsey et al. 2014, Pommier, Sun et al. 2016, Vann, Oviatt et al. 2021). Given that a double-stranded DNA break must form during the assembly of the binary enzyme-DNA complex, type II topoisomerases have the capacity to fragment the genome (Deweese and Osheroff 2009, Nitiss 2009, Aldred, Kerns et al. 2014, Ketron and Osheroff 2014, Pendleton, Lindsey et al. 2014,

Pommier, Sun et al. 2016, Vann, Oviatt et al. 2021). Consequently, the equilibrium between the forward cleavage reaction (enabling the subsequent strand passage) and the reverse religation reaction (resealing the DNA break) heavily favors religation to maintain genomic integrity during the catalytic cycle (Figure 1.6). The formation of covalent linkages between the enzyme active site tyrosine with the cleaved phosphate ends prevents them from being separated in the cell and masks them from DNA repair mechanisms. Under normal equilibrium conditions, ~0.5-1% of type II topoisomerases in an *in vitro* DNA scission reaction exist in a cleavage complex (Zechiedrich, Christiansen et al. 1989, Deweese, Burgin et al. 2008). This means that these covalent enzyme-cleaved DNA complexes are tightly regulated, present at low steady-state levels, short-lived, and tolerated in cells (Deweese, Osheroff et al. 2008, Nitiss 2009, Pommier, Sun et al. 2016, Ashley and Osheroff 2019, Vann, Oviatt et al. 2021). Conditions that significantly increase the frequency, concentration, or lifetime of cleavage complexes can trigger adverse, mutagenic, and potentially lethal cellular events (Levine, Hiasa et al. 1998, Anderson and Osheroff 2001, Felix, Kolaris et al. 2006, Deweese, Osheroff et al. 2008, Deweese and Osheroff 2009, Nitiss 2009, Aldred, Kerns et al. 2014, Pendleton, Lindsey et al. 2014, Pommier, Sun et al. 2016, Gibson, Ashley et al. 2018, Vann, Oviatt et al. 2021).

In biological systems, the processes of DNA replication and transcription require the formation of cleavage complexes in order for strand passage to be performed and to remove the (+)SCs that accumulate. If (+)SCs are left unresolved, movement of DNA tracking machinery becomes impeded and genetic material cannot be replicated or transcribed (Deweese and Osheroff 2009, Aldred, Kerns et al. 2014, Pendleton, Lindsey et al. 2014, Vann, Oviatt et al. 2021). However, the formation of cleavage complexes ahead of these DNA tracking systems can be potentially lethal when polymerases or helicases approach or attempt to traverse the covalently

bound topoisomerase “roadblock” in the genetic material (Deweese, Osheroff et al. 2008, Deweese and Osheroff 2009, Nitiss 2009, Aldred, Kerns et al. 2014, Ketron and Osheroff 2014, Pendleton, Lindsey et al. 2014, Pommier, Sun et al. 2016, Vann, Oviatt et al. 2021). Such an action disrupts cleavage complexes and prevents the bound enzyme from religating the double-stranded DNA breaks (Howard, Neece et al. 1994). Consequently, the transient DNA cuts are converted to non-ligatable DNA lesions that need to be repaired by recombination repair pathways. Increased frequencies of these pathways can trigger unwanted chromosomal insertions, deletions, translocations, and other DNA aberrations (Deweese and Osheroff 2009, Aldred, Kerns et al. 2014, Pendleton, Lindsey et al. 2014, Vann, Oviatt et al. 2021). In sufficient numbers, they can initiate a series of detrimental events that can culminate in cell death. Because overwound DNA that needs to be resolved accumulates ahead of tracking systems, cleavage complexes formed with (+)SC DNA are potentially the most lethal to cells (Deweese and Osheroff 2009, Aldred, Kerns et al. 2014, Ketron and Osheroff 2014, Pendleton, Lindsey et al. 2014, Pommier, Sun et al. 2016, Ashley and Osheroff 2019, Vann, Oviatt et al. 2021). As such, it is important to understand the effects of DNA topology on type II topoisomerase function in humans and bacteria.

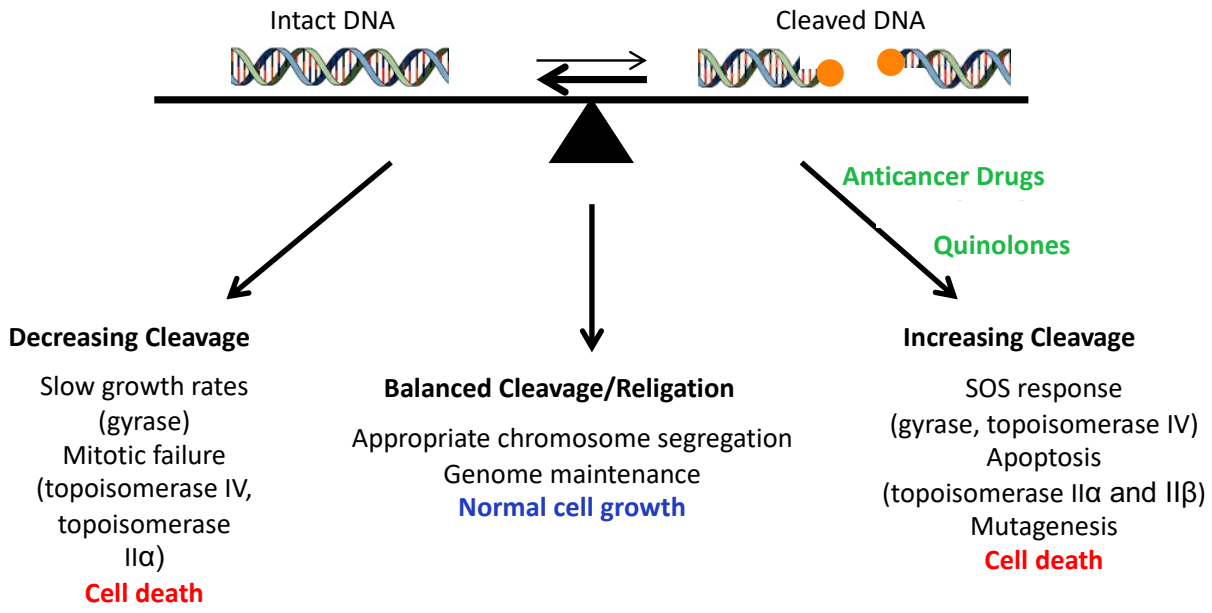

Figure 1.6: The critical balance between DNA cleavage and religation. The activity of type II topoisomerases must be tightly regulated in the cell. When cleavage/religation is balanced, the genome can be appropriately maintained and the cell can grow normally. If the level of cleavage/religation decrease, slow growth rates and mitotic failure can cause cell death. Conversely, if the levels of cleavage/relegation are too high, DNA damage can overwhelm the cell, leading to mutagenesis and cell death. Figure adapted from Pendleton *et al.*, 2014.

Antibacterial Drugs

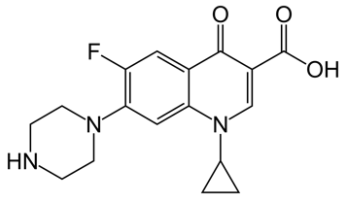

Ciprofloxacin

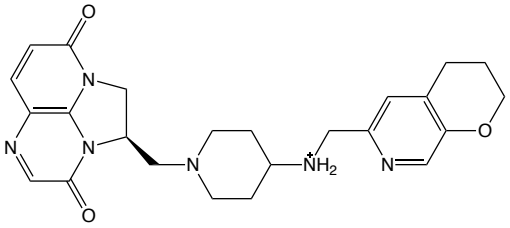

Gepotidacin

Anticancer Drugs

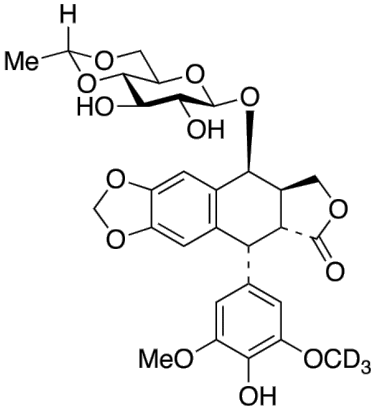

Etoposide

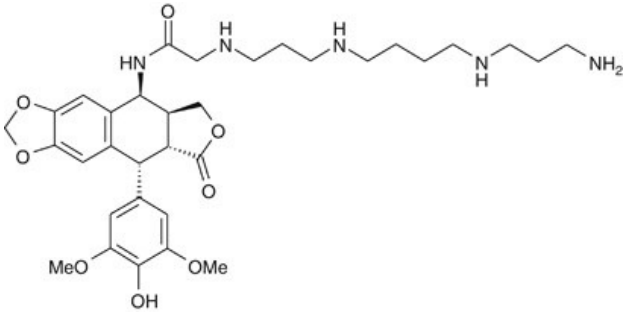

F14512

Figure 1.7: Structures of antibacterial and anticancer drugs. Structures of selected antibacterial drugs targeted to DNA gyrase and topoisomerase IV (ciprofloxacin, top left; gepotidacin, top right), and anticancer drugs targeted to human type II topoisomerases (etoposide, bottom left; F14512, bottom right).

Type II Topoisomerases as Drug Targets

The formation of cleavage complexes by type II topoisomerases is a requisite, but potentially dangerous step in the process of regulating the topological state of DNA. Because of this potentially lethal property, type II topoisomerases are the targets for a variety of anticancer and antibacterial drugs (Baldwin and Osheroff 2005, Deweese, Osheroff et al. 2008, Deweese and Osheroff 2009, Drlica, Hiasa et al. 2009, Nitiss 2009, Bax, Chan et al. 2010, Pommier, Leo et al. 2010, Aldred, Kerns et al. 2014, Pendleton, Lindsey et al. 2014, Hooper and Jacoby 2016, Pommier, Sun et al. 2016, Gibson, Ashley et al. 2018, Hiasa 2018, Bax, Murshudov et al. 2019, Vann, Oviatt et al. 2021). In contrast to many therapeutics, these drugs do not function by preventing enzymatic activity, though they can impair enzyme function (Deweese, Osheroff et al. 2008, Deweese and Osheroff 2009, Nitiss 2009, Aldred, Kerns et al. 2014, Ketron and Osheroff 2014, Pendleton, Lindsey et al. 2014, Pommier, Sun et al. 2016, Gibson, Ashley et al. 2018, Bax, Murshudov et al. 2019, Vann, Oviatt et al. 2021). Rather, these chemical agents kill cells by increasing the concentration or stability (i.e., lifetime) of covalent enzyme-DNA cleavage complexes. Drugs that target the type II topoisomerases convert these essential enzymes into potent cellular toxins that can have mutagenic and lethal consequences (Bandele and Osheroff 2008, Deweese and Osheroff 2009, Wu, Li et al. 2011, Pommier and Marchand 2012, Dalvie, Gopas et al. 2019, Vann, Oviatt et al. 2021). In doing so, these agents are collectively referred to as topoisomerase "poisons." Type II topoisomerase poisons stand in contrast to drugs or compounds that act as topoisomerase inhibitors, which decrease the overall activity of the enzyme but does not necessarily increase the concentration of cleavage complexes.

Anticancer drugs

Type II topoisomerase poisons currently represent some of the most widely-prescribed anticancer drugs in clinical use (Deweese, Osheroff et al. 2008, Deweese and Osheroff 2009, Nitiss 2009, Pommier, Leo et al. 2010, Pendleton, Lindsey et al. 2014, Vann, Oviatt et al. 2021). These drugs encompass a variety of natural and synthetic compounds that are commonly prescribed to treat many human malignancies (Deweese and Osheroff 2009, Nitiss 2009, Ketron and Osheroff 2014, Pendleton, Lindsey et al. 2014, Pommier, Sun et al. 2016, Ashley and Osheroff 2019, Dalvie and Osheroff 2021). All of these chemical agents act as type II topoisomerase poisons and function mainly by inhibiting enzyme-mediated religation of the cleaved DNA substrate (Deweese and Osheroff 2009, Nitiss 2009, Ketron and Osheroff 2014, Pendleton, Lindsey et al. 2014, Pommier, Sun et al. 2016, Vann, Oviatt et al. 2021). In cellular contexts, preventing the religation of cleaved DNA effectively traps the enzyme-DNA cleavage complex. The lifetime of this enzyme-DNA-drug tertiary structure has been shown previously to be longer than that of the enzyme-DNA binary complex (Bandele and Osheroff 2008, Gentry, Pitts et al. 2011). As both the frequency and stability of cleavage complexes are increased, so does the probability of approaching DNA tracking systems, such as polymerases and helicases, converting these transient-cleaved breaks in the double helical backbone into nonligatable lesions that need to be repaired (Deweese and Osheroff 2009, Nitiss 2009, Ketron and Osheroff 2014, Pendleton, Lindsey et al. 2014, Pommier, Sun et al. 2016, Vann, Oviatt et al. 2021).

Drugs targeting one or more type II topoisomerases in humans are efficacious for three primary reasons. First, cancer cells are highly proliferative and express higher levels of topoisomerases, resulting in more drug-stabilized cleavage complexes (Hsiang, Wu et al. 1988, Woessner, Mattern et al. 1991, Nitiss 2009, Nitiss 2009, Pendleton, Lindsey et al. 2014). Second,

the higher metabolic rates of cancer cells mean that replication forks and transcription complexes are constantly moving along the DNA substrate, increasing the probability that cleavage complexes will be converted into nonligatable DNA lesions (Baldwin and Osheroff 2005, Deweese and Osheroff 2009, Chen, Qiu et al. 2012, Puigvert, Sanjiv et al. 2016, Vann, Oviatt et al. 2021). Third, the impaired cell cycle checkpoints and DNA damage response mechanisms in cancer cells make them more susceptible to drug-induced topoisomerase II-mediated DNA damage (Murai 2017).

Given the expression patterns, cellular functions, and localizations of human type II topoisomerases, drugs that favor one isoform over the other have clinical implications (Deweese and Osheroff 2009, Pommier, Leo et al. 2010, Vos, Tretter et al. 2011, Pommier, Sun et al. 2016). In humans, topoisomerase IIα is not expressed appreciably in quiescent cells (i.e., cells that are not actively proliferating) (Markovits, Pommier et al. 1987, Hsiang, Wu et al. 1988, Woessner, Mattern et al. 1991). Thus, the actions of chemical agents against the β isoform in differentiated tissues, such as cardiac cells (i.e., cardiotoxicity), are most likely responsible for much of the off-target toxicity of these drugs (Lyu, Kerrigan et al. 2007, Menna, Salvatorelli et al. 2008, Cowell, Sondka et al. 2012, Pendleton, Lindsey et al. 2014). Alternatively, because topoisomerase IIα and topoisomerase IIβ are involved in different cellular processes, it may be that cleavage complexes formed with one or the other isoform can be more likely converted to nonligatable DNA lesions.

One of the earliest type II topoisomerase-targeted drugs was etoposide, a chemical derivative from the natural plant substance podophyllotoxin (Hande 1998, Baldwin and Osheroff 2005, Deweese and Osheroff 2009, Vos, Tretter et al. 2011, Pendleton, Lindsey et al. 2014). Etoposide has been approved for use against cancer since the 1980s and for several years was the most commonly-prescribed antineoplastic drug in the world (Baldwin and Osheroff 2005,

Deweese and Osheroff 2009, Pommier, Leo et al. 2010, Vos, Tretter et al. 2011, Pendleton, Lindsey et al. 2014, Pommier, Sun et al. 2016). Etoposide and its derivatives have thus become highly prescribed for a variety of systemic cancers and solid tumors, including leukemias, lymphomas, sarcomas and breast, lung, and germline cancers (Baldwin and Osheroff 2005, Azarova, Lyu et al. 2007, Nitiss 2009, Pommier, Leo et al. 2010, Pendleton, Lindsey et al. 2014, Pommier, Sun et al. 2016, Delgado, Hsieh et al. 2018). Currently, ~50% of all cancer chemotherapy regimens contain drugs targeting topoisomerase II, with six approved for use in the United States (doxorubicin, daunorubicin, idarubicin, mitoxantrone, etoposide, and teniposide) (Hande 1998, Velez-Cruz and Osheroff 2004, Baldwin and Osheroff 2005, McClendon and Osheroff 2007). Every form of cancer that can be cured by systemic chemotherapy is treated with these agents. Nonetheless the off-target and side effects of etoposide necessitated the development of stronger and more specific anticancer drugs (Hande 1998, Felix 2001, Baldwin and Osheroff 2005). The etoposide derivative F14512 was eventually synthesized to take advantage of the polyamine transport system (PAS) in some cancer cells (Barret, Kruczynski et al. 2008). Instead of a glycosyl moiety at the C4 site, F14512 contains spermidine, which was found to both increase specificity for PAS transport and cellular uptake, as well as have increased efficacy against tumors (Barret, Kruczynski et al. 2008, Kruczynski, Vandenberghe et al. 2011). In the presence of etoposide or F14512, both human topoisomerase IIα and IIβ have observed lower levels of cleavage intermediates with (+)SC DNA than with (-)SC DNA (McClendon and Osheroff 2006, Gentry, Pitts et al. 2011).

Despite the benefits, there have also been dangers associated with anticancer drugs targeting type II topoisomerases, namely the formation of off-target effects and secondary malignancies (Baguley and Ferguson 1998, Felix 2001, Baldwin and Osheroff 2005, Felix, Kolaris

et al. 2006, McClendon and Osheroff 2007, Pendleton, Lindsey et al. 2014). In humans there are high levels of type II topoisomerase activity in rapidly proliferating cells, such as tumors. It therefore would make logical sense to apply type II topoisomerase poisons as antineoplastic agents, by increasing the frequency or lifetime of cleavage complexes that form in cancer cells. However, due to the greater induction of double- stranded DNA breaks in cancer cells, the use of these anticancer drugs has also been associated with off-target effects, such as the generation of unwanted chromosomal translocations that result in secondary leukemias in a small proportion of patients (Felix 2001, Baldwin and Osheroff 2005, Joannides and Grimwade 2010, Joannides, Mays et al. 2011, Ezoe 2012, Rashidi and Fisher 2013, Pendleton, Lindsey et al. 2014). Approximately 2-3% of patients treated with etoposide develop acute myeloid leukemia (AML) characterized by translocations with breakpoints in the mixed lineage leukemia (*MLL*) gene at chromosomal band 11q23 (Baldwin and Osheroff 2005, Azarova, Lyu et al. 2007, Nitiss 2009, Pendleton, Lindsey et al. 2014, Delgado, Hsieh et al. 2018). The application of other anticancer drugs to treat diseases such as breast cancer and multiple sclerosis carries the risk of developing acute promyelocytic leukemia (APL) characterized by chromosome 15:17 translocations involving the promyelocytic leukemia gene (*PML*) and the retinoic acid receptor α (*RARA*) genes (Joannides and Grimwade 2010, Joannides, Mays et al. 2011, Pendleton, Lindsey et al. 2014, Ellis, Brown et al. 2015). Sites of breakpoints in the chromosome have been found in close proximity to sites of type II topoisomerase-mediated DNA cleavage (Baldwin and Osheroff 2005, Azarova, Lyu et al. 2007, Hasan, Mays et al. 2008, Cowell, Sondka et al. 2012, Baranello, Kouzine et al. 2014, Delgado, Hsieh et al. 2018, McKie, Maxwell et al. 2020). Additionally, because both cancerous and noncancerous tissues can express type II topoisomerases, specifically the IIβ isoform, it has been identified as the type II enzyme in humans that may be responsible for the side effects of these

chemotherapeutic drugs. Lastly, other secondary effects such as increased risk of cardiotoxicity has been associated with topoisomerase IIβ (Lyu, Kerrigan et al. 2007, Menna, Salvatorelli et al. 2008, Cowell, Sondka et al. 2012, Pendleton, Lindsey et al. 2014).

Antibacterial Drugs

In bacteria, DNA gyrase and topoisomerase IV are the targets for a class of antibacterials known as fluoroquinolones (Aldred, Kerns et al. 2014, Gibson, Ashley et al. 2018, Bax, Murshudov et al. 2019). These drugs are the most active and broad spectrum oral antibacterial agents in clinical use and are among the most widely prescribed antibacterials worldwide (Hooper 1998, Hooper 2001, Linder, Huang et al. 2005, Drlica, Hiasa et al. 2009, Pommier, Leo et al. 2010, Aldred, Kerns et al. 2014). Fluoroquinolones were first discovered as the quinolone parent compound nalidixic acid in the 1960s (Lesher, Froelich et al. 1962). Modifications to nalidixic acid by adding fluorine substituents led to newer generations of fluoroquinolones (i.e. ciprofloxacin, moxifloxacin) to continue to treat bacterial infections (Stein 1988, Anderson and Osheroff 2001, Drlica, Hiasa et al. 2009, Pommier, Leo et al. 2010). Drugs such as ciprofloxacin are routinely prescribed for a wide variety of Gram-negative and Gram-positive bacterial infections, including gastrointestinal tract and bone and joint infections (Anderson and Osheroff 2001, Drlica, Hiasa et al. 2009, Pommier, Leo et al. 2010). Ciprofloxacin and related fluoroquinolones are also used to treat various sexually transmitted diseases as well as anthrax infections, caused by the Gram-positive bacterial species *Bacillus anthracis*, and tuberculosis, which is caused by *Mycobacterium tuberculosis* (a species that is neither Gram-positive nor Gram-negative) (Aldred, Blower et al. 2016, Ashley, Blower et al. 2017, Gibson, Ashley et al. 2018, Ashley and Osheroff 2019).

Fluoroquinolones are topoisomerase poisons that increase the overall level of cleavage complexes formed by DNA gyrase and topoisomerase IV (Aldred, McPherson et al. 2012, Aldred, Blower et al. 2016, Ashley, Blower et al. 2017, Ashley, Lindsey et al. 2017, Gibson, Ashley et al. 2018). These drugs also inhibit the other essential functions of these enzymes, including supercoiling, relaxation, untangling, and unknotting. In the presence of ciprofloxacin, DNA gyrase-mediated cleavage is greater with (-)SC than with (+)SC DNA. This difference has been shown for gyrase from *E. coli*, *B. anthracis*, and *M. tuberculosis* (Aldred, McPherson et al. 2012, Aldred, Blower et al. 2016, Ashley, Blower et al. 2017, Ashley, Lindsey et al. 2017, Gibson, Ashley et al. 2018). Moreover, enzyme-cleaved DNA complexes formed in the presence of ciprofloxacin display longer lifetimes as the ternary structure, suggesting increased overall complex stability. In contrast to gyrase, topoisomerase IV from *E. coli* and *B. anthracis* do not display a strong preference for supercoil handedness during the DNA scission reaction (Aldred, McPherson et al. 2012, Aldred, Blower et al. 2016, Ashley, Blower et al. 2017, Ashley, Lindsey et al. 2017).

Unfortunately, the rapid increase in antibacterial resistance over the course of the last several decades has rendered it difficult to continue solely relying on fluoroquinolone treatments (Andriole 2005, Drlica, Hiasa et al. 2009, Aldred, Kerns et al. 2014). Consequently, new classes of drugs that also target bacterial type II topoisomerases while retaining activity against fluoroquinolone-resistant strains are currently in development (Bax, Chan et al. 2010, Gibson, Ashley et al. 2018, Gibson, Blower et al. 2018, Bax, Murshudov et al. 2019). The most advanced of these compounds are known as novel bacterial topoisomerase inhibitors (NBTIs); one example of an NBTI is gepotidacin (Dougherty, Nayar et al. 2014, Biedenbach, Bouchillon et al. 2016, O'Riordan, Tiffany et al. 2017, Gibson, Blower et al. 2018, Gibson, Bax et al. 2019). In contrast

to fluoroquinolones, which generate enzyme-mediated double-stranded DNA breaks during the scission reaction, NBTIs generate single-stranded breaks. These drugs have also the capacity to inhibit DNA supercoiling and relaxation reactions mediated by bacterial type II enzymes.

The Effects of DNA Topology on Human and Bacterial Type II Topoisomerases

Relaxation of Supercoiled DNA

Given the critical roles of type II topoisomerases in their respective cellular environments, it is important to understand how DNA topology can affect the function of both the bacterial and human enzymes. As previously mentioned, DNA in bacterial and human cells is globally underwound (Bates and Maxwell 2005, Buck 2009). Overwound or (+)SC DNA that accumulates ahead of replication forks and transcription complexes results in torsional stress that needs to be alleviated for these nucleic acid processes to continue (Linka, Porter et al. 2007, Deweese and Osheroff 2009, Baxter, Sen et al. 2011, Ashley and Osheroff 2019, Vann, Oviatt et al. 2021). Fortunately, humans and bacterial species encode at least one type II topoisomerase that can preferentially resolve these unwanted topological structures.

In humans, a major distinguishing characteristic between topoisomerase IIα from topoisomerase IIβ is that the IIα isoform relaxes (+)SC 10–fold faster than it does (-)SC DNA (McClendon, Rodriguez et al. 2005, McClendon, Dickey et al. 2006, McClendon, Gentry et al. 2008). In contrast, topoisomerase IIβ, which appears to play no role in DNA replication, does not distinguish between (+)SC or (-)SC substrates during relaxation (McClendon, Rodriguez et al. 2005, McClendon, Dickey et al. 2006, McClendon, Gentry et al. 2008). Similar to those observed with bacterial gyrase versus topoisomerase IV, these disparities between topoisomerase IIα and topoisomerase IIβ can be attributed to differences in elements of their respective C-terminal

domains(McClendon, Dickey et al. 2006, McClendon and Osheroff 2006, McClendon, Gentry et al. 2008). The region of the human type II enzymes where the greatest sequence difference can be observed is in the C-terminal domain (~31% sequence overlap). This disparity stands in marked contrast to the ~79% similarity in their N-terminal domain and catalytic core region, suggesting that the ability to differentially recognize supercoil handedness during relaxation may be attributable to differences in sequence identity between the C-termini of the two isoforms (Austin, Sng et al. 1993, McClendon, Gentry et al. 2008). Human topoisomerase IIα mutants that have the C-terminal domain removed relaxed (+)SC and (-)SC DNA at similar rates (Dickey and Osheroff 2005). Moreover, studies that switched the C-terminal domain of topoisomerase IIα with that of topoisomerase IIβ demonstrated that topoisomerase IIβ gained the ability to recognize and preferentially relax (+)SC DNA (McClendon, Gentry et al. 2008). Topoisomerase IIα that received the C-terminal domain of the β isoform lost handedness preference during strand passage (i.e., relax both (+)SC and (-)SC supercoiled DNA at similar rates) (McClendon, Gentry et al. 2008). Additional studies on DNA substrate binding by human type II enzymes did not show differences based on supercoil handedness (McClendon and Osheroff 2006). While there is evidence that topoisomerase IIα can function ahead of DNA tracking machinery during replication (Heintzman, Campos et al. 2019), it is believed to primarily function ahead of the fork and it is unclear where the IIβ isoform is located during replication (Heintzman, Campos et al. 2019). Taken together, these results indicate that the ability to recognize supercoil handedness during DNA relaxation resides in the C-terminus (McClendon, Dickey et al. 2006, McClendon and Osheroff 2006, McClendon, Gentry et al. 2008).

In bacteria, gyrase removes (+)SC DNA substantially faster than it generates (-)SCs in relaxed substrates (Aldred, McPherson et al. 2012, Ashley, Blower et al. 2017, Ashley, Dittmore

et al. 2017, Ashley, Lindsey et al. 2017). Bacterial topoisomerase IV, although primarily working behind replication forks as a decatenase, also preferentially removes (+)SC over (-)SC DNA (Ashley, Blower et al. 2017, Ashley, Dittmore et al. 2017). Elements in the C-terminal domains of bacterial enzymes explain the differences in ability to distinguish between supercoil handedness during DNA relaxation (Vos, Lee et al. 2013, Ashley, Blower et al. 2017, Ashley, Dittmore et al. 2017, Ashley and Osheroff 2019). When DNA substrate recognition and binding affinities were assessed based on supercoil handedness, gyrase from *E. coli* appeared to preferentially bind to (+)SC over (-)SC DNA, whereas topoisomerase IV did not discriminate (Ashley, Dittmore et al. 2017, Ashley and Osheroff 2019).

Catenation/Decatenation of Supercoiled DNA

In addition to recognition of DNA topology during relaxation of supercoils, type II topoisomerases can also preferentially decatenate (+)SC over (-)SC DNA (Baxter, Sen et al. 2011, Zawadzki, Stracy et al. 2015, Dalvie, Stacy et al. 2022). Previous studies in bacteria and yeast have suggested that DNA becomes positively supercoiled immediately prior to decatenation (Baxter, Sen et al. 2011, Zawadzki, Stracy et al. 2015). Given that formation of catenanes during processes such as DNA replication must be resolved for proper chromosome segregation during mitosis, catenated sister chromatids might be particularly susceptible to the dangers of cleavage complexes as the forces induced by the mitotic spindle have the potential to pull apart these structures, generating double-stranded breaks (Dalvie, Stacy et al. 2022). Human topoisomerase IIα was able to distinguish between different supercoiled states of DNA during the catenation reaction while topoisomerase IIβ was not. The α isoform was found to catenate relaxed and underwound molecules faster than it did overwound substrates, which was a result opposite that of relaxation

reactions (human topoisomerase IIα relaxes overwound substrates faster) (Dalvie, Stacy et al. 2022). In bacterial topoisomerase IV, (+)SC DNA was the preferred substrate for catenation (Dalvie, Stacy et al. 2022). However, as topoisomerase IV primarily functions behind replication forks, this behavior may help keep daughter chromosomes together until separation during anaphase. Comparing catenated with monomeric DNA, both human topoisomerase IIα and bacterial topoisomerase IV maintain lower levels of cleavage complexes with catenated substrates, which would allow these enzymes to perform their cellular functions in a safer manner (Dalvie, Stacy et al. 2022).

Cleavage of Supercoiled DNA

Type II topoisomerases can also recognize supercoil geometry during DNA cleavage (McClendon, Rodriguez et al. 2005, McClendon and Osheroff 2006, Gentry, Pitts et al. 2011, Vos, Lee et al. 2013, Ashley, Blower et al. 2017, Ashley, Dittmore et al. 2017, Gibson, Ashley et al. 2018, Gibson, Bax et al. 2019).

In humans, topoisomerase IIα and IIβ both maintain ~3-4-fold lower levels of cleavage complexes on (+)SC than (-)SC DNA (McClendon, Rodriguez et al. 2005, McClendon and Osheroff 2006). Given that (+)SCs accumulate ahead of replication forks and transcription complexes, this supercoil handedness preference during cleavage could help prevent the conversion of transiently-cleaved double-stranded DNA breaks into non-ligatable lesions in the genome. The studies on recognition of supercoil handedness during relaxation proposed that the functional differences could have also been attributable to differences in degrees of DNA scission (McClendon, Rodriguez et al. 2005, McClendon, Gentry et al. 2008). While this could have been the case for the IIα isoform, it did not explain the behavior of human topoisomerase IIβ

(McClendon, Rodriguez et al. 2005, McClendon and Osheroff 2006, McClendon, Gentry et al. 2008). Structurally, the ability to recognize supercoil handedness during the DNA cleavage reaction appeared to lie within the catalytic core region (Lindsey, Pendleton et al. 2014). Mutations in the catalytic core of human topoisomerase IIα reduced its ability to preferentially cleave (-)SC substrates (Lindsey, Pendleton et al. 2014). As with the experiments in bacteria, differences in rates of relaxation of supercoiled DNA did not correlate with differences in levels of cleavage. In other words, how type II enzymes discriminated between supercoil handedness during the DNA cleavage reaction could not necessarily explain differences in their respective abilities to relax supercoiled substrates.

In bacteria, gyrase maintains greater levels of cleavage complexes on (-)SC DNA than on (+)SC DNA, whereas topoisomerase IV shows no large difference in cleavage of (+)SC versus (-)SC DNA (Crisona, Strick et al. 2000, Stone, Bryant et al. 2003, Ashley, Blower et al. 2017, Ashley, Dittmore et al. 2017). These differences in DNA cleavage stand in contrast to the abilities of gyrase and topoisomerase IV to preferentially relax (+)SC. In biological systems, the ability of gyrase to quickly relax (+)SC DNA while maintaining lower levels of cleavage complexes supports its function to remove torsional stress, as it can safely work ahead of the replication fork and therefore is less likely to form non-ligatable DNA lesions. Topoisomerase IV does not discriminate between supercoil handedness as strongly during the DNA cleavage reaction, but as it primarily works behind the replication fork, it is less likely to be disrupted by DNA tracking systems (Ashley, Dittmore et al. 2017). The C-terminal domain for gyrase in most bacterial species, such as *E. coli* and *B. anthracis*, contributes to its ability to preferentially cleave (-)SC over (+)SC substrates (Ashley, Dittmore et al. 2017). However, it is the N-terminus of *M. tuberculosis* gyrase that confers supercoil recognition during the DNA cleavage reaction (Ashley,

Blower et al. 2017). The observation that bacterial type II topoisomerases preferentially relax (+)SC DNA therefore could not be explained by the differences in levels of scission during DNA cleavage.

Scope of the Dissertation

Although human and bacterial type II topoisomerases are important targets for anticancer and antibacterial drugs, respectively, much about the interactions between the enzymes, drugs that target them, and their DNA substrates remains unclear. The goal of this dissertation is to further investigate the mechanism of action and the basis behind the determination and preference of specific topological states of DNA by human and bacterial type II topoisomerases.

Chapter I provides an overview of DNA topology, human and bacterial type II topoisomerases, and topoisomerase-targeting drugs.

Chapter 2 provides an overview of the experimental materials and methods, and examines the basis for the preference for supercoil geometry during the DNA cleavage reaction. Previous studies have shown that certain type II topoisomerases cleave DNA substrates of a specific topological state better than they do others. (-)SC DNA is preferentially cleaved over (+)SC DNA by human type II topoisomerases and bacterial gyrase. Topoisomerase IV-mediated cleavage does not vary as substantially by supercoil handedness. Results shown in this chapter demonstrate that human topoisomerase IIα maintains more stable cleavage complexes with (-)SC over (+)SC DNA in the presence of drugs. Human topoisomerase IIβ does not discriminate supercoil handedness when maintaining stable cleavage complexes. Bacterial gyrase from *E. coli, B. anthracis,* and *M. tuberculosis* displays a pattern similar to that of human topoisomerase IIα. Bacterial topoisomerase IV does not maintain as stable cleavage complexes as gyrase, nor do the lifetimes of these

complexes vary by supercoil handedness. Rates of religation appear to play no substantial role in the ability to distinguish supercoil handedness during DNA cleavage in the absence or presence of drugs. Human topoisomerase IIα and IIβ, and bacterial gyrase generate higher levels of cleavage complexes with (-)SC over (+)SC DNA, at least in part, because they cleave the DNA more rapidly. Forward rates of topoisomerase IV-mediated cleavage do not vary by supercoil handedness. The results presented in this chapter have been published (Jian, McCarty, et al. 2023).

Chapter 3 discusses the conclusions and implications of the work presented in this dissertation.

CHAPTER TWO

BASIS FOR THE DISCRIMINATION OF SUPERCOIL HANDEDNESS DURING DNA CLEAVAGE BY TYPE II TOPOISOMERASES

Introduction

As discussed in Chapter 1, the formation of cleavage complexes by type II topoisomerases is an intrinsic threat to genomic stability (Levine, Hiasa et al. 1998, Deweese, Osheroff et al. 2008, Deweese and Osheroff 2009, Bax, Chan et al. 2010, Aldred, Kerns et al. 2014, Pendleton, Lindsey et al. 2014, Pommier, Sun et al. 2016, Ashley and Osheroff 2019). When nucleic acid processes such as replication and transcription begin, movement of DNA tracking machinery generates (+)SC DNA that need to be resolved. Given that cleavage complexes formed ahead of replication forks and transcription complexes can be converted into nonligatable DNA lesions by the approach of DNA tracking systems, complexes formed on (+)SC DNA are the most dangerous to the cell (Deweese and Osheroff 2009, Pendleton, Lindsey et al. 2014, Gibson, Ashley et al. 2018, Ashley and Osheroff 2019). The approaching DNA tracking systems render the type II enzymes incapable of ligating the DNA, resulting in fragmentation of the genome. Because of this potentially lethal property, type II topoisomerases are the targets for a variety of anticancer and antibacterial drugs (Baldwin and Osheroff 2005, Deweese, Osheroff et al. 2008, Deweese and Osheroff 2009, Nitiss 2009, Bax, Chan et al. 2010, Pommier, Leo et al. 2010, Aldred, Kerns et al. 2014, Pendleton, Lindsey et al. 2014, Pommier, Sun et al. 2016, Gibson, Ashley et al. 2018, Ashley and Osheroff 2019, Bax, Murshudov et al. 2019). As such, it is imperative to understand how type II topoisomerases recognize and interact with DNA substrates of different supercoil handedness.

Previous studies have shown that human and bacterial type II topoisomerases vary in their abilities to recognize supercoil handedness during the DNA cleavage reaction. Human topoisomerase IIα and topoisomerase IIβ, and bacterial gyrase preferentially cleave (-)SC over (+)SC DNA (McClendon, Rodriguez et al. 2005, McClendon and Osheroff 2006, Gentry, Pitts et al. 2011, Ashley, Blower et al. 2017, Ashley, Dittmore et al. 2017, Gibson, Bax et al. 2019). In contrast, bacterial topoisomerase IV does not differentiate supercoil handedness during cleavage (Ashley, Blower et al. 2017, Ashley, Dittmore et al. 2017). Despite these reports, the basis for the recognition of supercoil handedness during the DNA cleavage reaction is unclear. As such, the effects of DNA topology on the stability (i.e., lifetime), rates of enzyme-mediated DNA ligation, and rate of formation of cleavage complexes were examined. Results indicate that the forward rate of cleavage is the determining factor of how topoisomerase IIα, topoisomerase IIβ, gyrase, and topoisomerase IV distinguish supercoil handedness in the absence or presence of anticancer or antibacterial drugs. In the presence of drugs, this ability can be enhanced by the formation of more stable cleavage complexes between topoisomerase IIα or gyrase and (-)SC DNA. Finally, rates of enzyme-mediated DNA ligation do not contribute to the recognition of DNA supercoil geometry during cleavage. These results suggest that different type II topoisomerases may use different mechanisms to distinguish supercoil handedness during DNA cleavage.

METHODS

Enzymes

Recombinant human topoisomerase IIα and IIβ were expressed and purified from *Saccharomyces cerevisiae* by the protocol originally described for the isolation of the α isoform

(Worland and Wang 1989, Kingma, Greider et al. 1997). Enzymes were untagged and purified by size-exclusion column. Enzymes were stored in liquid N_2 in 50 mM Tris-HCl (pH 7.9), 0.1 mM NaEDTA, 750 mM KCl, and 40% (v/v) glycerol. *Escherichia coli* gyrase subunits GyrA and GyrB, and *Bacillus anthracis* gyrase subunits GyrA and GyrB were expressed and purified as previously described (Ashley, Dittmore et al. 2017). Untagged *E. coli* topoisomerase IV subunits (ParC and ParE) were expressed and purified using ion exchange chromatography as described by Peng and Marians (Peng and Marians 1993). *Bacillus anthracis* topoisomerase IV subunits (GrlA and GrlB) were expressed in *Escherichia coli* and purified using a C-terminal His-tag as described by Dong *et al* (Dong, McPherson et al. 2010). *M. tuberculosis* gyrase subunits (GyrA and GyrB) were expressed and purified as previously described (Ashley, Blower et al. 2017). Enzymes were stored at -80 °C in 40 mM HEPES-KOH (pH 7.6), 1 mM NaEDTA, 150 mM KGlu, and 40% (v/v) glycerol.

DNA Substrates

Negatively supercoiled pBR322 and pUC18 plasmid DNA were prepared from *E. coli* using a Plasmid Mega Kit (Qiagen) as described by the manufacturer. Relaxed pBR322 plasmid DNA was generated by treating (-)SC pBR322 DNA with calf thymus topoisomerase I (Invitrogen) in 10 mM Tris-HCl (pH 7.5), 10 mM KCl, 2 mM $MgCl_2$, 0.1 mM DTT, 0.02 mM EDTA, and 6 µg/ml bovine serum albumin (BSA) and purified as described previously (Fortune, Velea et al. 1999).

Positively supercoiled plasmid DNA was prepared by treating (-)SC DNA with recombinant *Archaeoglobus fulgidus* reverse gyrase as described previously (McClendon, Rodriguez et al. 2005). Briefly, reaction mixtures contained 35 nM (-)SC pBR322 or pUC18 DNA and 420 nM reverse gyrase in a total of 500 µl of 50 mM Tris-HCl (pH 8.0), 10 mM NaCl, 10 mM $MgCl_2$, and

1 mM ATP. Reactions were incubated at 95°C for 10 min, stopped by the addition of 20 µl of 250 mM Na_2EDTA, and cooled on ice. 5 µl Proteinase K (Affymetrix, 8 mg/ml) was added and reactions were incubated at 45°C for 30 min to digest the enzyme. Samples were extracted with phenol:chloroform:isoamyl alcohol (25:24:1), and DNA was precipitated with 100% ice-cold ethanol. Plasmids were resuspended in 50 µl of 5 mM Tris (pH 8.0), 0.5 mM EDTA (pH 8.0) and were purified using Bio-Spin P-30 gel columns (Bio-Rad, #7326231). Eluted samples were assessed for purity by the A260/A280 absorbance ratio using a spectrophotometer. To ensure that differences between (-)SC and (+)SC DNA substrates were not influenced by temperature or other conditions used in the preparation protocol, (-)SC plasmid substrates were treated in parallel with the omission of reverse gyrase.

Drugs

Etoposide was obtained from Sigma and was stored at 4°C as a 20 mM stock solution in 100% DMSO. F14512 was a gift from Christian Bally and was stored at -20°C as a 20 mM stock solution in 100% DMSO. Ciprofloxacin was obtained from LKT and was stored at 4°C as a 40 mM stock solution in 0.1 N NaOH. All chemicals were analytical reagent grade.

DNA Cleavage

DNA cleavage assays with human type II topoisomerases were performed using the procedure of Fortune and Osheroff (Fortune, Velea et al. 1999). Reaction mixtures contained 0-200 µM etoposide or F14512, 110 nM topoisomerase IIα or topoisomerase IIβ, and 10 nM (-)SC, (+)SC, or relaxed pBR322 DNA in a total of 20 µl of 10 mM Tris-HCl (pH 7.9), 100 mM KCl, 0.1 mM EDTA, 5 mM $MgCl_2$, and 2.5% glycerol (v/v). Reactions were incubated at 37 ºC for 6 min.

Reactions with bacterial type II topoisomerases contained 0-200 μM ciprofloxacin. DNA cleavage assays with *E. coli* gyrase or topoisomerase IV were carried out as described previously (Aldred, Breland et al. 2014, Ashley, Dittmore et al. 2017). Assay mixtures contained 10 nM (-)SC, (+)SCS, or relaxed pBR322 DNA and 100 nM *E. coli* gyrase (1:1 GyrA:GyrB ratio) or 20 nM topoisomerase IV (1:1 ParC:ParE ratio) in 20 μl of 40 mM Tris-HCl (pH 7.9), 50 mM NaCl, 5 mM $MgCl_2$ and 2.5% glycerol (v/v). The stated enzyme concentration reflects that of the holoenzyme (A_2B_2). Reactions were incubated at 37 ºC for 20 or 10 min for gyrase or topoisomerase IV, respectively.

DNA cleavage assays with *B. anthracis* gyrase and topoisomerase IV were carried out as described previously (Aldred, McPherson et al. 2012, Ashley, Dittmore et al. 2017). Assay mixtures for *B. anthracis* gyrase contained 500 nM enzyme (1:2 GyrA:GyrB ratio) in 20 μl of 50 mM Tris-HCl (pH 7.5), 100 mM potassium glutamate (KGlu), 5 mM $MgCl_2$, 5 mM dithiothreitol (DTT) and 50 μg/ml BSA. The stated enzyme concentration reflects that of the holoenzyme (A_2B_2). Assay mixtures for *B. anthracis* topoisomerase IV contained 150 nM enzyme (1:2 GrlA:GrlB ratio) in 40 mM Tris-HCl (pH 7.9), 50 mM NaCl, 5 mM $MgCl_2$ and 2.5% glycerol (v/v). Reactions were incubated at 37 ºC for 30 or 10 min for gyrase or topoisomerase IV, respectively.

DNA cleavage assays with *M. tuberculosis* gyrase were carried out as previously described (Aldred, Blower et al. 2016, Ashley, Blower et al. 2017, Gibson, Blower et al. 2018). Assay mixtures contained 100 nM *M. tuberculosis* gyrase (1.5:1 GyrA:GyrB ratio) in 20 μl of 10 mM Tris-HCl (pH 7.5), 40 mM KCl, 6 mM $MgCl_2$, 0.1 mg/ml BSA, and 10% glycerol (v/v). The stated enzyme concentration reflects that of the holoenzyme (A_2B_2). Reactions were incubated 37 ºC for 10 min.

For all reactions, DNA cleavage intermediates were trapped by the addition of 2 µl of 5% sodium dodecyl sulfate (SDS) followed by 2 µl of 250 mM Na_2EDTA (pH 8.0). Reaction mixtures were digested with 2 µl of proteinase K and incubated at 45°C for 30 min to digest the topoisomerases. Samples were mixed with 2 µl of 60% sucrose (w/v), 10 mM Tris-HCl (pH 7.9), 0.5% bromophenol blue, and 0.5% xylene cyanole FF, heated at 45°C for 2 min, and subjected to electrophoresis in 1% agarose gels in 40 mM Tris-acetate (pH 8.3) and 2 mM EDTA containing 0.5 µg/ml ethidium bromide. DNA bands were visualized with medium-range ultraviolet light and quantified using a Protein Simple digital imaging system. Levels of double-stranded DNA cleavage were monitored by the conversion of circular plasmid to linear molecules.

Rates of DNA cleavage were determined as described above over a 0–10 min time course. However, shorter reaction times (0–60 s) required the use of a rapid-quench flow (RQF-3) apparatus (KinTek, Snow Shoe, PA). The RQF-3 is a rapid mixing device that operates by first pushing equal volumes of two reaction mixtures into an internal chamber. The combined solution is allowed to incubate for a predetermined period of time, prior to dilution in quench solution and expulsion from the apparatus. In these reactions, the first solution contained the DNA substrate, drug, and buffer, while the second solution contained the enzyme and buffer. Reaction mixtures were incubated across a 0–60 s time course at 37 °C and quenched using 2% SDS. Resulting samples were expelled into collection vials, processed, analyzed by gel electrophoresis, and quantified using digital imaging as described above.

Half-lives (i.e. $t_{1/2}$ values) were determined by GraphPad Prism. $T_{1/2}$ values were calculated based on the loss of the linear, doubly cleaved DNA band, and were fitted to a one-phase decay, nonlinear regression.

Persistence of Topoisomerase-DNA Cleavage Complexes

DNA persistence assays were carried out for both human and bacterial type II enzymes as previously described (Gentry, Pitts et al. 2011, Ashley, Blower et al. 2017, Ashley, Dittmore et al. 2017). For all enzymes, DNA cleavage/religation equilibria were established in the buffers described above at 37 ºC at the given times. However, enzyme and DNA concentrations were five times higher than indicated in cleavage assays to increase baseline visualization. Assays with human topoisomerase IIα and topoisomerase IIβ were carried out in the absence of drug or in the presence of 100 μM etoposide or 20 μM F14512. Assays with bacterial gyrase or topoisomerase IV were carried out in the absence of drug or in the presence of 100 μM ciprofloxacin. Following the establishment of DNA cleavage/religation equilibria, samples were diluted 20-fold with the appropriate assay buffer (see above) that lacked divalent cations and were further incubated at 37 ºC. Samples were removed at times up to 2 h and cleavage complexes were trapped, processed, and analyzed by gel electrophoresis as described earlier. Levels of linear DNA cleavage products were set to 100% at time zero, and the persistence of cleavage complexes was determined by the decay of the linear DNA product over time.

Because of the rapidity by which topoisomerase-DNA cleavage complexes disassemble in the absence of drug, persistence assays that utilized a rapid-quench approach were necessary to determine the lifetime of enzyme-DNA cleavage complexes that lacked drugs. Experiments were performed at 37 °C using a KinTek rapid-quench apparatus with some modifications. Cleavage/religation equilibria were initiated as described in the rapid-quench section above. Because of machine constraints, samples were diluted 5-fold (rather than the 20-fold dilution in benchtop experiments) with buffer that lacked divalent cation. After a predetermined period of time, the mixture was expelled and cleavage complexes were trapped using 5% SDS, processed,

analyzed by gel electrophoresis, and quantified using digital imaging as described above. Half-lives (i.e. $t_{1/2}$ values) were determined by GraphPad Prism software. $T_{1/2}$ values were calculated based on the loss of the linear, doubly cleaved DNA band, and were fitted to a one-phase decay, nonlinear regression.

DNA Religation

DNA religation assays were carried out as previously described (McClendon and Osheroff 2006, Aldred, McPherson et al. 2012, Ashley, Dittmore et al. 2017). For all enzymes, DNA cleavage/religation equilibria were established in the buffers described above at 37 ºC at the given time points. Assays with human topoisomerase IIα and IIβ were carried out in the absence of drug or in the presence of 100 μM etoposide. Assays with bacterial gyrase or topoisomerase IV were carried out in the absence of drug or in the presence of 100 μM ciprofloxacin. Following the establishment of DNA cleavage/religation equilibria, DNA religation was initiated by shifting samples from 37 to 0 °C to permit ligation but prevent further cleavage. In all cases, reactions were stopped at time points up to 120 s by the addition of 2 μl of 5% SDS. Samples were processed, analyzed by gel electrophoresis, and quantified using digital imaging as described above.

RESULTS

Effects of supercoil handedness on DNA cleavage mediated by type II topoisomerases and the persistence of cleavage complexes

Although type II topoisomerases must generate double-stranded DNA breaks to carry out their catalytic functions, the presence of covalent enzyme-cleaved DNA complexes in the genome has potentially negative ramifications (Levine, Hiasa et al. 1998, Deweese, Osheroff et al. 2008, Deweese and Osheroff 2009, Nitiss 2009, Bax, Chan et al. 2010, Aldred, Kerns et al. 2014, Pendleton, Lindsey et al. 2014, Pommier, Sun et al. 2016, Gibson, Ashley et al. 2018, Ashley and Osheroff 2019, Bax, Murshudov et al. 2019, Vann, Oviatt et al. 2021). Because cleavage complexes formed with (+)SC DNA are more likely to encounter DNA tracking systems and be converted to non-ligatable DNA breaks, they may be intrinsically more lethal than complexes formed with (-)SC DNA (Levine, Hiasa et al. 1998, Deweese, Osheroff et al. 2008, Deweese and Osheroff 2009, Nitiss 2009, Bax, Chan et al. 2010, Aldred, Kerns et al. 2014, Pendleton, Lindsey et al. 2014, Pommier, Sun et al. 2016, Gibson, Ashley et al. 2018, Ashley and Osheroff 2019, Bax, Murshudov et al. 2019, Vann, Oviatt et al. 2021). Consequently, it is important to characterize the effects of DNA supercoil handedness on the formation and stability of topoisomerase-DNA cleavage complexes.

As a first step in this characterization, the intrinsic ability of different type II topoisomerases to cleave (-)SC and (+)SC DNA was assessed. In order to maintain the superhelicity of DNA throughout the cleavage reaction, assays were carried out in the absence of ATP. Under these conditions, strand passage does not take place (Deweese, Osheroff et al. 2008, Deweese and Osheroff 2009, Vos, Tretter et al. 2011, Chen, Chan et al. 2013, Ashley and Osheroff

2019, McKie, Neuman et al. 2021) and topoisomerase-mediated DNA cleavage can be simplified to the following equation:

$$E + S \underset{k_{-1}}{\overset{k_1}{\rightleftharpoons}} E{\bullet}S \underset{k_{-2}}{\overset{k_2}{\rightleftharpoons}} E{-}S^*$$

In this equation, E represents the enzyme, S represents the DNA substrate of different superhelical handedness, E•S represents the non-covalent enzyme•DNA complex, and E–S* represents the covalent enzyme-cleaved DNA complex. Levels of DNA cleavage at equilibrium can be affected by changes in any of the reaction steps (k_1, rate of enzyme•DNA association; k_{-1}, rate of enzyme•DNA dissociation; k_2, rate of DNA cleavage; k_{-2}, rate of DNA religation).

The results of DNA cleavage assays are shown in Figures 2.1 and 2.2. Consistent with previous reports (McClendon, Rodriguez et al. 2005, McClendon and Osheroff 2006, Lindsey, Pendleton et al. 2014, Ashley, Blower et al. 2017, Ashley, Dittmore et al. 2017), human topoisomerase IIα and IIβ, as well as gyrase from *E. coli, B. anthracis,* and *M. tuberculosis* all maintain ~2- to 4-fold higher levels of DNA cleavage with (-)SC over (+)SC pBR322 (top panel). Conversely, topoisomerase IV from *E. coli* and *B. anthracis* displayed less ability to distinguish supercoil handedness [~1.2- to 1.3-fold higher cleavage with (-)SC pBR322].

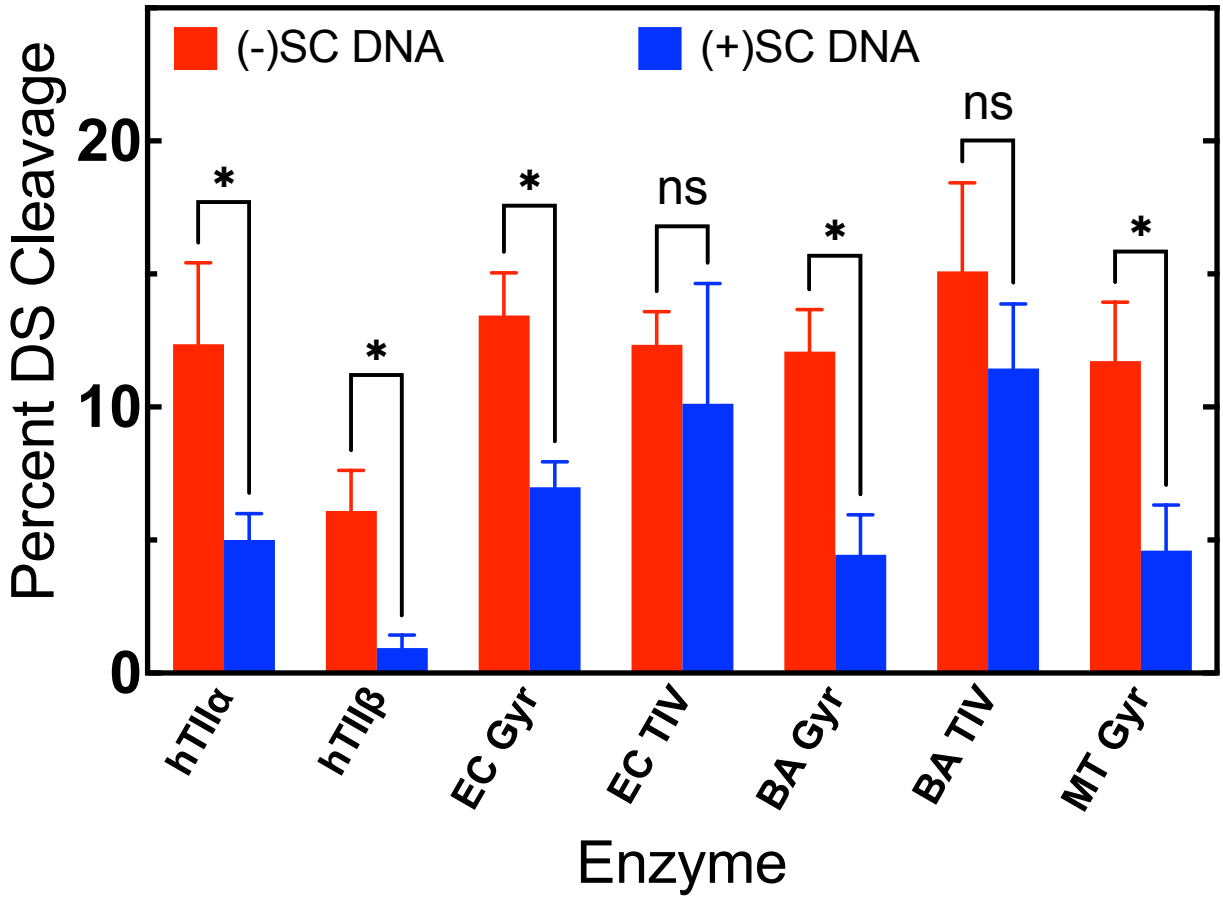

Figure 2.1. Effects of supercoil geometry on DNA cleavage mediated by type II topoisomerases in the absence of drugs. DNA cleavage mediated by human topoisomerase IIα (hTIIα) and IIβ (hTIIβ), *E. coli* gyrase (EC Gyr) and topoisomerase IV (EC TIV), *B. anthracis* gyrase (BA Gyr) and topoisomerase IV (BA TIV), and *M. tuberculosis* gyrase (MTs Gyr) with (-)SC (red) or (+)SC (blue) DNA are shown. Error bars represent the standard deviation of at least three independent assays. Significance was determined using a Student's t-test. Asterisks represents a p-value < 0.05; ns = not significant.

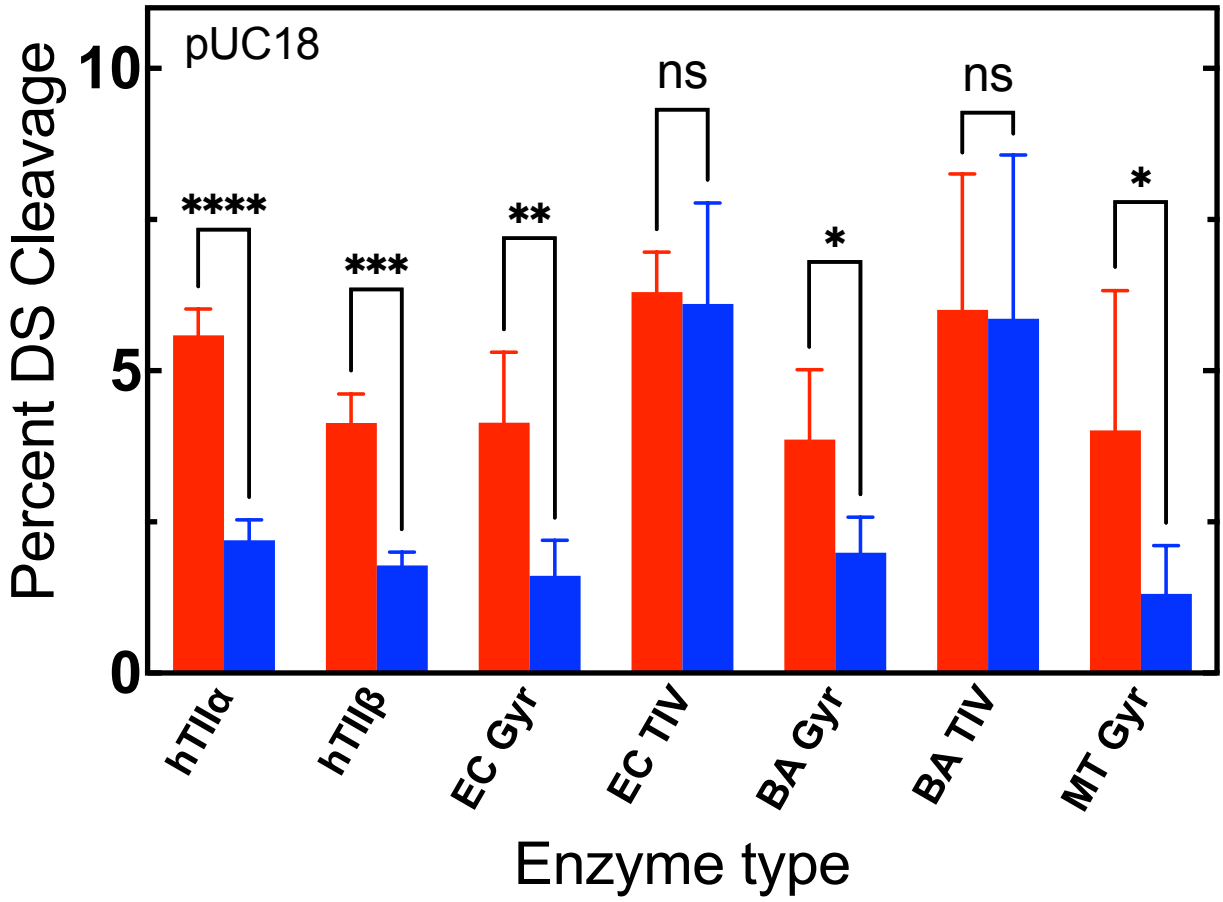

Figure 2.2. Effects of pUC18 supercoil geometry on DNA cleavage mediated by type II topoisomerases in the absence of drugs. DNA cleavage mediated by human topoisomerase IIα (hTIIα) and IIβ (hTIIβ), *E. coli* gyrase (EC Gyr) and topoisomerase IV (EC TIV), *B. anthracis* gyrase (BA Gyr) and topoisomerase IV (BA TIV), and *M. tuberculosis* gyrase (MTs Gyr) with (-)SC (red) or (+)SC (blue) pUC18 DNA are shown. Error bars represent the standard deviation of at least three independent assays. Significance was determined using a Student's t-test. Asterisks represents a p-value < 0.05; ns = not significant.

Similar results were observed comparing enzyme activity with (-)SC and (+)SC pUC18 (Figure 2.2). This latter plasmid is considerably smaller than pBR322 (2686 bp vs 4361 bp, respectively), demonstrating that the recognition of supercoil handedness by type II topoisomerases is consistent with plasmids of different sizes and sequences. Furthermore, the ability of human topoisomerase IIα and IIβ, and gyrase from *E. coli*, *B. anthracis*, and *M. tuberculosis* to distinguish the handedness of DNA supercoils during cleavage holds true over a range (4- to 10-fold) of enzyme concentrations (McClendon, Rodriguez et al. 2005, McClendon and Osheroff 2006, Lindsey, Pendleton et al. 2014, Ashley, Blower et al. 2017, Ashley, Dittmore et al. 2017). Conversely, over a twenty-fold range that was examined (20–400 nM enzyme), *E. coli* and *B. anthracis* topoisomerase IV displayed similar levels of DNA cleavage with (-)SC and (+)SC pBR322 (data not shown).

To investigate the basis for the differential effects of supercoil handedness on DNA cleavage, a series of experiments was carried out that examined individual steps in the DNA cleavage-religation equation shown above. In the first series, a persistence assay was used to monitor the stability of total enzyme-DNA complexes (E•S + E–S*) formed by type II topoisomerases with (-)SC or (+)SC DNA (Bandele and Osheroff 2008, Gentry, Pitts et al. 2011, Ashley, Blower et al. 2017, Ashley, Dittmore et al. 2017). In this assay, enzyme-DNA complexes are allowed to come to a cleavage/religation equilibrium, and then diluted in buffer that lacks the essential divalent cation. Under these conditions, the DNA cleavage-religation equilibrium is relatively unaffected because it is zero-order and the catalytic divalent cations that are required for cutting and rejoining of the DNA substrate do not leave the complex (Osheroff 1987). However, following dilution and the decreased concentration of the divalent cation, enzyme•DNA complexes that dissociate are unlikely to reform. Thus, the conditions used in the persistence assay block the

k_1 step. Although the readout for the persistence assay is the loss of the covalent enzyme-cleaved DNA complex (E–S*) as monitored by the decrease of double-stranded DNA breaks (i.e., the linear DNA band), we propose that the assay reflects the lifetime of all the enzyme-DNA complexes (E•S + E–S*) and is comprised of a combination of k_{-1}, k_2, and k_{-2} (Bandele and Osheroff 2008) as shown below.

$$E + S \underset{k_{-1}}{\overset{\cancel{k_1}}{\rightleftharpoons}} E{\bullet}S \underset{k_{-2}}{\overset{k_2}{\rightleftharpoons}} E\text{–}S^*$$

Under the conditions of the persistence assay, in the absence of anticancer or antibacterial drugs, cleavage complexes (E–S*) displayed poor stability and levels of double-stranded breaks decreased rapidly within the first few seconds of the assay (Figures 2.3–2.6). With all enzymes, the concentration of cleavage complexes dropped to ~10% by 5 s, which was the first time point that could be reliably measured at the benchtop. An example is shown for human topoisomerase IIα Figure 2.3, left panel. This short lifetime of cleavage complexes confounded our ability to compare the persistence of cleavage complexes with (-)SC vs (+)SC substrates in the absence of drugs. Therefore, a rapid-quench kinetic system was used to track persistence over time periods as short as 50 ms (Figure 2.3, insets). For all enzymes examined, irrespective of whether they were able to distinguish supercoil handedness during cleavage, very little difference in persistence was observed in reactions that compared (-)SC vs (+)SC DNA (Figures 2.3–2.6, table 2.1). Therefore, in the absence of drugs, the intrinsic ability of human and bacterial type II topoisomerases to discern supercoil handedness during DNA cleavage is not caused by parallel changes in the lifetime of enzyme-DNA complexes (Figures 2.3-2.6, Table 2.1).

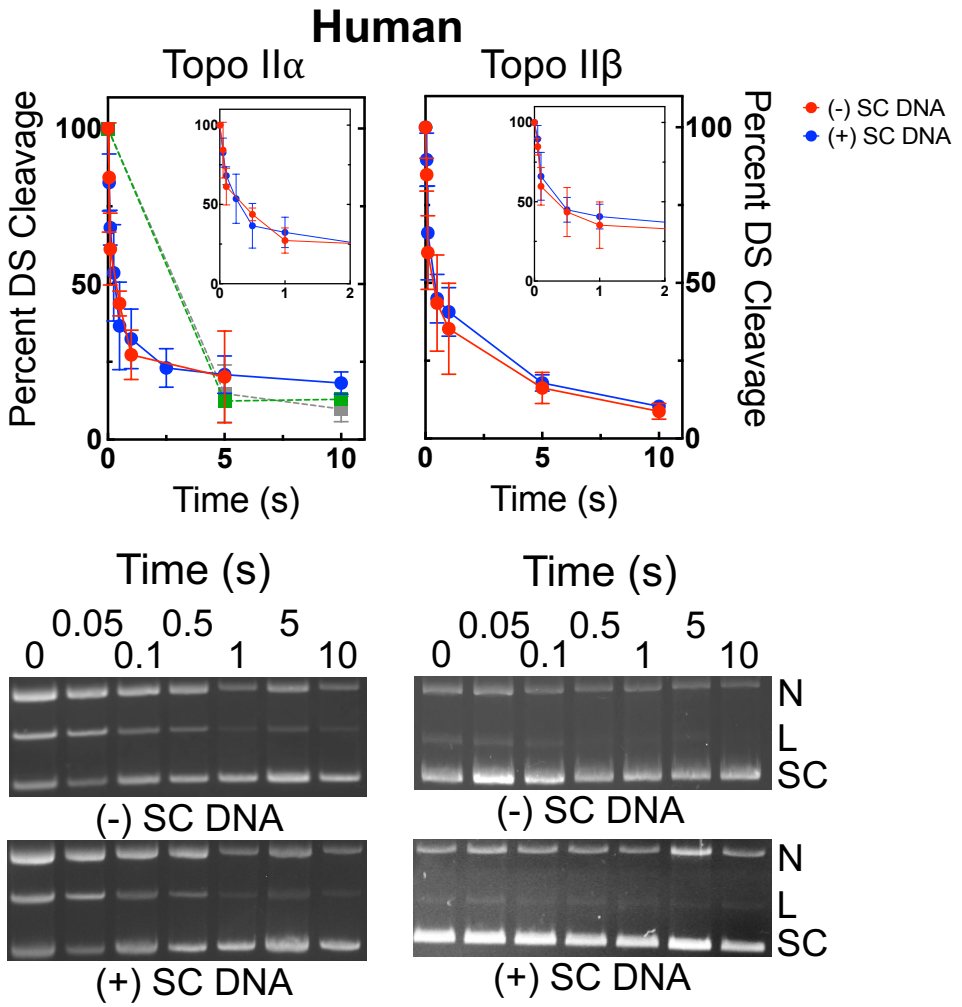

Figure 2.3. Effects of supercoil geometry on the persistence of DNA cleavage complexes generated by human type II topoisomerases in the absence of drugs. Persistence of DNA cleavage complexes generated by human topoisomerase IIα (Topo IIα, left) and topoisomerase IIβ (Topo IIβ, right) with (-)SC (red) or (+)SC (blue) pBR322 DNA are shown. The green and gray dashed lines shown in the panel with Topo IIα represent benchtop assays with (-)SC and (+)SC DNA, respectively. All other data shown were generated by rapid-quench flow assays. Representative gel images for human topoisomerase IIα and IIβ with (-)SC or (+)SC DNA are shown. The positions of supercoiled (SC), nicked (N), and linear (L) DNA are indicated. The control DNA substrate is marked (Ctrl). Insets show expanded time courses up to 2 s. Error bars represent the standard deviation of at least three independent assays. $T_{1/2}$ values are displayed in Table 2.1.

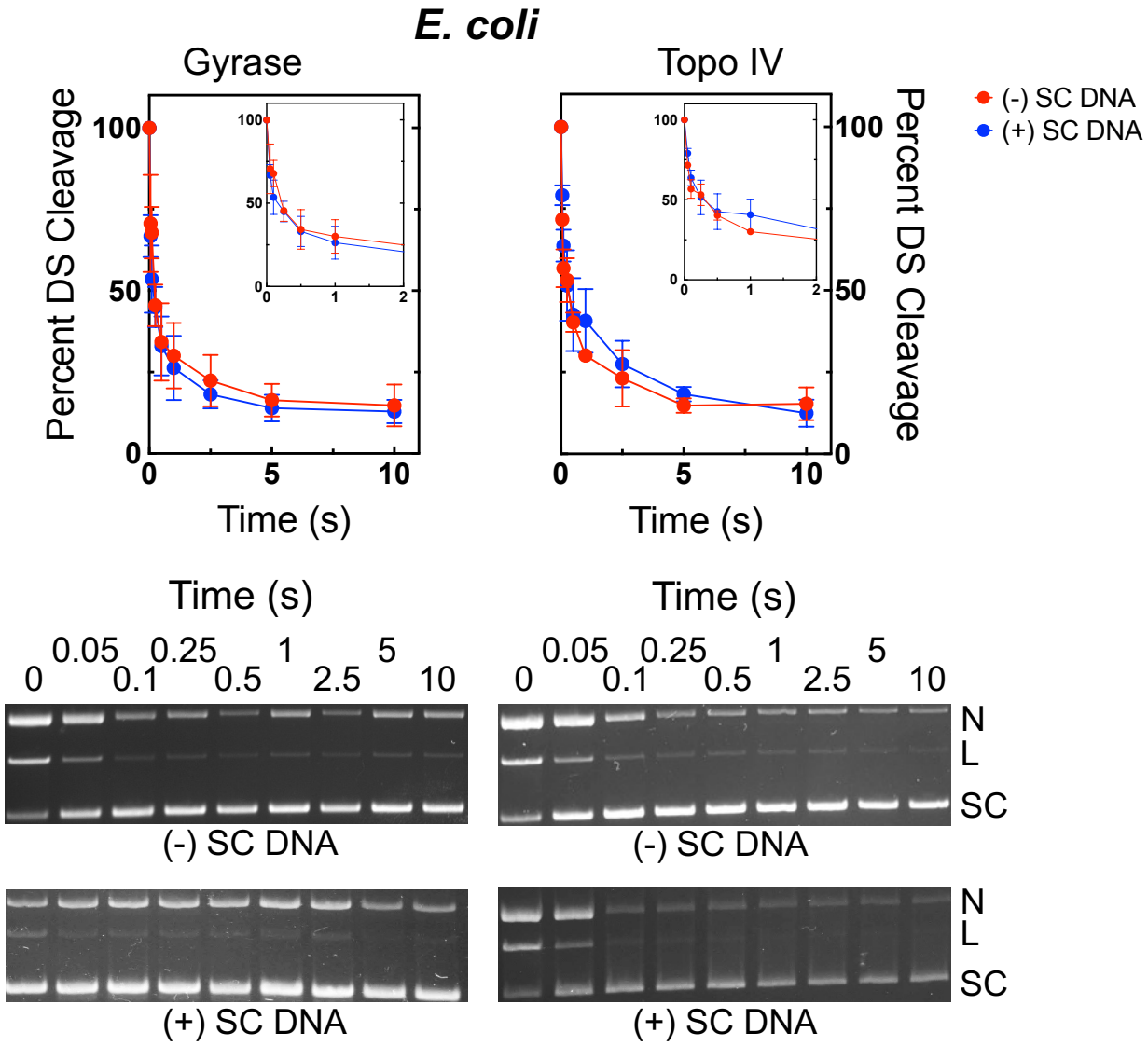

Figure 2.4. Effects of supercoil geometry on the persistence of DNA cleavage complexes generated by *E. coli* type II topoisomerases in the absence of drugs. Persistence of DNA cleavage complexes generated by *E. coli* gyrase (left) and topoisomerase IV (Topo IV, right) with (-)SC (red) or (+)SC (blue) pBR322 DNA are shown. All data shown were generated by rapid-quench flow assays. Representative gel images for *E. coli* gyrase and topoisomerase IV with (-)SC or (+)SC DNA are shown. The positions of supercoiled (SC), nicked (N), and linear (L) DNA are indicated. Insets show expanded time courses up to 2 s. Error bars represent the standard deviation of at least three independent assays. $T_{1/2}$ values are displayed in Table 2.1.

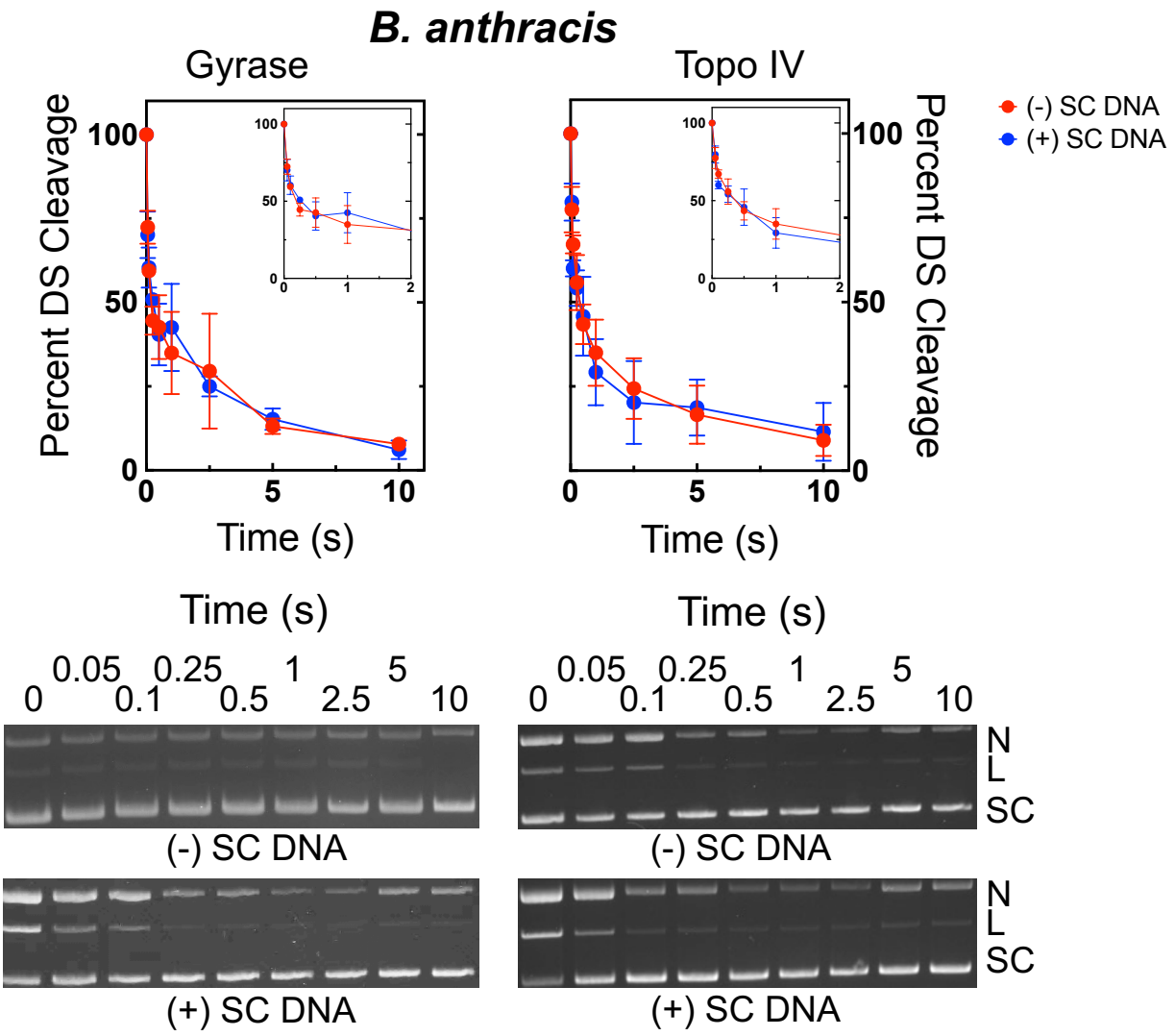

Figure 2.5. Effects of supercoil geometry on the persistence of DNA cleavage complexes generated by *B. anthracis* type II topoisomerases in the absence of drugs. Persistence of DNA cleavage complexes generated by *B. anthracis* gyrase (left) and topoisomerase IV (Topo IV, right) with (-)SC (red) or (+)SC (blue) pBR322 DNA are shown. All data shown were generated by rapid-quench flow assays. Representative gel images for *B. anthracis* gyrase and topoisomerase IV with (-)SC or (+)SC DNA are shown. The positions of supercoiled (SC), nicked (N), and linear (L) DNA are indicated. Insets show expanded time courses up to 2 s. Error bars represent the standard deviation of at least three independent assays. $T_{1/2}$ values are displayed in Table 2.1.

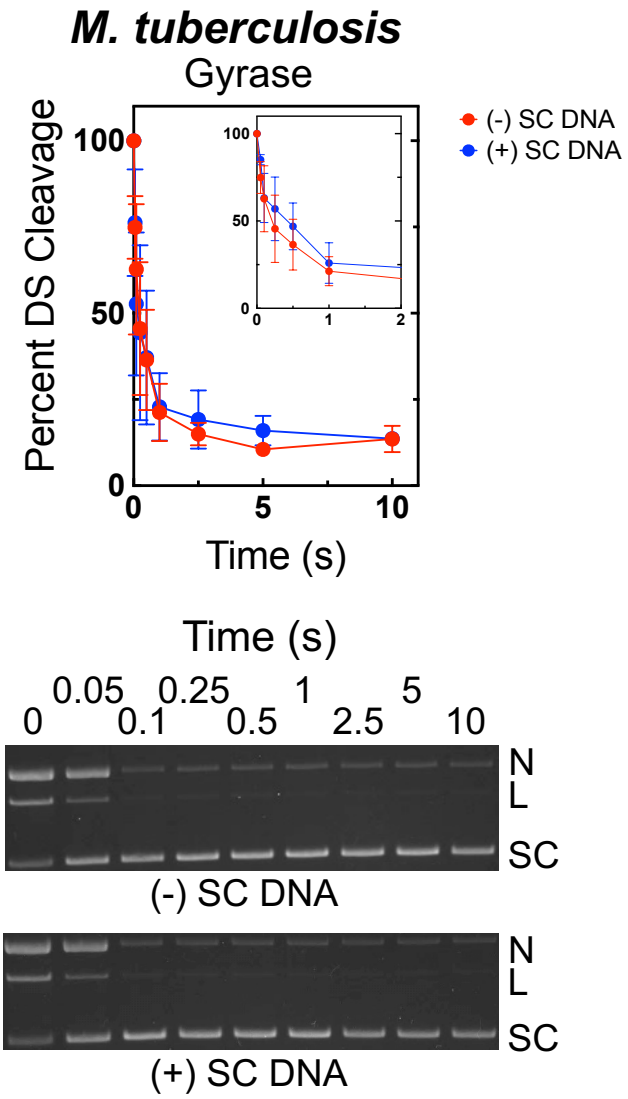

Figure 2.6. Effects of supercoil geometry on the persistence of DNA cleavage complexes generated by *M. tuberculosis* type II topoisomerases in the absence of drugs. Persistence of DNA cleavage complexes generated by *M. tuberculosis* gyrase with (-)SC (red) or (+)SC (blue) pBR322 DNA are shown. All data shown were generated by rapid-quench flow assays. Representative gel images for *M. tuberculosis* gyrase with (-)SC or (+)SC DNA are shown. The positions of supercoiled (SC), nicked (N), and linear (L) DNA are indicated. Insets show expanded time courses up to 2 s. Error bars represent the standard deviation of at least three independent assays. $T_{1/2}$ values are displayed in Table 2.1.

Species	Enzyme	DNA Type	$T_{1/2}$ (s)
Human	IIα	(-) SC	0.15
		(+) SC	0.19
Human	IIβ	(-) SC	0.37
		(+) SC	0.41
E. coli	Gyrase	(-) SC	0.16
		(+) SC	0.13
E. coli	Topo IV	(-) SC	0.21
		(+) SC	0.22
B. anthracis	Gyrase	(-) SC	0.16
		(+) SC	0.30
B. anthracis	Topo IV	(-) SC	0.31
		(+) SC	0.28
M. tuberculosis	Gyrase	(-) SC	0.19
		(+) SC	0.13

Table 2.1: $T_{1/2}$ values for Figures 2.3–2.6

Table 2.1. Effects of supercoil geometry on the lifetime of cleavage complexes generated by human and bacterial type II topoisomerases in the absence of stabilizing drugs. Lifetime of cleavage complexes (represented by $T_{1/2}$) by human IIα and human topoisomerase IIβ, and *E. coli*, *B. anthracis*, and *M. tuberculosis* gyrase and topoisomerase IV with (-)SC (red) or (+)SC (blue) DNA in the absence of stabilizing drugs are shown.

With all enzymes, the concentration of cleavage complexes dropped to ~10% by 5 s, which was the first time point that could be reliably measured at the benchtop. An example is shown for human topoisomerase IIα Figure 2.3, left panel. This rapid dissociation of cleavage complexes confounded our ability to compare the persistence of cleavage complexes with (-)SC vs (+)SC substrates in the absence of drugs. Therefore, a rapid-quench kinetic system was used to track persistence over time periods as short as 50 ms (Figures 2.3-2.6, insets). For all enzymes examined, irrespective of whether they were able to distinguish supercoil handedness during cleavage, very little difference in persistence was observed in reactions that compared (-)SC vs (+)SC DNA (Figures 2.3-2.6, table 2.1). Therefore, in the absence of drugs, the intrinsic ability of human and bacterial type II topoisomerases to discern supercoil handedness during DNA cleavage is not caused by parallel changes in the lifetime of enzyme-DNA complexes.

Effects of supercoil handedness on DNA cleavage mediated by human type II topoisomerases and the persistence of total enzyme-DNA cleavage complexes in the presence of anticancer drugs

Many clinically relevant anticancer and antibacterial drugs that target type II topoisomerases act by increasing levels of enzyme-DNA cleavage complexes (Levine, Hiasa et al. 1998, Deweese, Osheroff et al. 2008, Deweese and Osheroff 2009, Nitiss 2009, Bax, Chan et al. 2010, Aldred, Kerns et al. 2014, Pendleton, Lindsey et al. 2014, Pommier, Sun et al. 2016, Gibson, Ashley et al. 2018, Ashley and Osheroff 2019, Bax, Murshudov et al. 2019, Vann, Oviatt et al. 2021). Previous studies with human topoisomerase IIα and IIβ suggest that, all else being equal, drugs that form the most stable cleavage complexes are the most lethal (Bandele and Osheroff 2008, Deweese and Osheroff 2009, Austin, Lee et al. 2018, Vann, Oviatt et al. 2021). Therefore,

the effects of supercoil handedness on the persistence of total enzyme-DNA complexes (E•S + E–S*) formed in the presence of drugs were assessed (as above) by monitoring the lifetime of cleavage complexes under the conditions of the assay.

Initial studies focused on the effects of etoposide and its derivative, F14512, on human topoisomerase IIα and IIβ (Figures 2.7–2.10). This compound was developed to be used to treat cancers with active polyamine transport systems (Barret, Kruczynski et al. 2008), but also was found to be considerably more potent than etoposide against the human type II topoisomerases (Gentry, Pitts et al. 2011). Both of these drugs generated ~2- to 5-fold higher levels of cleavage with (-)SC over (+)SC DNA (Figures 2.7–2.10; cleavage panels). For topoisomerase IIα, this enhanced scission was accompanied by a greater stability of cleavage complexes formed with (-)SC DNA (Figures 2.7 and 2.9, persistence panels; table 2.2). This was not the case for topoisomerase IIβ; the stability of cleavage complexes formed with (-)SC and (+)SC DNA were similar (Figures 2.8 and 2.10, persistence panels; table 2.2). The basis for the differences between the two isoforms is not known. However, it could be related to the lower overall stability of cleavage complexes formed by topoisomerase IIβ (Figures 2.8 and 2.10)(Willmore, Frank et al. 1998, Bandele and Osheroff 2008). Additional experiments were carried out with relaxed DNA substrates in the presence of etoposide. For both isoforms, results with relaxed DNA were similar to those with (+)SC molecules (Figures 2.7–2.8, table 2.2).

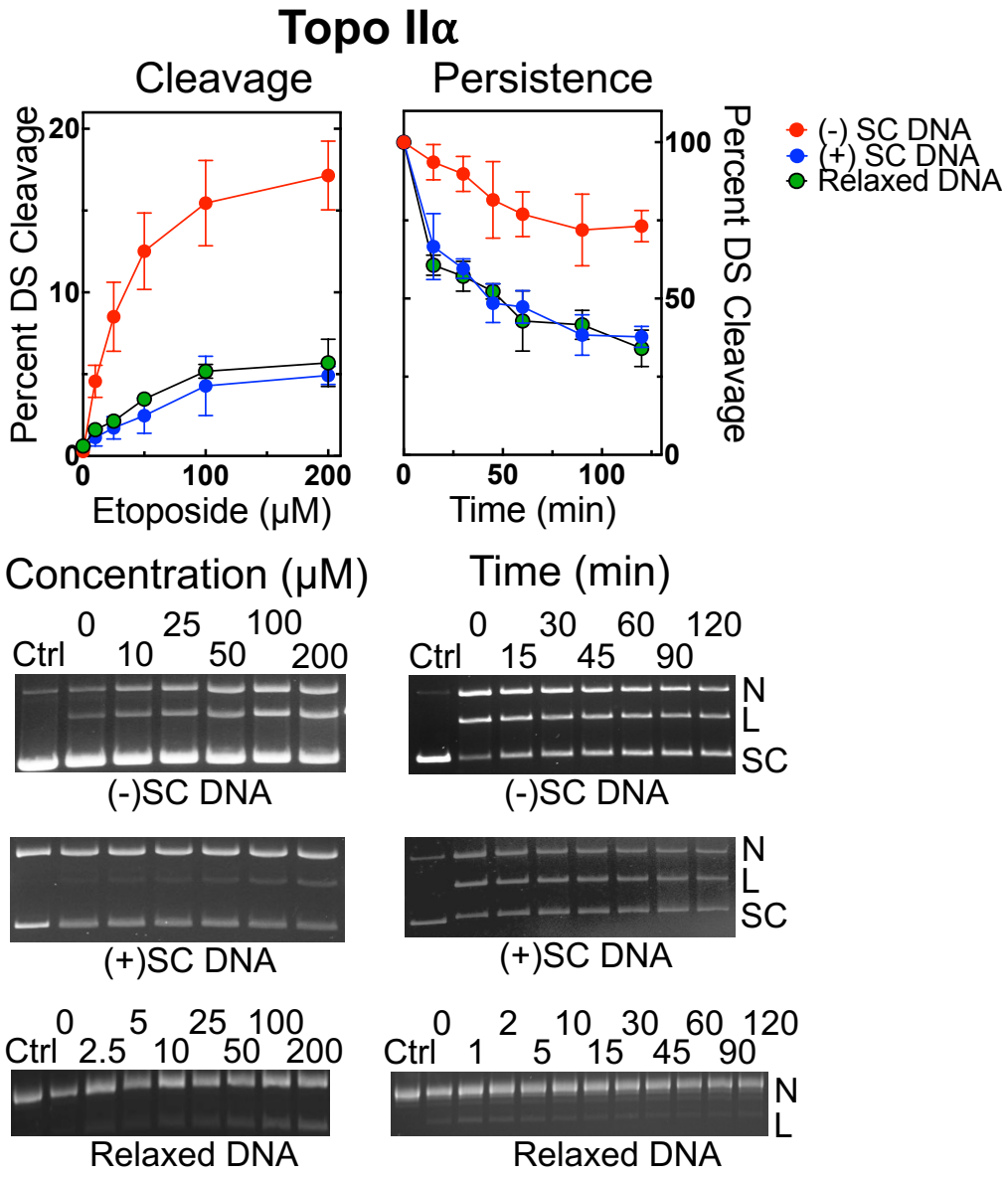

Figure 2.7. Effects of supercoil geometry on DNA cleavage and the persistence of cleavage complexes generated by human topoisomerase IIα in the presence of etoposide. DNA cleavage and the persistence of cleavage complexes by human topoisomerase IIα (Topo IIα) with (-)SC (red), (+)SC (blue), or relaxed pBR322 DNA (green) in the presence of 100 μM etoposide are shown. Representative gel images for human topoisomerase IIα-mediated cleavage and persistence with (-)SC, (+)SC, or relaxed DNA are shown. The positions of supercoiled (SC), nicked (N), and linear (L) DNA are indicated. Error bars represent the standard deviation of at least three independent assays. $T_{1/2}$ values are displayed in Table 2.2.

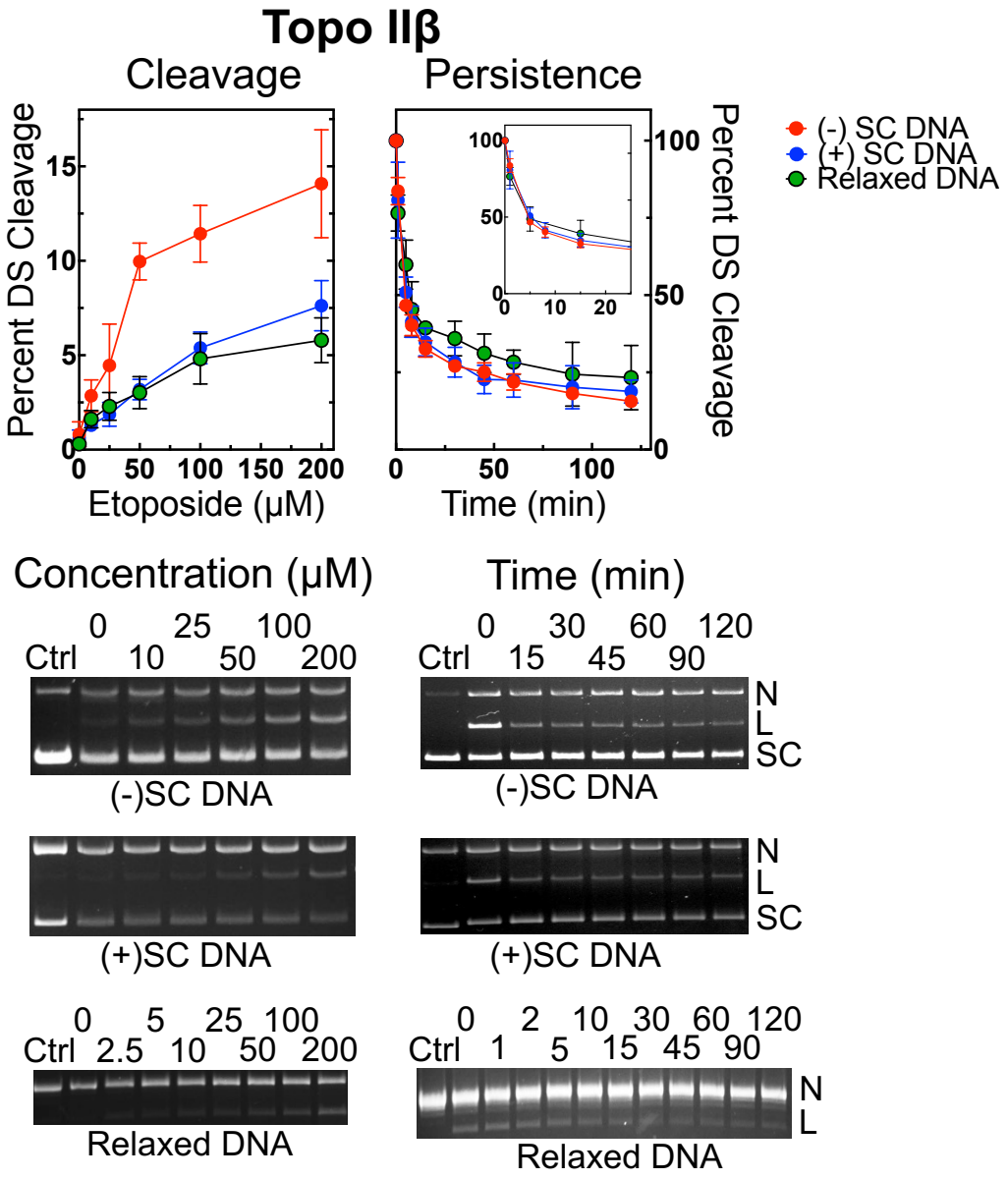

Figure 2.8. Effects of supercoil geometry on DNA cleavage and the persistence of cleavage complexes generated by human topoisomerase IIβ in the presence of etoposide. DNA cleavage and the persistence of cleavage complexes by human topoisomerase IIβ (Topo IIβ) with (-)SC (red), (+)SC (blue), or relaxed pBR322 DNA (green) in the presence of 100 μM etoposide are shown. Representative gel images for human topoisomerase IIβ-mediated cleavage and persistence with (-)SC, (+)SC, or relaxed DNA are shown. The positions of supercoiled (SC), nicked (N), and linear (L) DNA are indicated. Error bars represent the standard deviation of at least three independent assays. $T_{1/2}$ values are displayed in Table 2.2.

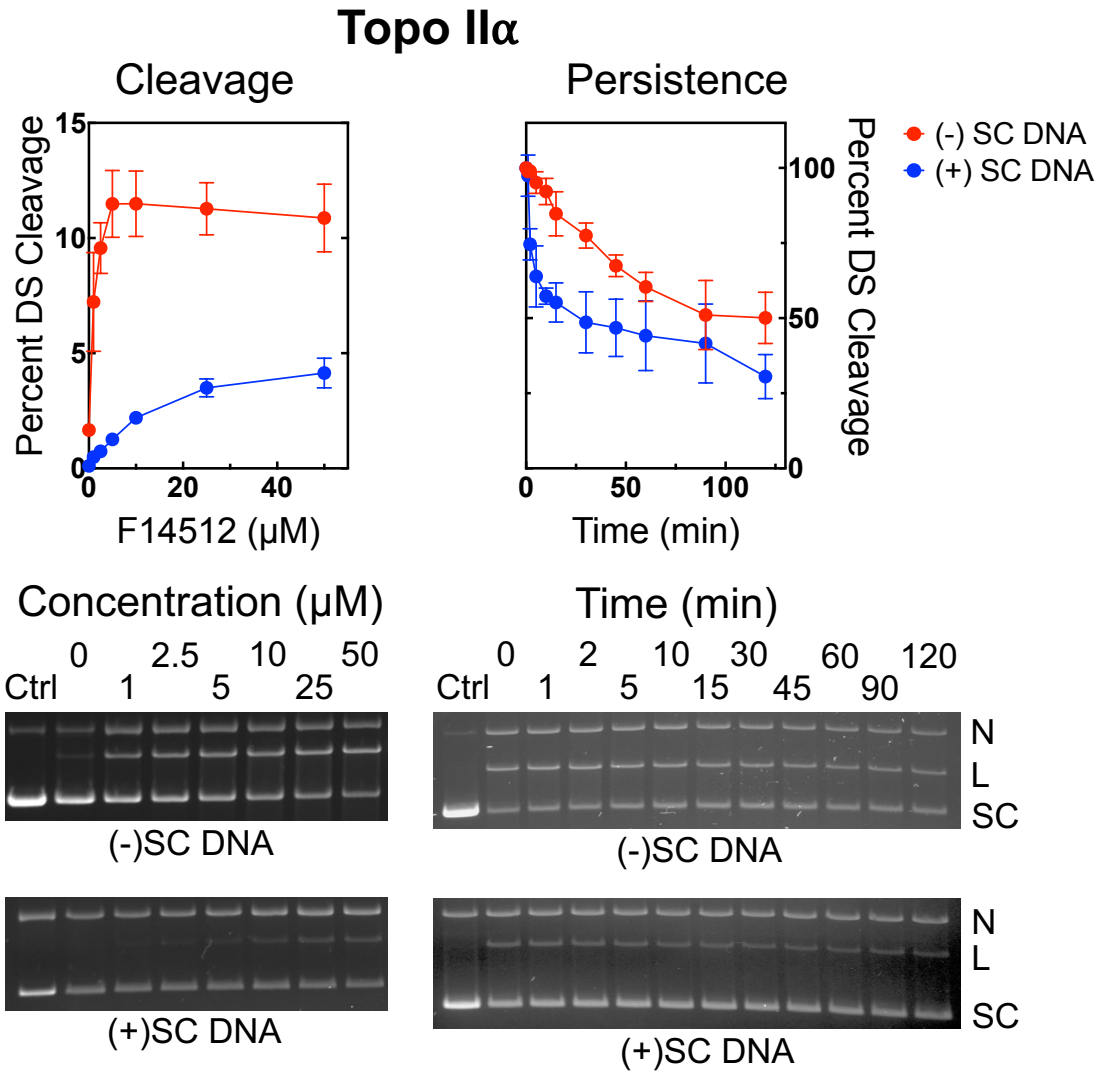

Figure 2.9. Effects of supercoil geometry on DNA cleavage and the persistence of cleavage complexes generated by human topoisomerase IIα in the presence of F14512. DNA cleavage and the persistence of cleavage complexes by human topoisomerase IIα (Topo IIα) with (-)SC (red) or (+)SC (blue) pBR322 DNA in the presence of 20 μM of the etoposide analog F14512 are shown. Representative gel images for human topoisomerase IIα-mediated cleavage and persistence with (-)SC, (+)SC, or relaxed DNA are shown. The positions of supercoiled (SC), nicked (N), and linear (L) DNA are indicated. Error bars represent the standard deviation of at least three independent assays. $T_{1/2}$ values are displayed in Table 2.2.

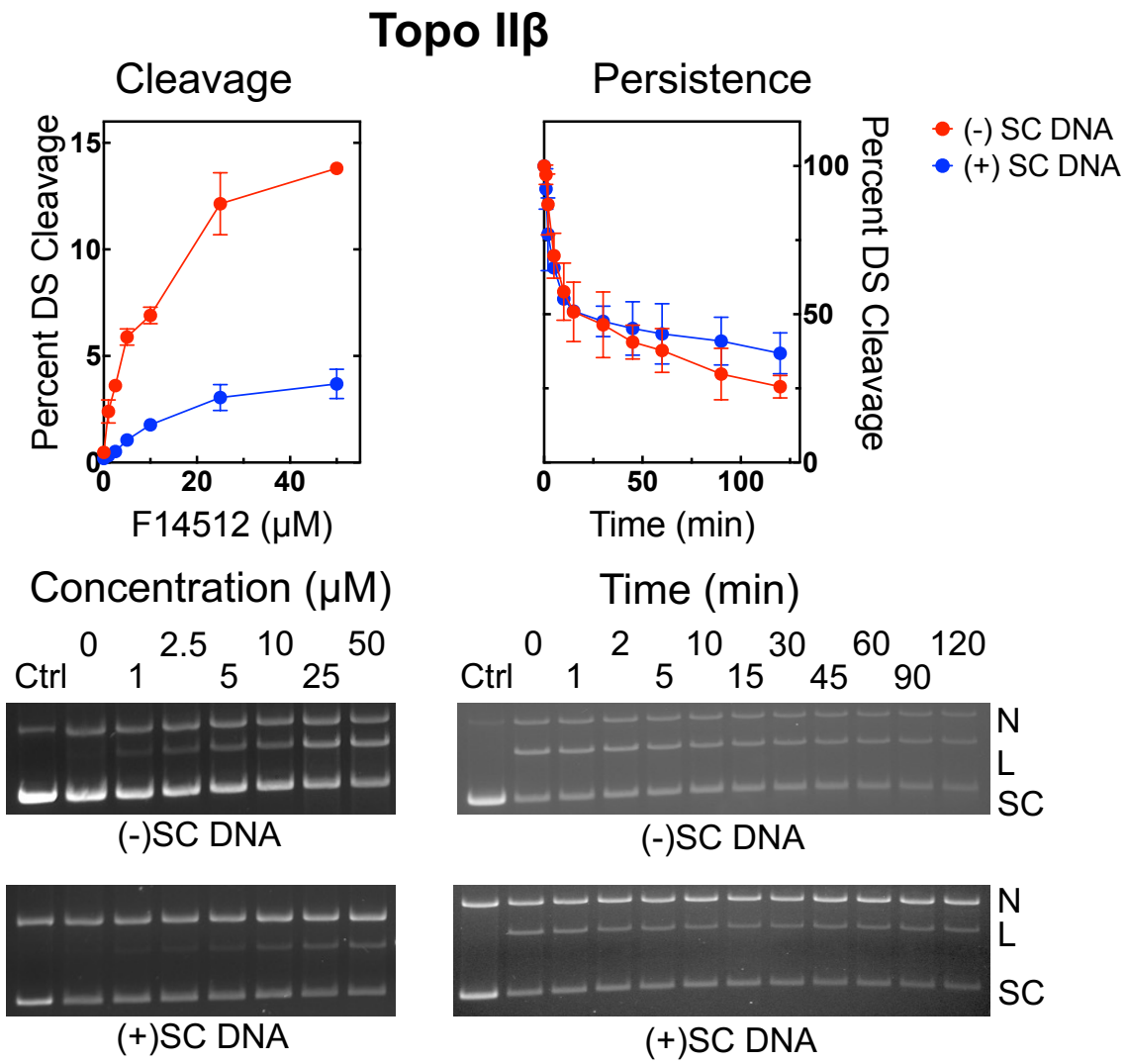

Figure 2.10. Effects of supercoil geometry on DNA cleavage and the persistence of cleavage complexes generated by human topoisomerase IIβ in the presence of F14512. DNA cleavage and the persistence of cleavage complexes by human topoisomerase IIβ (Topo IIβ) with (-)SC (red) or (+)SC (blue) pBR322 DNA in the presence of 20 μM of F14512 are shown. Representative gel images for human topoisomerase IIβ-mediated cleavage and persistence with (-)SC, (+)SC, or relaxed DNA are shown. The positions of supercoiled (SC), nicked (N), and linear (L) DNA are indicated. Error bars represent the standard deviation of at least three independent assays. $T_{1/2}$ values are displayed in Table 2.2.

Species	Enzyme	Drug	DNA Type	$T_{1/2}$ (min)
Human	IIα	Etoposide	(-) SC	>120
			(+) SC	70.5
			Relaxed	64.2
Human	IIβ	Etoposide	(-) SC	3.45
			(+) SC	3.85
			Relaxed	4.28
Human	IIα	F14512	(-) SC	37.1
			(+) SC	4.33
Human	IIβ	F14512	(-) SC	7.23
			(+) SC	4.08

Table 2.2: $T_{1/2}$ values for Figures 2.7–2.10

Table 2.2. Effects of supercoil geometry on DNA cleavage and the lifetime of cleavage complexes generated by human type II topoisomerases in the presence of etoposide or F14512. Lifetime of cleavage complexes (represented by $T_{1/2}$) by human topoisomerase IIα and human topoisomerase IIβ with (-)SC (red), (+)SC (blue), or relaxed pBR322 DNA (green) in the presence of etoposide or F14512 are shown.

Effects of supercoil handedness on DNA cleavage mediated by bacterial type II topoisomerases and the persistence of total enzyme-DNA cleavage complexes in the presence of antibacterial drugs

A series of parallel experiments was carried out with bacterial gyrase and topoisomerase IV to discern the effects of supercoil handedness on DNA scission and the stability of total cleavage complexes (E•S + E–S*) in the presence of ciprofloxacin (Figures 2.11–2.15, tables 2.3–2.4). Results with *E. coli, B. anthracis,* and *M. tuberculosis* gyrase were similar to those observed with human topoisomerase IIα (Figures 2.11–2.13). In all cases, enzymes produced ~2–4 times higher levels of cleavage with (-)SC DNA (Figures 2.11–2.13, cleavage panels). Furthermore, total enzyme-DNA complexes (as reflected by the lifetime of the enzyme-DNA cleavage complexes) formed with (-)SC DNA were more stable than those formed with (+)SC DNA (Figures 2.11–2.13, persistence panels; table 2.3). One notable difference observed between gyrase and topoisomerase IIα was that levels of cleavage generated by gyrase with relaxed DNA were considerably lower than those generated with (+)SC substrates.

In contrast to results with gyrase, neither *E. coli* nor *B. anthracis* topoisomerase IV displayed an ability to discern DNA supercoil handedness during cleavage in the presence of ciprofloxacin (Figures 2.14–2.15, cleavage panels). Indeed, both enzymes maintained similar levels of cleavage complexes formed with either (-)SC or (+)SC DNA (Figures 2.14–2.15, cleavage panels). Despite the inability to distinguish between (-)SC and (+)SC DNA, topoisomerase IV easily discerned between plasmid molecules with supercoils from those without (i.e., relaxed) and maintained substantially higher levels of cleavage with supercoiled substrates. These features of *E. coli* and *B. anthracis* topoisomerase IV were reflected in persistence assays (Figures 2.14–2.15, persistence panels; table 2.4). Whereas the persistence of total enzyme-DNA

complexes was similar between (-)SC or (+)SC DNA, the stability of complexes formed on relaxed DNA was substantially lower (Figures 2.14–2.15, persistence panels; table 2.4).

Effects of supercoil handedness on the ability of human and bacterial type II topoisomerases to religate DNA.

Although the stability of total enzyme-DNA complexes (E•S + E–S*) may partially explain the basis for the recognition of supercoil geometry during cleavage with some type II topoisomerases, it cannot offer a complete explanation. Therefore, the effects of supercoil handedness on topoisomerase-mediated DNA religation (the k_{-2} step in the above equations) were examined. Because DNA in cleavage complexes has to be religated before the ternary enzyme-DNA-drug complex can dissociate, the k_{-2} religation step may represent a rate-determining step that affects overall levels of DNA scission of substrates with different supercoil geometry.

In the DNA religation assay, the DNA cleavage-religation equilibrium (E•S ⇌ E–S*) is established (in the presence or absence of drugs) at 37 ºC. Reaction mixtures are then switched to 0 ºC, a temperature that supports DNA religation (k_{-2}) but not cleavage (k_2) (Bromberg and Osheroff 2001). Consequently, the reaction monitors the unidirectional rate of enzyme-mediated DNA religation. In schematic terms, the temperature shift blocks the k_2 step and is believed to primarily reflect the k_{-2} step in the reaction scheme shown below.

$$E + S \underset{k_{-1}}{\overset{k_1}{\rightleftharpoons}} E{\bullet}S \underset{k_{-2}}{\overset{\cancel{k_2}}{\rightleftharpoons}} E\text{–}S^*$$

The results of DNA religation assays are shown in Figures 2.16–2.19. Consistent with previous literature (Osheroff 1989, McClendon, Rodriguez et al. 2005, Gentry, Pitts et al. 2011, Aldred, McPherson et al. 2012, Gibson, Blower et al. 2018), rates of religation with all enzymes tested were considerably slower in the presence of anticancer or antibacterial drugs than in their

absence. Together with persistence assays that compared the stability of total enzyme-DNA complexes formed in the absence (Figure 2.3–2.6) or presence (Figures 2.7–2.15, persistence panels) of drugs, these data strongly suggest that drug-induced increases in DNA scission can be explained by slower rates of religation and higher stabilities of cleavage complexes. However, these assays cannot explain the ability of human and bacterial type II topoisomerases to discern supercoil handedness during the DNA cleavage reaction. With all enzymes examined, rates of religation (k_{-2}) of (-)SC vs (+)SC substrates in the presence of drugs were similar to each other (Figures 2.16–2.19, closed circles), as were rates of religation (albeit much faster) for these substrates in the absence of drugs (Figure 2.16–2.19, open circles).

Effects of supercoil handedness on the rate of DNA cleavage by human and bacterial type II topoisomerases

When cleavage complexes are formed by type II topoisomerases, an equilibrium is established between the formation of the cleaved DNA (E–S* complex) and its religation to the intact molecule (E•S complex) (Deweese, Burgin et al. 2008, Deweese and Osheroff 2009, Vann, Oviatt et al. 2021). Because the rate of religation (k_{-2} in the equation shown below) did not correlate with the effects of supercoil handedness on levels of DNA cleavage, we determined the pre-equilibrium rates of enzyme-mediated cleavage of (-)SC and (+)SC DNA (Figures 2.20–2.25, tables 2.5–2.6). The forward rate of enzyme-DNA binding (k_1) is likely to be diffusion controlled. Furthermore, a previous study has demonstrated that human topoisomerase IIα and IIβ display equal binding affinities for (-)SC and (+)SC DNA (McClendon, Rodriguez et al. 2005). Therefore, it is believed that pre-equilibrium rates of cleavage reflect primarily the k_2 step in the equation below.

$$E + S \underset{k_{-1}}{\overset{k_1}{\rightleftharpoons}} E{\bullet}S \underset{k_{-2}}{\overset{k_2}{\rightleftharpoons}} E{-}S^*$$

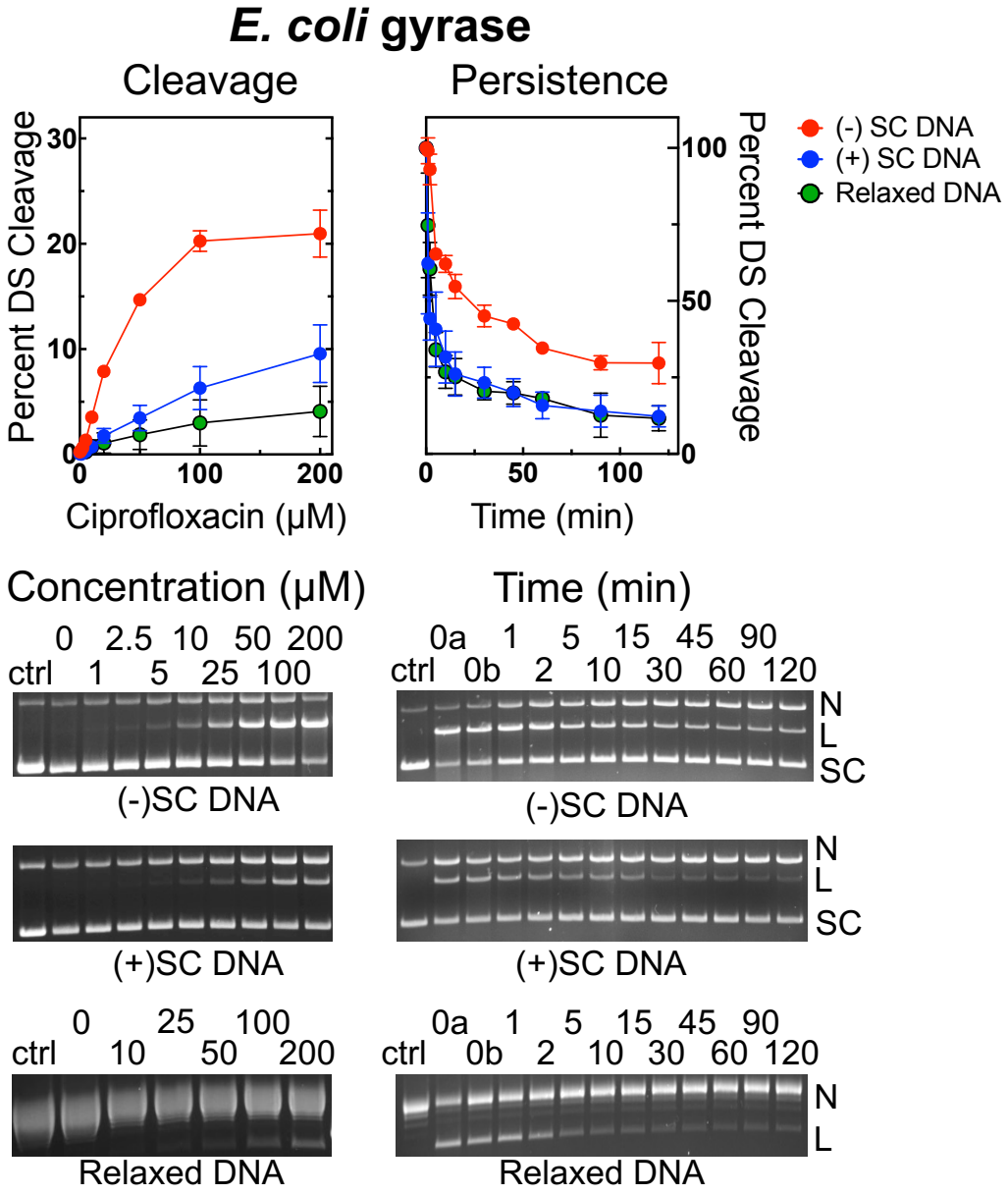

Figure 2.11. Effects of supercoil geometry on DNA cleavage and the persistence of cleavage complexes generated by *E. coli* gyrase in the presence of ciprofloxacin. DNA cleavage and the persistence of cleavage complexes by *E. coli* gyrase with (-)SC (red), (+)SC (blue), or relaxed pBR322 DNA (green) in the presence of 100 μM ciprofloxacin are shown. Representative gel images for *E. coli* gyrase cleavage and persistence with (-)SC, (+)SC, or relaxed DNA are shown. The positions of supercoiled (SC), nicked (N), and linear (L) DNA are indicated. Error bars represent the standard deviation of at least three independent assays. $T_{1/2}$ values are displayed in Table 2.3.

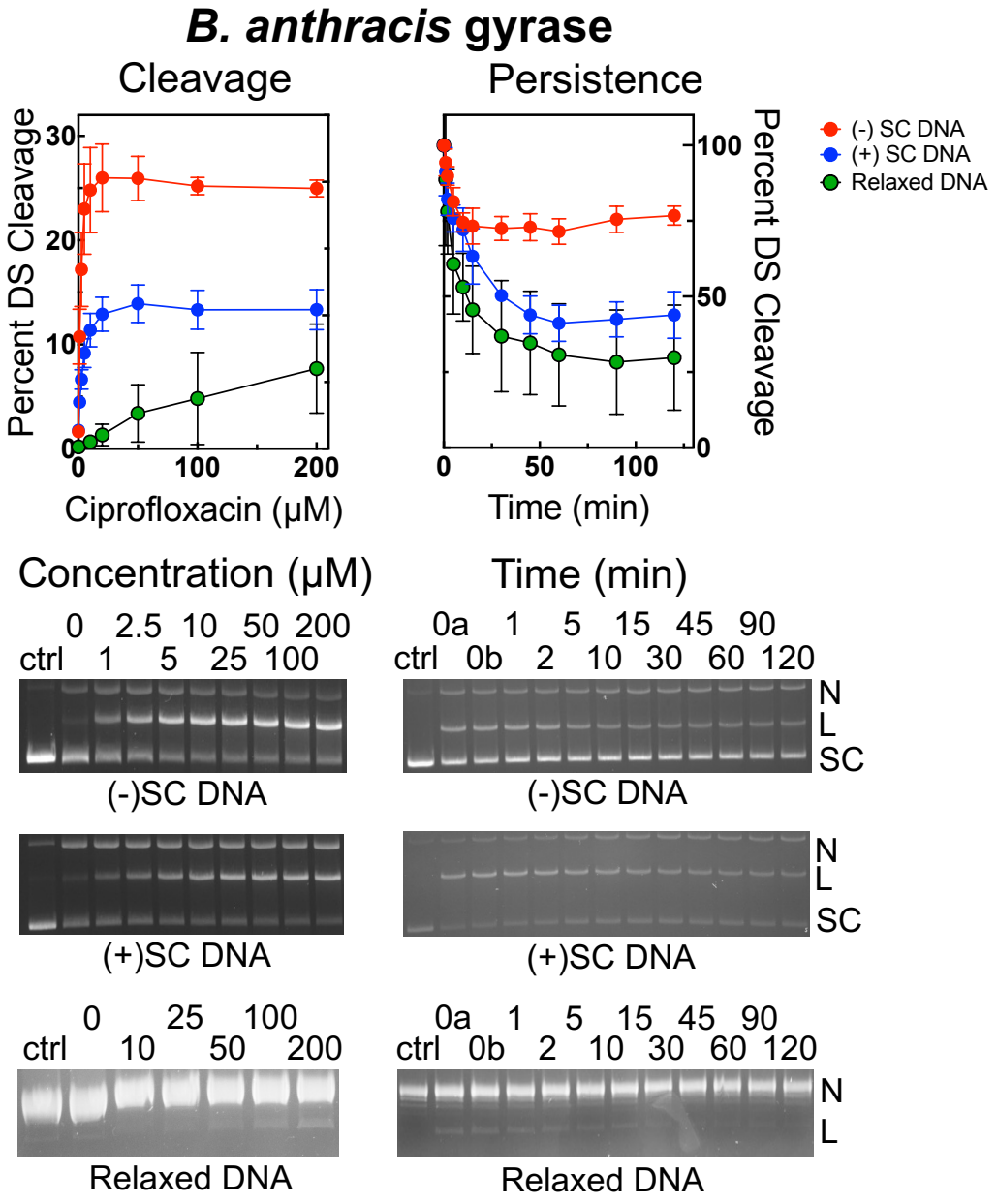

Figure 2.12. Effects of supercoil geometry on DNA cleavage and the persistence of cleavage complexes generated by *B. anthracis* gyrase in the presence of ciprofloxacin. DNA cleavage and the persistence of cleavage complexes by *B. anthracis* gyrase with (-)SC (red), (+)SC (blue), or relaxed pBR322 DNA (green) in the presence of 100 μM ciprofloxacin are shown. Representative gel images for *B. anthracis* gyrase cleavage and persistence with (-)SC, (+)SC, or relaxed DNA are shown. The positions of supercoiled (SC), nicked (N), and linear (L) DNA are indicated. Error bars represent the standard deviation of at least three independent assays. $T_{1/2}$ values are displayed in Table 2.3.

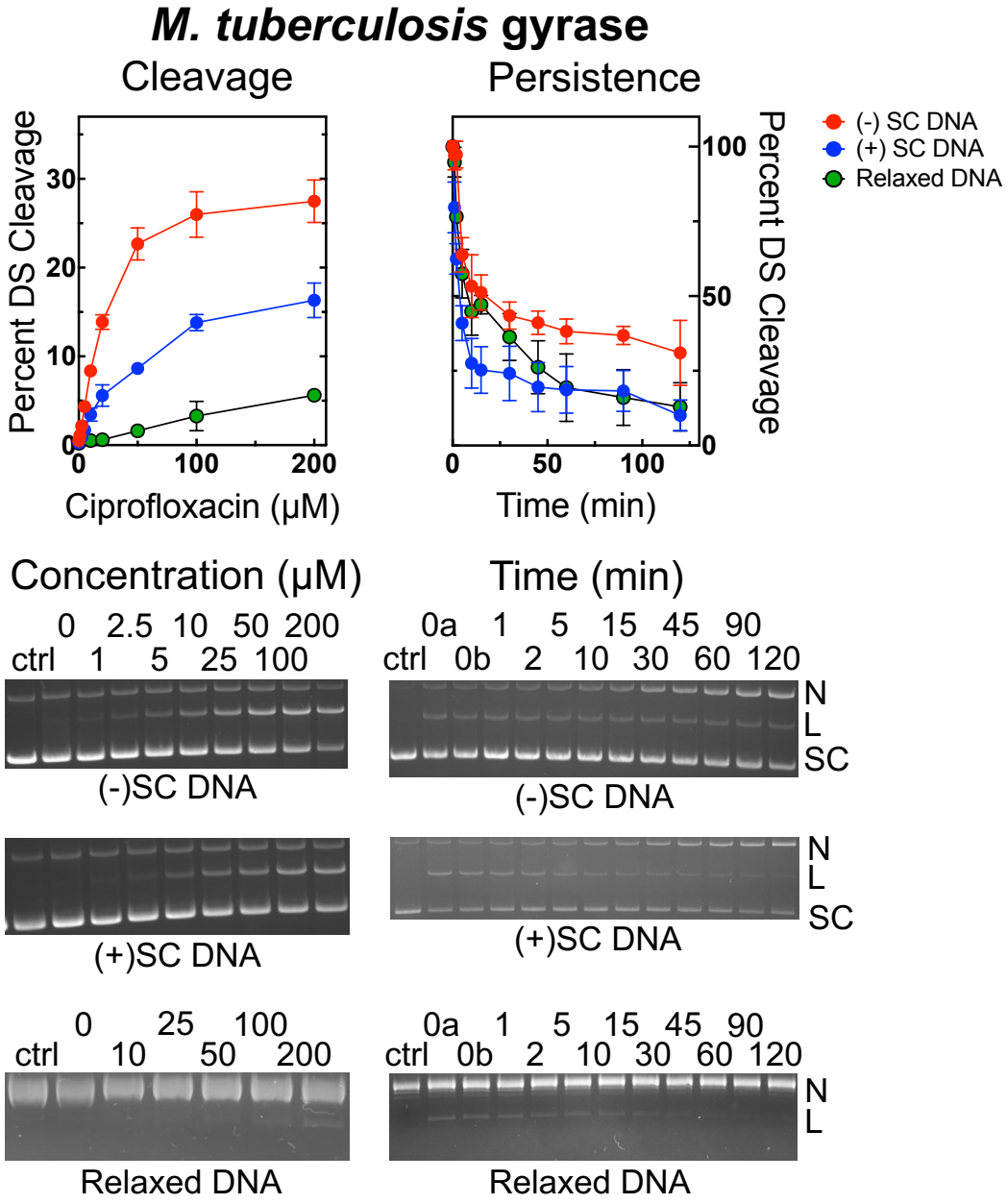

Figure 2.13. Effects of supercoil geometry on DNA cleavage and the persistence of cleavage complexes generated by *M. tuberculosis* gyrase in the presence of ciprofloxacin. DNA cleavage and the persistence of cleavage complexes by *M. tuberculosis* gyrase with (-)SC (red), (+)SC (blue), or relaxed pBR322 DNA (green) in the presence of 100 μM ciprofloxacin are shown. Representative gel images for *M. tuberculosis* gyrase cleavage and persistence with (-)SC, (+)SC, or relaxed DNA are shown. The positions of supercoiled (SC), nicked (N), and linear (L) DNA are indicated. Error bars represent the standard deviation of at least three independent assays. $T_{1/2}$ values are displayed in Table 2.3.

Species	Enzyme	Drug	DNA Type	$T_{1/2}$ (min)
E. coli	Gyrase	Ciprofloxacin	(-) SC	7.90
			(+) SC	1.40
			Relaxed	2.20
B. anthracis	Gyrase	Ciprofloxacin	(-) SC	>120
			(+) SC	54.1
			Relaxed	2.20
M. tuberculosis	Gyrase	Ciprofloxacin	(-) SC	5.17
			(+) SC	2.61
			Relaxed	3.89

Table 2.3: $T_{1/2}$ values for Figures 2.11–2.13

Table 2.3. Effects of supercoil geometry on DNA cleavage and the lifetime of cleavage complexes generated by bacterial gyrase in the presence of ciprofloxacin. Lifetime of cleavage complexes (represented by $T_{1/2}$) by *E. coli*, *B. anthracis*, and *M. tuberculosis* gyrase with (-)SC (red), (+)SC (blue), or relaxed pBR322 DNA (green) in the presence of ciprofloxacin are shown.

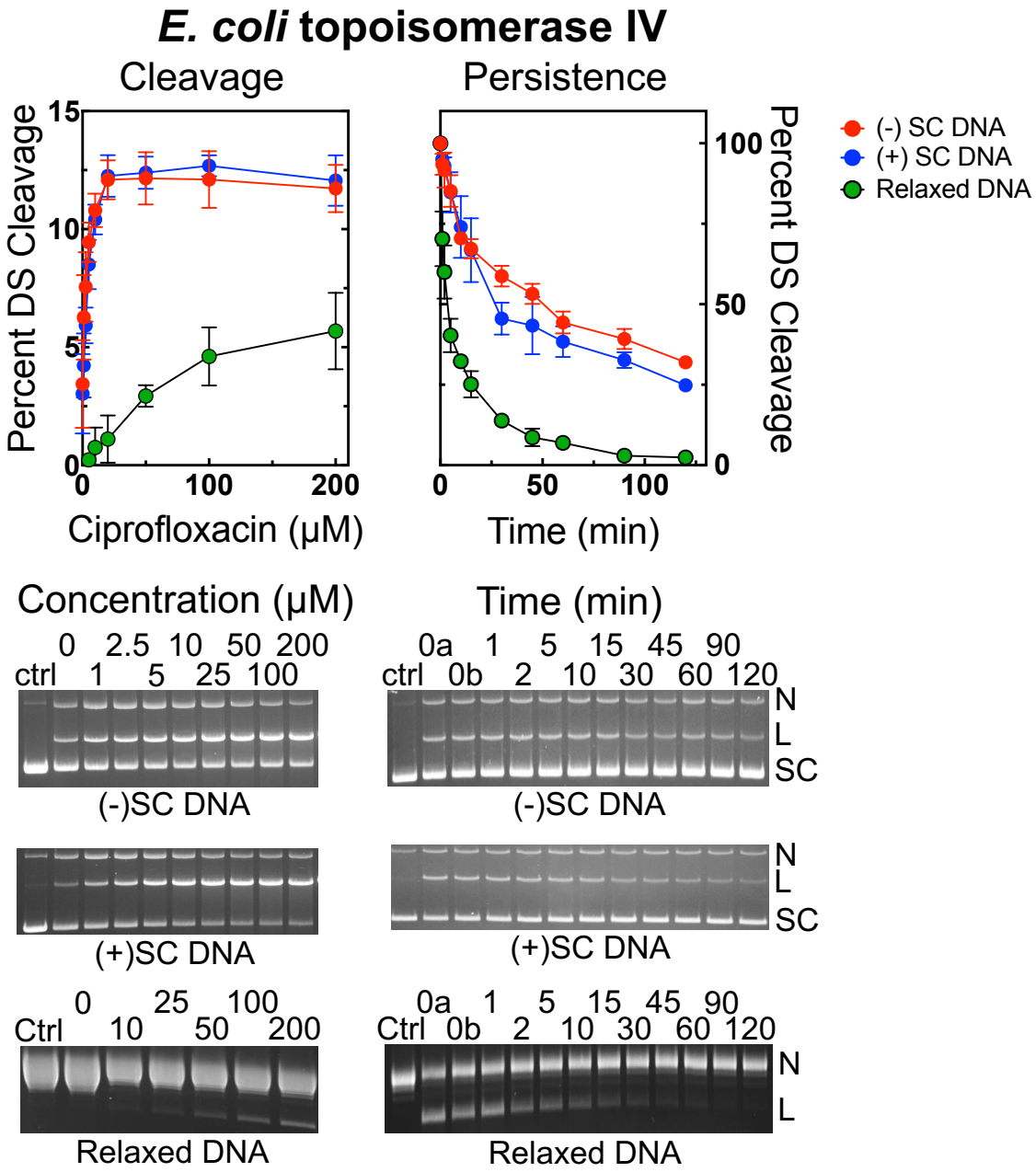

Figure 2.14. Effects of supercoil geometry on DNA cleavage and the persistence of cleavage complexes generated by *E. coli* topoisomerase IV in the presence of ciprofloxacin. DNA cleavage and the persistence of cleavage complexes by *E. coli* topoisomerase IV with (-)SC (red), (+)SC DNA (blue), or relaxed pBR322 DNA (green) in the presence of ciprofloxacin are shown. Representative gel images for *E. coli* topoisomerase IV cleavage and persistence with (-)SC, (+)SC, or relaxed DNA are shown. The positions of supercoiled (SC), nicked (N), and linear (L) DNA are indicated. Error bars represent the standard deviation of at least three independent assays. $T_{1/2}$ values are displayed in Table 2.4.

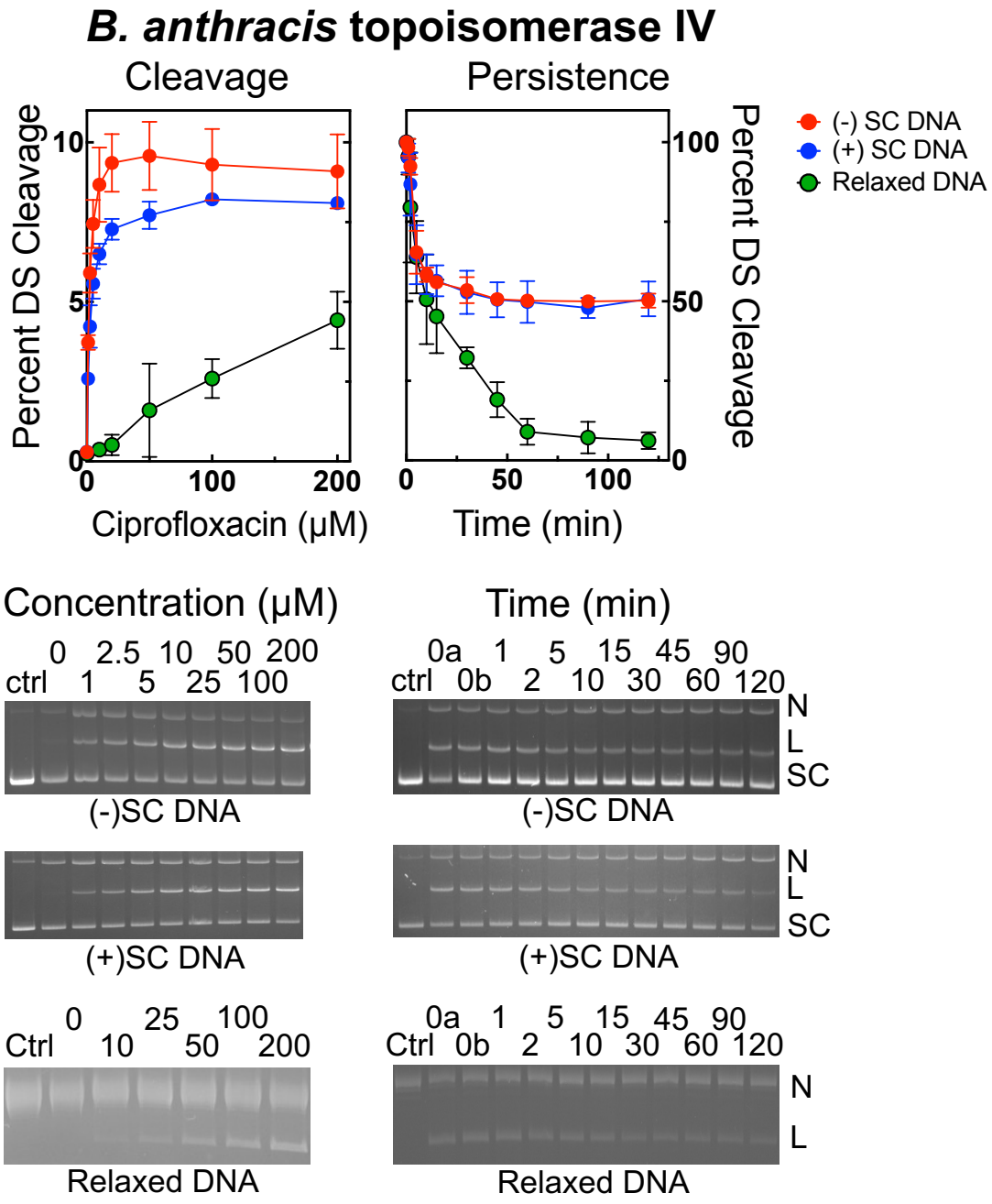

Figure 2.15. Effects of supercoil geometry on DNA cleavage and the persistence of cleavage complexes generated by *B. anthracis* topoisomerase IV in the presence of ciprofloxacin. DNA cleavage and the persistence of cleavage complexes by *B. anthracis* topoisomerase IV with (-)SC (red), (+)SC DNA (blue), or relaxed pBR322 DNA (green) in the presence of ciprofloxacin are shown. Representative gel images for *B. anthracis* topoisomerase IV cleavage and persistence with (-)SC, (+)SC, or relaxed DNA are shown. The positions of supercoiled (SC), nicked (N), and linear (L) DNA are indicated. Error bars represent the standard deviation of at least three independent assays. $T_{1/2}$ values are displayed in Table 2.4.

Species	Enzyme	Drug	DNA Type	$T_{1/2}$ (min)
E. coli	Topo IV	Ciprofloxacin	(-) SC	27.1
			(+) SC	24.2
			Relaxed	4.54
B. anthracis	Topo IV	Ciprofloxacin	(-) SC	50.9
			(+) SC	50.8
			Relaxed	4.54

Table 2.4: $T_{1/2}$ values for Figures 2.14–2.15

Table 2.4. Effects of supercoil geometry on DNA cleavage and the lifetime of cleavage complexes generated by bacterial topoisomerase IV in the presence of ciprofloxacin. Lifetime of cleavage complexes (represented by $T_{1/2}$) by *E. coli*, *B. anthracis*, and *M. tuberculosis* topoisomerase IV with (-)SC (red), (+)SC (blue), or relaxed pBR322 DNA (green) in the presence of ciprofloxacin are shown.

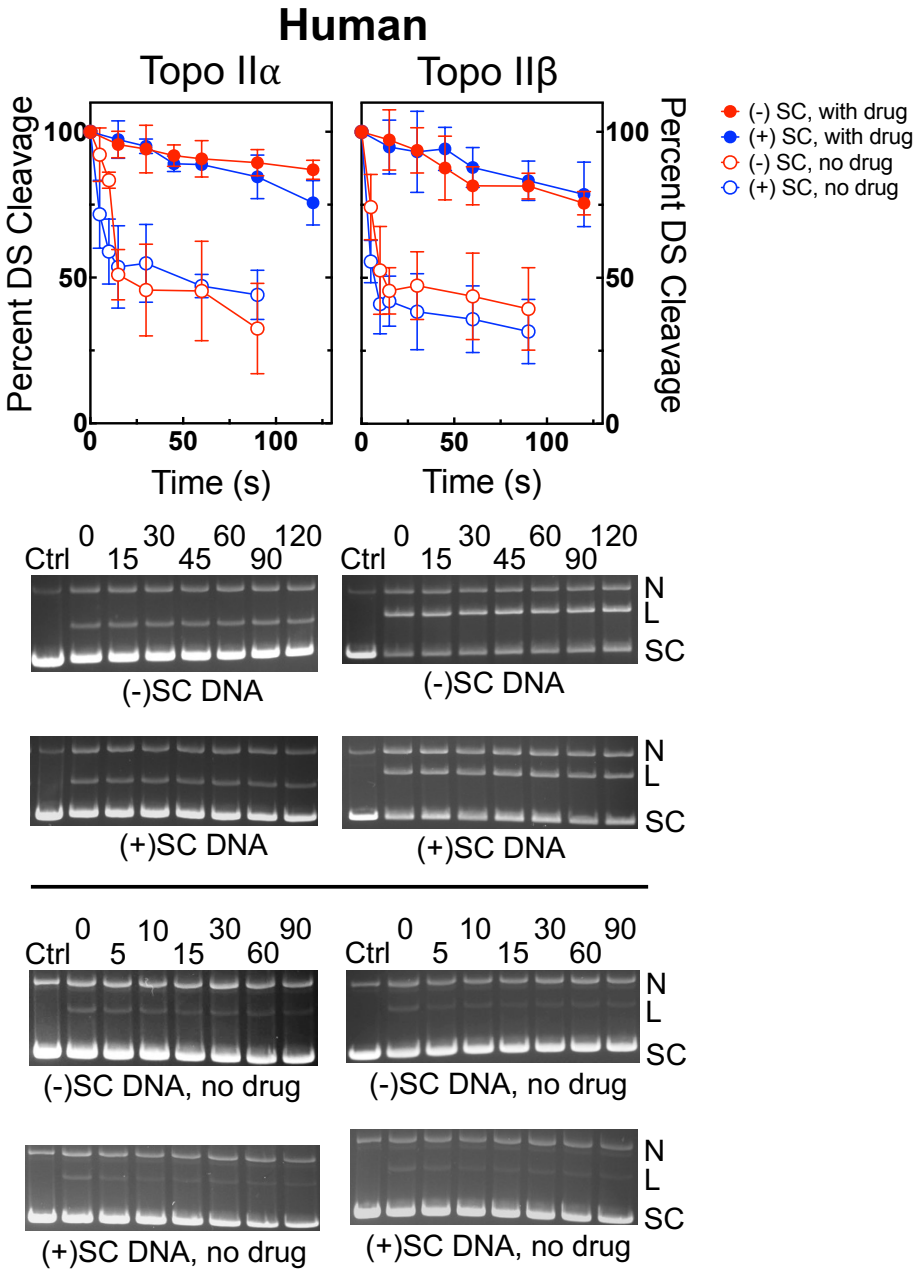

Figure 2.16. Effects of supercoil geometry on DNA religation by human type II topoisomerases in the presence or absence of drugs. DNA religation catalyzed by human topoisomerase IIα (Topo IIα, left) and topoisomerase IIβ (Topo IIβ, right). Experiments were carried out with (-)SC (red) or (+)SC (blue) pBR322 DNA in the absence (open circles) or presence (filled circles) of 100 μM etoposide. Representative gel images for religation mediated by human topoisomerase IIα and IIβ with (-)SC or (+)SC DNA in the presence (upper gels) or absence (lower gels) of drug are shown. The positions of supercoiled (SC), nicked (N), and linear (L) DNA are indicated. Error bars represent the standard deviation of at least three independent assays.

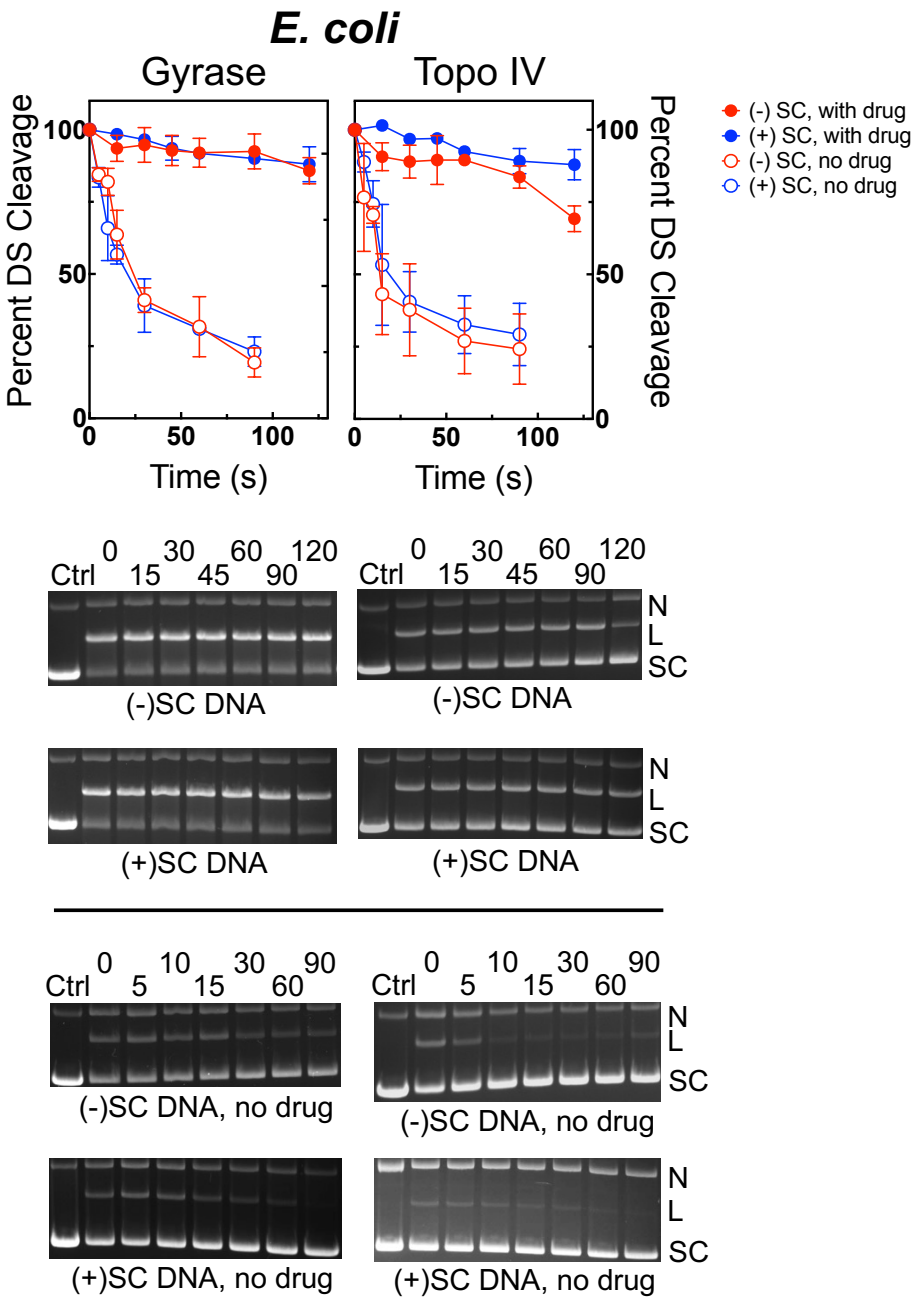

Figure 2.17. Effects of supercoil geometry on DNA religation by *E. coli* type II topoisomerases in the presence or absence of drugs. DNA religation catalyzed by *E. coli* gyrase (left) and topoisomerase IV (Topo IV, right) are shown. Experiments were carried out with (-)SC (red) or (+)SC (blue) pBR322 DNA in the absence (open circles) or presence (filled circles) of 100 μM ciprofloxacin. Representative gel images for religation mediated *E. coli* gyrase with (-)SC or (+)SC DNA in the presence (A, bottom; B, bottom) or absence (C, D) of drug are shown. The positions of supercoiled (SC), nicked (N), and linear (L) DNA are indicated. Error bars represent the standard deviation of at least three independent assays.

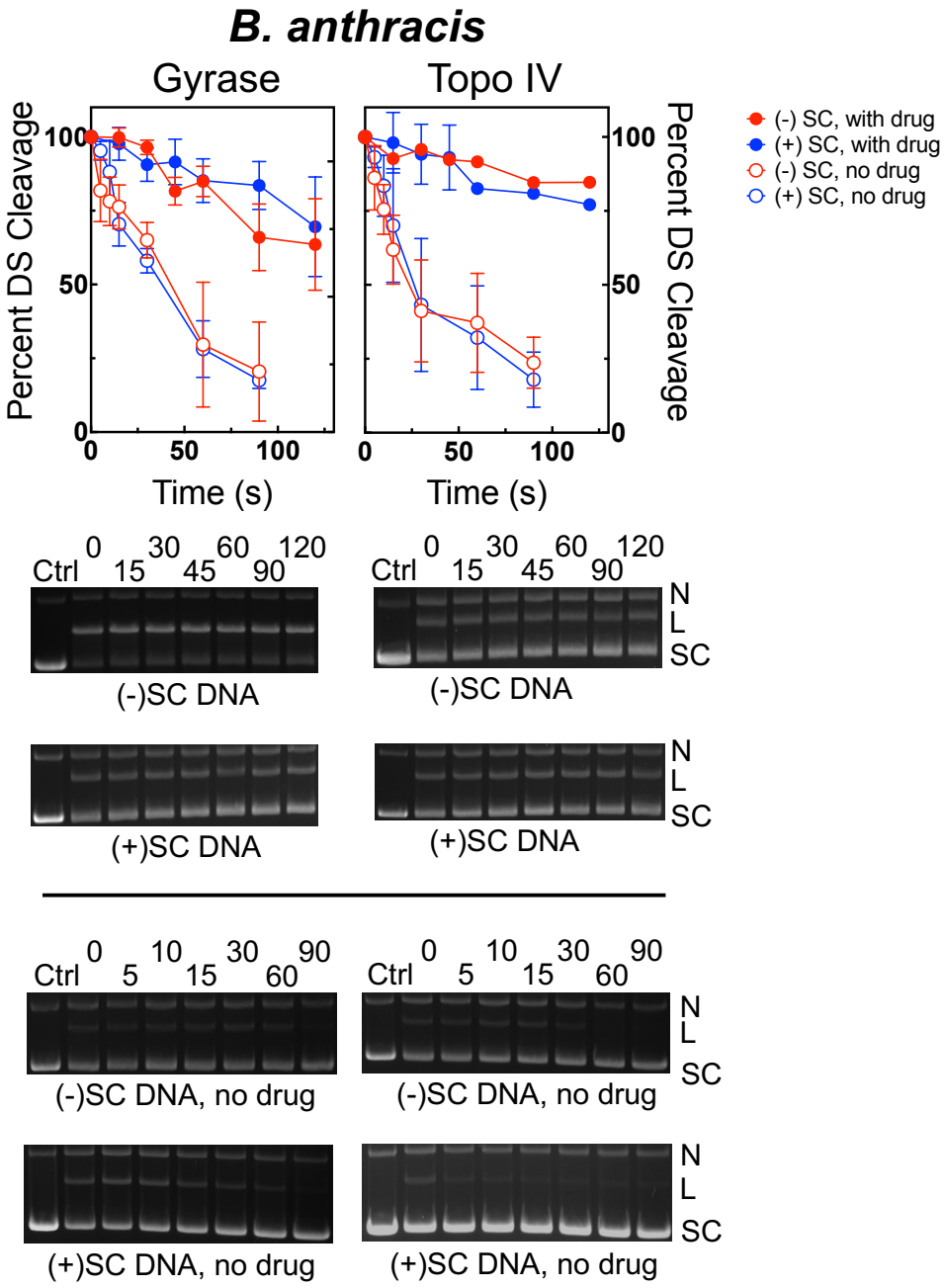

Figure 2.18. Effects of supercoil geometry on DNA religation by *B. anthracis* type II topoisomerases in the presence or absence of drugs. DNA religation catalyzed by *B. anthracis* gyrase (left) and topoisomerase IV (Topo IV, right) are shown. Experiments were carried out with (-)SC (red) or (+)SC (blue) pBR322 DNA in the absence (open circles) or presence (filled circles) of 100 μM ciprofloxacin. Representative gel images for religation mediated *B. anthracis* gyrase with (-)SC or (+)SC DNA in the presence (A, bottom; B, bottom) or absence (C, D) of drug are shown. The positions of supercoiled (SC), nicked (N), and linear (L) DNA are indicated. Error bars represent the standard deviation of at least three independent assays.

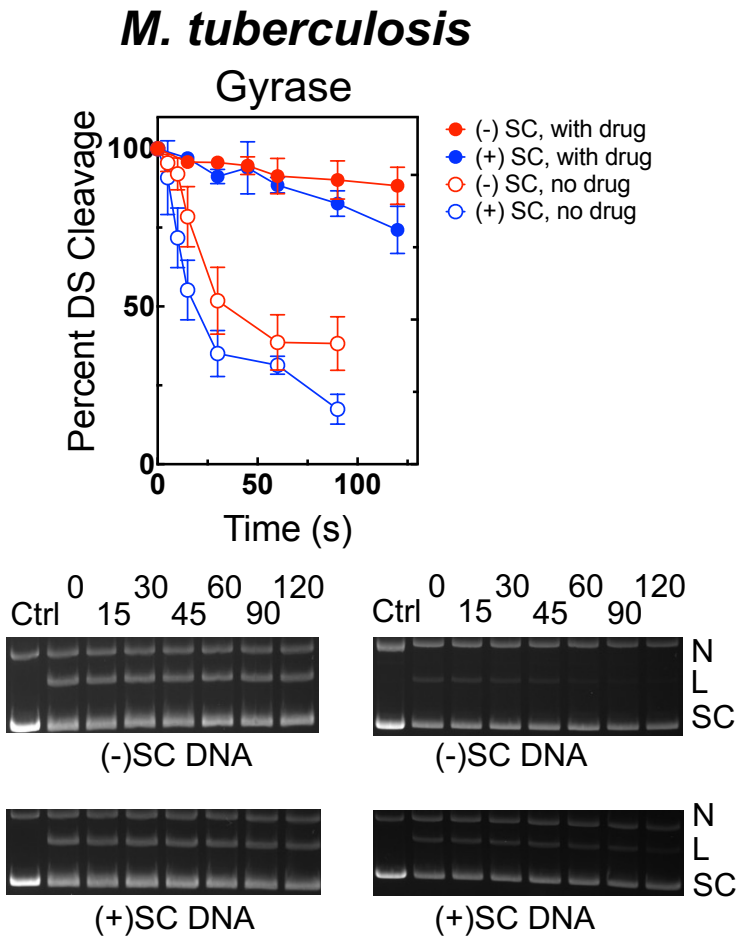

Figure 2.19. Effects of supercoil geometry on DNA religation by *M. tuberculosis* gyrase in the presence or absence of drugs. DNA religation catalyzed by *M. tuberculosis* is shown. Experiments were carried out with (-)SC (red) or (+)SC (blue) pBR322 DNA in the absence (open circles) or presence (filled circles) of 100 μM ciprofloxacin. Representative gel images for religation mediated by *M. tuberculosis* gyrase with (-)SC or (+)SC DNA in the presence (A, bottom; B, bottom) or absence (C, D) of drug are shown. The positions of supercoiled (SC), nicked (N), and linear (L) DNA are indicated. Error bars represent the standard deviation of at least three independent assays.

As a caveat to the above, a previous study demonstrated that human topoisomerase IIα and IIβ display ~2-fold higher binding affinities for (-)SC over (+)SC DNA ($K_D \approx 7.5$ nM vs 15 nM, respectively) (McClendon, Rodriguez et al. 2005). In addition, *E. coli* topoisomerase IV displayed similar affinities for substrates with either supercoil handedness. Thus, it is possible that k_1 plays some role in determining the pre-equilibrium rates of DNA cleavage (Stone, Bryant et al. 2003). However, as a counterpoint, the relative affinity of *M. tuberculosis* gyrase for (-)SC DNA is considerably lower than that for (+)SC plasmid (Ashley, Blower et al. 2017). Thus, we still posit that k_2 is an important factor in determining the initial rate of DNA cleavage.

Human topoisomerase IIα and IIβ, and *E. coli* gyrase and topoisomerase IV (as representative bacterial type II enzymes) were used for these experiments. Initial studies were carried out in the presence of etoposide (human enzymes) or ciprofloxacin (bacterial enzymes). The three enzymes that maintained higher levels of DNA cleavage with (-)SC substrates (topoisomerase IIα and IIβ, and gyrase) also displayed faster rates of cleavage with underwound versus overwound DNA (Figures 2.20–2.22, table 2.5). In contrast, topoisomerase IV, the enzyme that maintained similar levels of cleavage with (-)SC and (+)SC DNA, displayed similar rates of cleavage for both DNA substrates (Figure 2.23, table 2.5).

It can be argued that, as DNA cleavage/religation approaches equilibrium, the observed rate of cleavage will begin to reflect a component of the k_{-2} step. Therefore, to ensure that results reflected initial rates of cleavage (i.e., k_2), DNA scission that took place over the first few seconds of the reaction was monitored by rapid-quench flow (Figure 2.22–2.23). The results of these rapid-quench experiments paralleled those seen in slower benchtop assays. To determine whether the above relationships between drug-induced rates of scission and supercoil geometry reflected the intrinsic activity of the type II enzymes, rates of DNA cleavage were determined in the absence of

topoisomerase poisons (Figure 2.24–2.25, table 2.6). Again, topoisomerase IIα and IIβ, and gyrase displayed higher rates of cleavage with (-)SC over (+)SC DNA, while topoisomerase IV did not distinguish between the two substrates. Taken together, these results strongly suggest that the type II topoisomerases that distinguish supercoil geometry (topoisomerase IIα and IIβ, and gyrase) and generate higher levels of cleavage with (-)SC DNA do so, at least in part, by maintaining faster rates of scission with underwound substrates.

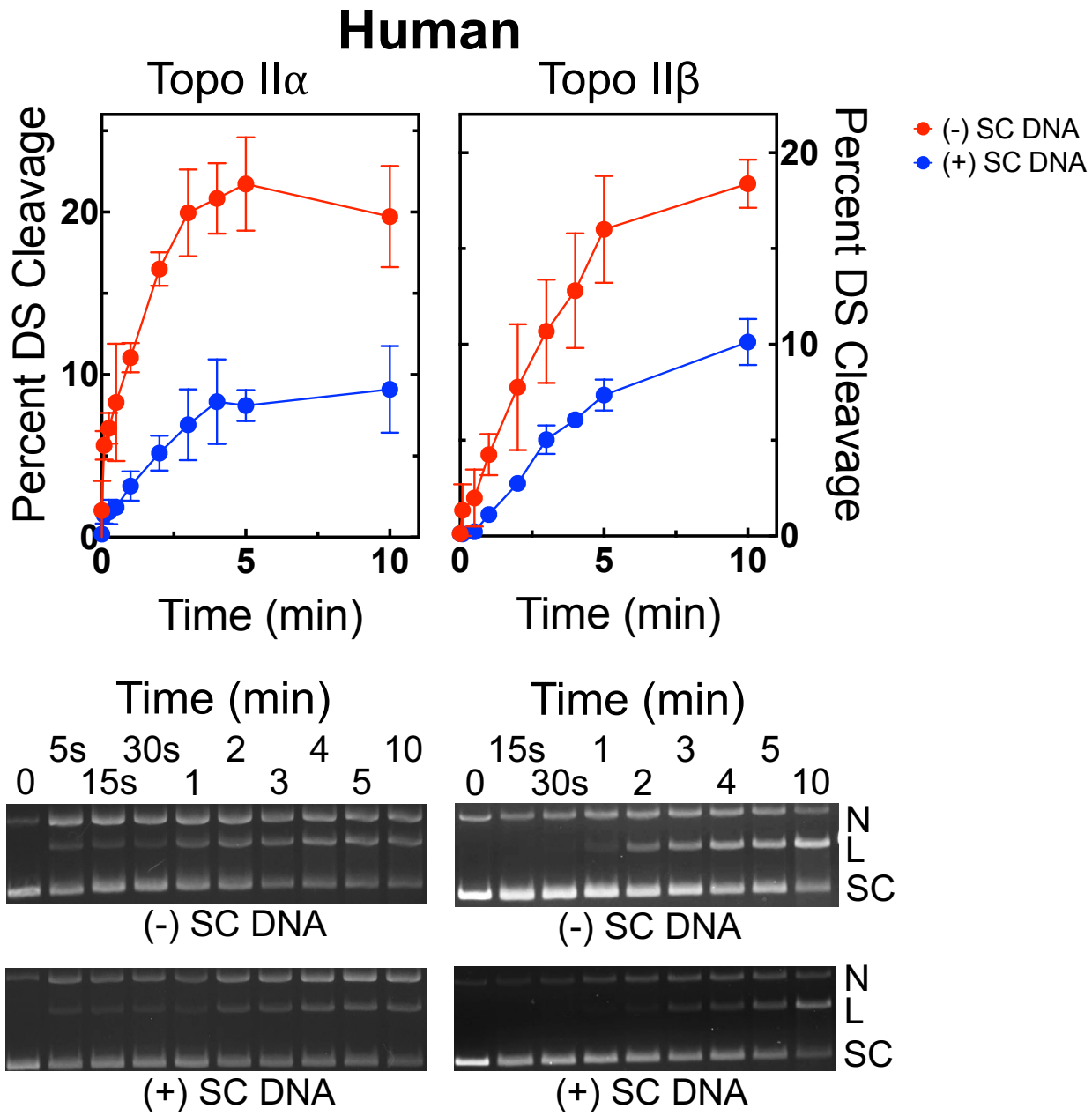

Figure 2.20. Effects of supercoil geometry on forward rates of DNA cleavage mediated by human type II topoisomerases in the presence of drugs. Initial rates of DNA cleavage mediated by human topoisomerase IIα (Topo IIα, left), and IIβ (Topo IIβ, right) are shown. Experiments were carried out with (-)SC (red) or (+)SC (blue) pBR322 DNA. Representative gel images for human topoisomerase IIα and IIβ with (-)SC or (+)SC DNA in the presence of drug are shown. The positions of supercoiled (SC), nicked (N), and linear (L) DNA are indicated. The positions of supercoiled (SC), nicked (N), and linear (L) DNA are indicated. Error bars represent the standard deviation of at least three independent assays. Rates are displayed in Table 2.5.

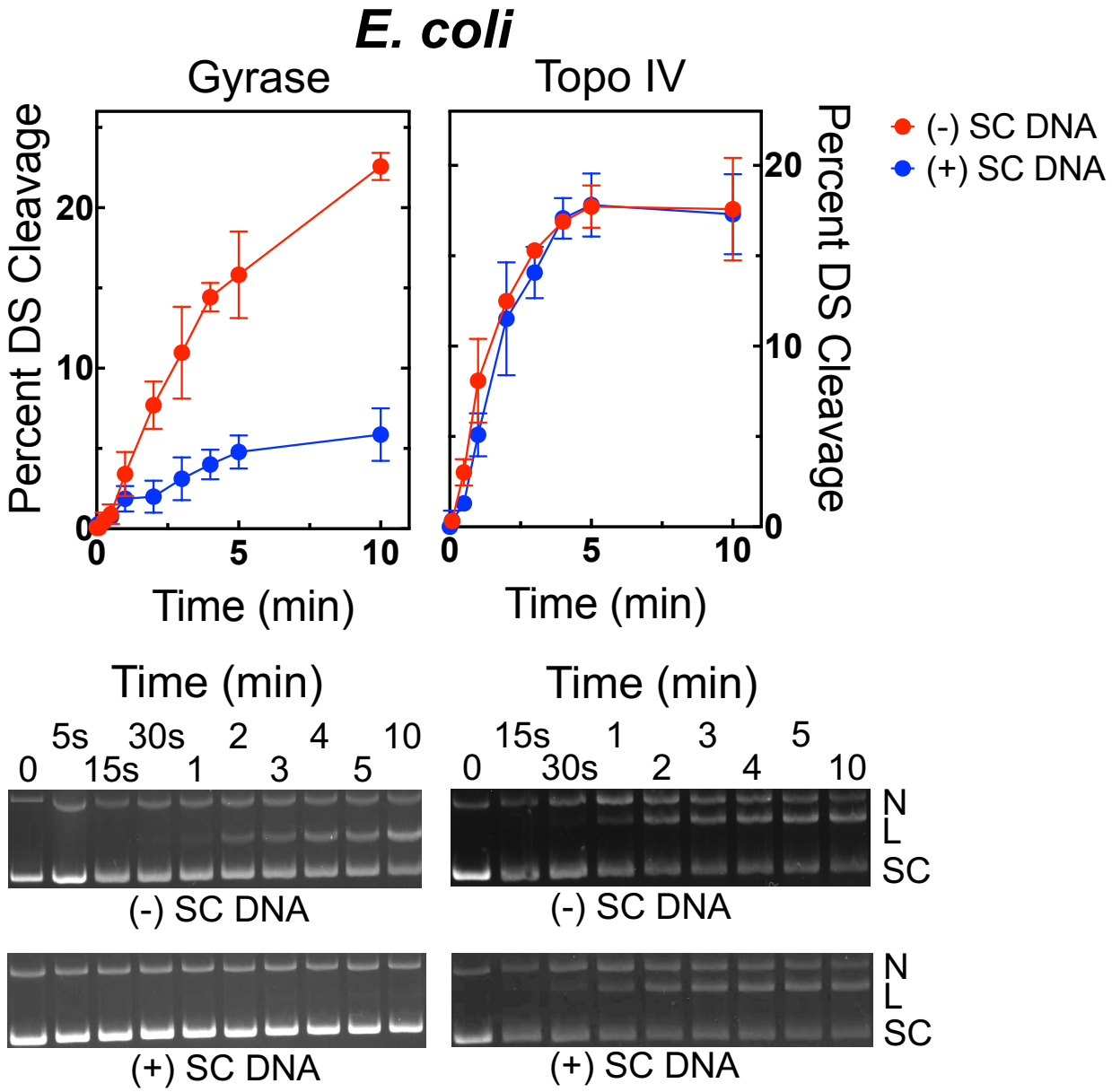

Figure 2.21. Effects of supercoil geometry on forward rates of DNA cleavage mediated by bacterial type II topoisomerases in the presence of drugs. Initial rates of DNA cleavage mediated by *E. coli* gyrase (left) and topoisomerase IV (Topo IV, right) are shown. Experiments were carried out with (-)SC (red) or (+)SC (blue) pBR322 DNA. Representative gel images for *E. coli* gyrase and topoisomerase IV cleavage with (-)SC or (+)SC DNA in the presence of drug are shown. The positions of supercoiled (SC), nicked (N), and linear (L) DNA are indicated. Error bars represent the standard deviation of at least three independent assays. Rates are displayed in Table 2.5.

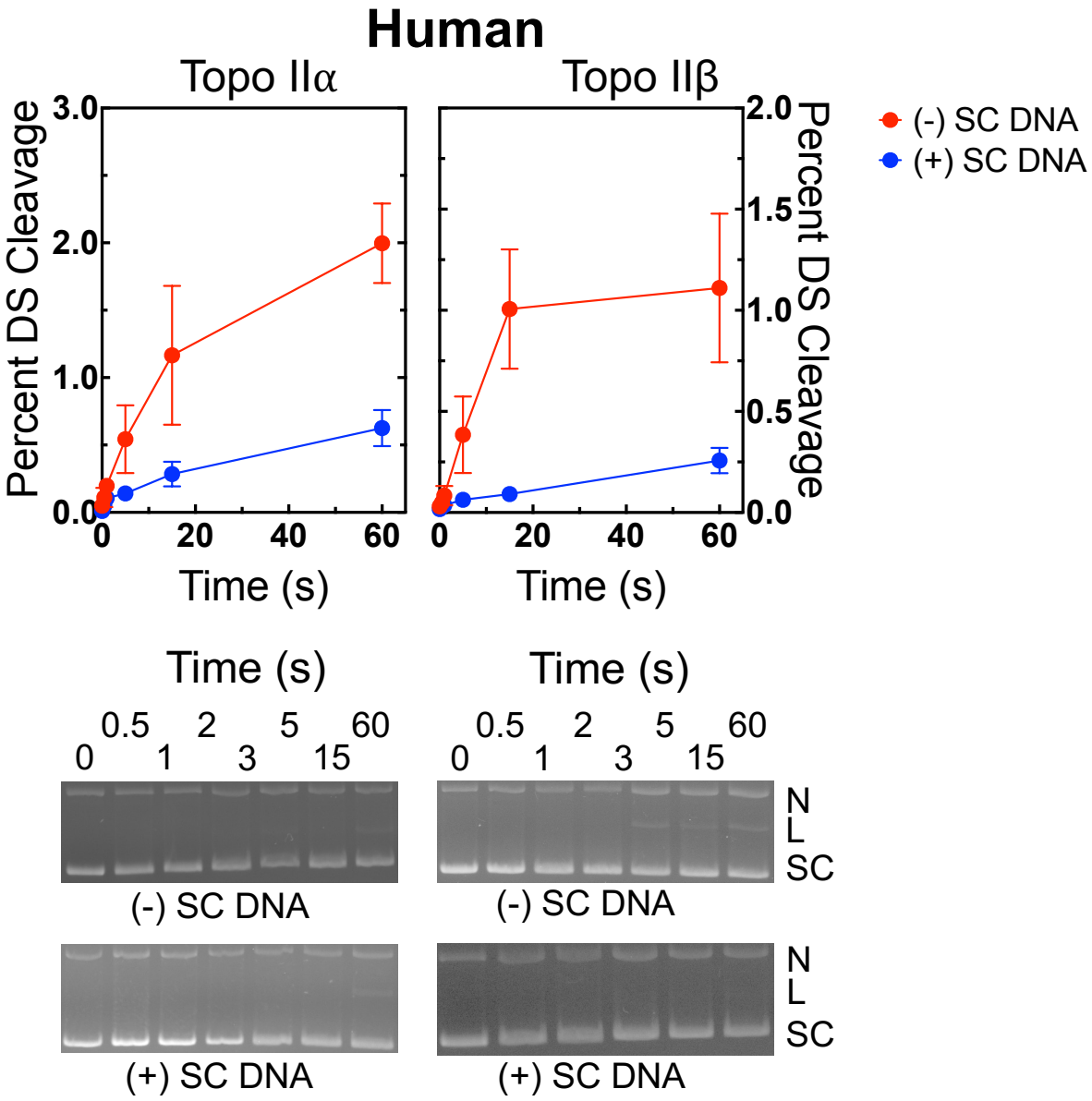

Figure 2.22. Effects of supercoil geometry on initial rates of DNA cleavage mediated by human type II topoisomerases in the presence of drugs. Initial rates of DNA cleavage mediated by human topoisomerase IIα (Topo IIα, left), and IIβ (Topo IIβ, right) are shown. Experiments were carried out with (-)SC (red) or (+)SC (blue) pBR322 DNA. Representative gel images for human topoisomerase IIα and IIβ with (-)SC or (+)SC DNA in the presence of drug are shown. The positions of supercoiled (SC), nicked (N), and linear (L) DNA are indicated. Error bars represent the standard deviation of at least three independent assays. Rates are displayed in Table 2.5.

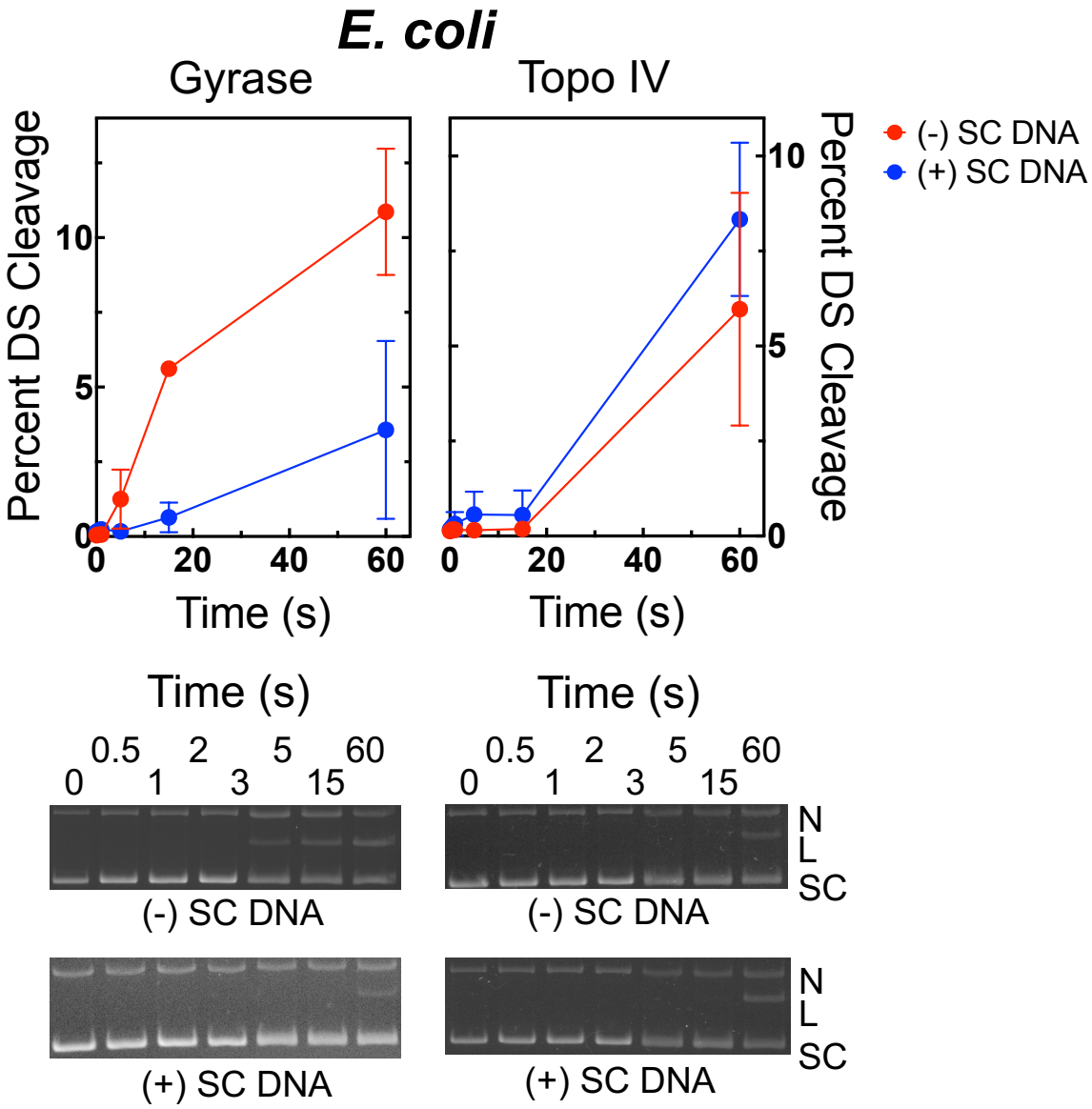

Figure 2.23. Effects of supercoil geometry on initial rates of DNA cleavage mediated by bacterial type II topoisomerases in the presence of drugs. Initial rates of DNA cleavage mediated by *E. coli* gyrase (left) and topoisomerase IV (Topo IV, right) are shown. Experiments were carried out with (-)SC (red) or (+)SC (blue) pBR322 DNA. Representative gel images for *E. coli* gyrase and topoisomerase IV cleavage with (-)SC or (+)SC DNA in the presence of drug are shown. The positions of supercoiled (SC), nicked (N), and linear (L) DNA are indicated. Error bars represent the standard deviation of at least three independent assays. Rates are displayed in Table 2.5.

Species	Enzyme	Setup	Drug	DNA Type	Rate (k) (%/min)
Human	IIα	Benchtop	Etoposide	(-) SC	0.97
		Benchtop		(+) SC	0.46
Human	IIβ	Benchtop	Etoposide	(-) SC	0.25
		Benchtop		(+) SC	0.13
E. coli	Gyrase	Benchtop	Ciprofloxacin	(-) SC	0.32
		Benchtop		(+) SC	0.16
E. coli	Topo IV	Benchtop	Ciprofloxacin	(-) SC	0.56
		Benchtop		(+) SC	0.43
Human	IIα	RQF	Etoposide	(-) SC	3.6
		RQF		(+) SC	1.8
Human	IIβ	RQF	Etoposide	(-) SC	6
		RQF		(+) SC	1.2
E. coli	Gyrase	RQF	Ciprofloxacin	(-) SC	1.8
		RQF		(+) SC	0.012
E. coli	Topo IV	RQF	Ciprofloxacin	(-) SC	0.006
		RQF		(+) SC	0.005

Table 2.5: k values for Figures 2.20–2.23

Table 2.5. Effects of supercoil geometry on forward rates of DNA cleavage generated by human and bacterial type II topoisomerases in the presence of stabilizing drugs. Forward rates of DNA cleavage, represented by rate (k; %/min), by human topoisomerase IIα and human topoisomerase IIβ, and *E. coli* gyrase and topoisomerase IV with (-)SC (red) or (+)SC (blue) DNA in the presence of stabilizing drug are shown. Experiments were either performed via benchtop assays or, to measure initial rates, via rapid-quench flow (RQF).

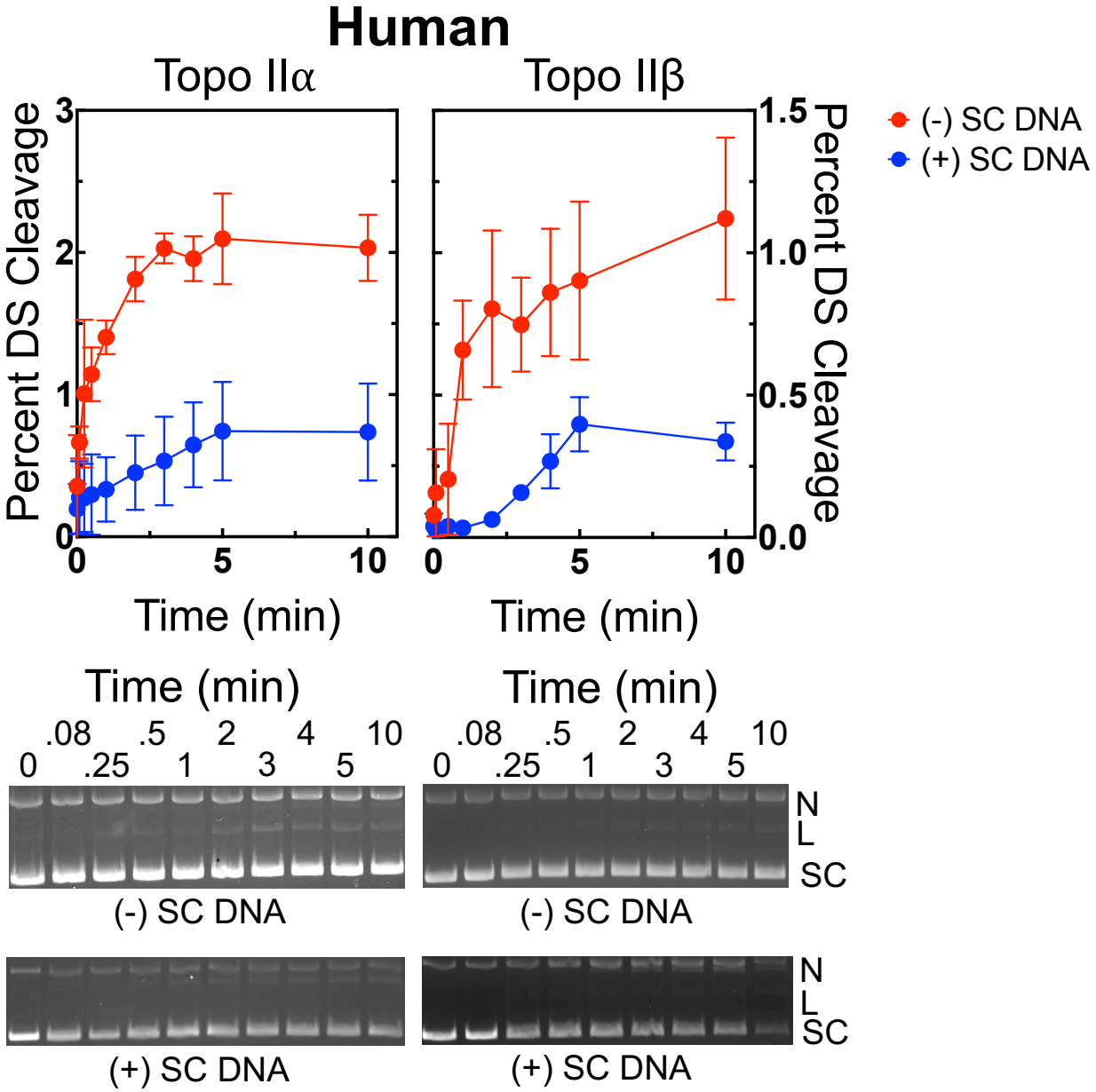

Figure 2.24. Effects of supercoil geometry on rates of DNA cleavage mediated by human type II topoisomerases in the absence of drugs. Rates of DNA cleavage mediated by human topoisomerase IIα (Topo IIα, left) and IIβ (Topo IIβ, right) are shown. Experiments were carried out with (-)SC (red) or (+)SC (blue) pBR322 DNA. Representative gel images for human topoisomerase IIα and topoisomerase IIβ cleavage with (-)SC or (+)SC DNA in the absence of drug are shown. The positions of supercoiled (SC), nicked (N), and linear (L) DNA are indicated. Error bars represent the standard deviation of at least three independent assays. Initial rates of DNA cleavage are displayed in Table 2.6.

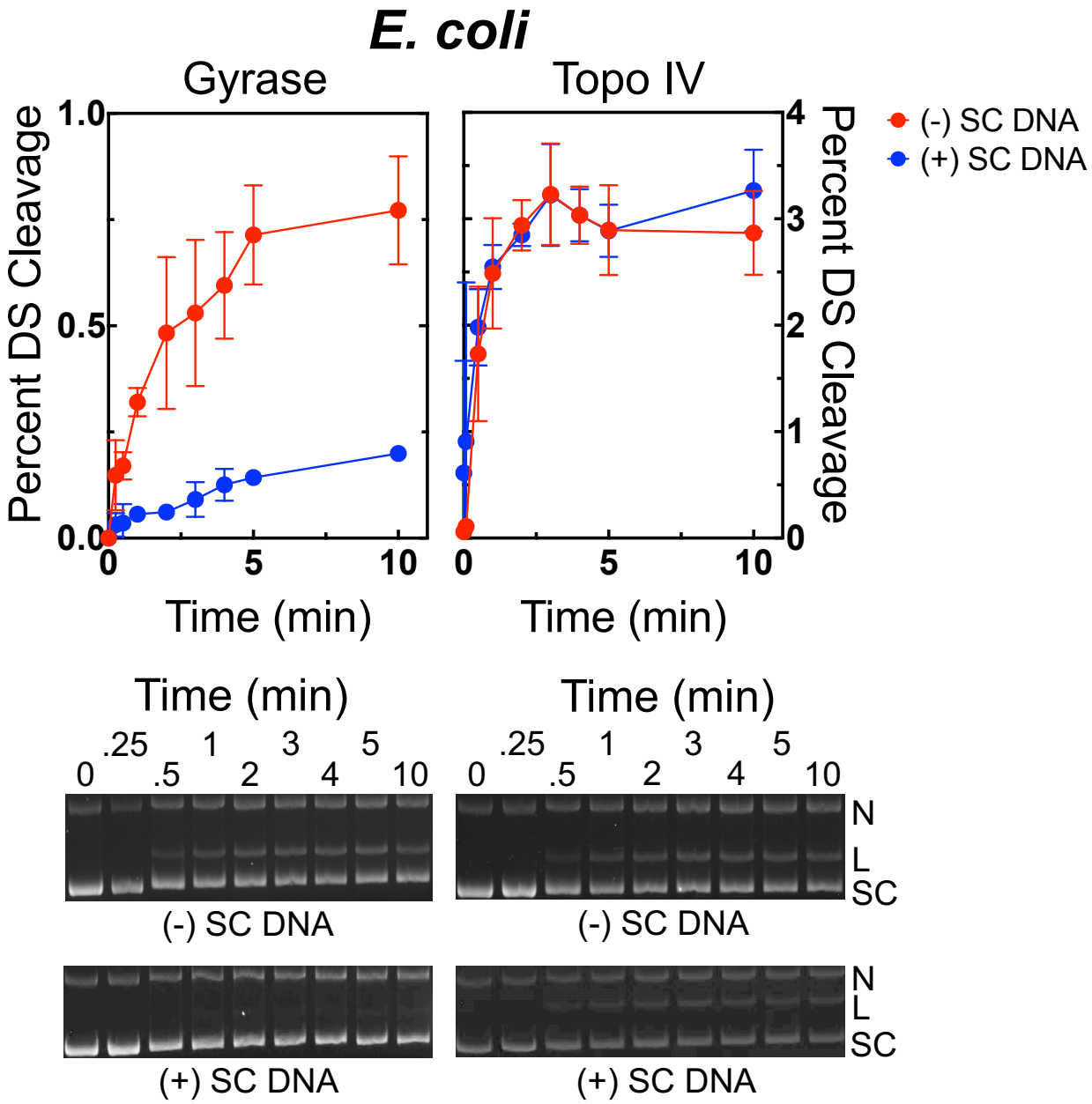

Figure 2.25. Effects of supercoil geometry on rates of DNA cleavage mediated by bacterial type II topoisomerases in the absence of drugs. Rates of DNA cleavage mediated by *E. coli* gyrase (left) and topoisomerase IV (Topo IV, right) are shown. Experiments were carried out with (-)SC (red) or (+)SC (blue) pBR322 DNA. Representative gel images for *E. coli* gyrase and topoisomerase IV cleavage with (-)SC or (+)SC DNA in the absence of drug are shown. The positions of supercoiled (SC), nicked (N), and linear (L) DNA are indicated. Error bars represent the standard deviation of at least three independent assays. Initial rates of DNA cleavage are displayed in Table 2.6.

Species	Enzyme	DNA Type	Rate (k)
Human	IIα	(-) SC	2.00
		(+) SC	0.76
Human	IIβ	(-) SC	0.72
		(+) SC	0.19
E. coli	Gyrase	(-) SC	0.48
		(+) SC	0.19
E. coli	Topo IV	(-) SC	0.41
		(+) SC	0.32

Table 2.6: k values for Figures 2.24–2.25

Table 2.6. Effects of supercoil geometry on forward rates of DNA cleavage generated by human and bacterial type II topoisomerases in the absence of stabilizing drugs. Forward rates of DNA cleavage, represented by rate (k; %/min), by human topoisomerase IIα and human topoisomerase IIβ, and *E. coli* gyrase and topoisomerase IV with (-)SC (red) or (+)SC (blue) DNA in the absence of stabilizing drug are shown. Experiments were performed using benchtop assays.

DISCUSSION

As mentioned earlier, several type II topoisomerases recognize supercoil handedness of DNA during enzymatic function. Human topoisomerase IIα and human topoisomerase IIβ preferentially relax (-)SC over (+)SC DNA. Bacterial gyrase and topoisomerase IV preferentially relax (+)SC DNA. Both human topoisomerase IIα and human topoisomerase IIβ, as well as bacterial gyrase from *E. coli*, *B. anthracis*, and *M. tuberculosis* preferentially cleave (-)SC over (+)SC DNA. Bacterial topoisomerase IV does not discriminate supercoil handedness during the cleavage reaction. The ability to recognize supercoil handedness is an important property of type II enzymes that potentially function on the overwound DNA ahead of replication forks, transcription complexes, or other tracking systems, as it makes them safer enzymes. Indeed, studies that mapped drug-induced topoisomerase IIα-DNA cleavage sites in human cells (Yu, Davenport et al. 2017) and gyrase-DNA cleavage sites in *E. coli* cells (Sutormin, Rubanova et al. 2019) found that these sites were enriched in regions of the genome that likely would be positively supercoiled during transcription elongation. The lower levels of cleavage complexes maintained by these enzymes on overwound vs underwound DNA makes them safer for cells (Figures 3 and 4). Conversely, bacterial topoisomerase IV, which works primarily behind replication forks, does not distinguish supercoil handedness during cleavage and maintains similar levels of cleavage complexes with underwound and overwound DNA (Ashley, Dittmore et al. 2017). Despite the importance of supercoil geometry to the functions of type II topoisomerases, the underlying basis for the recognition of supercoil handedness has not been determined previously.

Across all enzymes and species examined, there was a strong relationship between levels of DNA cleavage with substrates of different supercoil handedness and rates of DNA scission (k_2) in the presence or absence of drugs. The three enzymes that maintained lower levels of cleavage

complexes with (+)SC DNA (human topoisomerase IIα, human topoisomerase IIβ, gyrase) also displayed lower rates of cleavage. Conversely, topoisomerase IV, which maintained similar levels of cleavage with underwound and overwound DNA, displayed comparable rates of cleavage with both substrates. This finding suggests that human topoisomerase IIα and IIβ, and bacterial gyrase maintain higher levels of cleavage complexes with (-)SC DNA, at least in part, because they cleave the DNA more rapidly. In contrast, rates of religation appear to play no substantial role in the ability to distinguish supercoil handedness during DNA cleavage in the absence or presence of drugs.

A different result was found for the persistence of total enzyme-DNA complexes (E•S + E–S*) formed in the presence of anticancer/antibacterial drugs. In these cases, topoisomerase IIα and gyrase formed more stable cleavage complexes with (-)SC DNA. This result suggests that under certain circumstances, cleavage complex stability may also contribute to the ability of type II enzymes to distinguish supercoil geometry. However, this was not the case for human topoisomerase IIβ, which primarily relies on forward rates of cleavage in order to discriminate between (-)SC and (+)SC DNA.

Previous studies have identified the C-terminal domain of human and bacterial type II topoisomerases as being crucial for the recognition of supercoil handedness during the double-stranded DNA passage reaction (McClendon, Dickey et al. 2006, McClendon, Gentry et al. 2008, Seol, Gentry et al. 2013, Vos, Lee et al. 2013, Ashley, Blower et al. 2017, Ashley, Dittmore et al. 2017). Furthermore, at least with human topoisomerase IIα, the ability to recognize supercoil handedness depends on DNA writhe as opposed to twist (Seol, Gentry et al. 2013). It has been proposed that the differences in the crossover angles between (+)SC and (-)SC substrates control

interactions between the DNA and the C-terminal domain that enhance the rate of double-stranded DNA passage with (+)SC DNA.

In contrast to the above, the structural elements in type II topoisomerases that allow the enzymes to distinguish supercoil geometry during cleavage are not obvious. As determined by deletion and mutagenesis studies, the C-terminal domain does not appear to play a role in the ability of type II topoisomerases to distinguish DNA supercoil geometry during the cleavage event (McClendon, Dickey et al. 2006, McClendon, Gentry et al. 2008, Ashley, Blower et al. 2017, Ashley, Dittmore et al. 2017). Although elements in the N-terminal domain of *M. tuberculosis* gyrase may be necessary for the recognition of supercoil handedness during cleavage (Ashley, Blower et al. 2017), this property of the enzyme is embedded in the catalytic core of human topoisomerase IIα and IIβ (Lindsey, Pendleton et al. 2014). Given that the catalytic cores of the human type II enzymes lack the structural elements of the C-terminal domain that are involved in the recognition of DNA writhe (Seol, Gentry et al. 2013), it is not apparent how writhe could be contributing to the recognition of supercoil geometry during cleavage. An intriguing possibility is that this recognition of supercoil handedness is dependent on DNA twist. To this point, the angle of gate opening during the double-stranded DNA passage reaction should align with the directionality of torsional stress in underwound (i.e., negatively supercoiled) DNA (Schmidt, Osheroff et al. 2012). Conversely, the directionality of overwound (i.e., positively supercoiled) DNA should oppose gate opening. Further studies will be necessary to better understand the roles of twist and writhe in the recognition of supercoil geometry during DNA cleavage.

Taken together, our results provide at least a partial mechanism that explains the differential abilities of human and bacterial type II topoisomerases to distinguish supercoil handedness during the DNA cleavage reaction. This ability to recognize DNA geometry

contributes to the safety of type II topoisomerases and impacts the clinical efficacy of anticancer and antibacterial drugs.

CHAPTER 3

CONCLUSIONS AND IMPLICATIONS

The Recognition of DNA Supercoil Handedness During the Cleavage Reaction

As mentioned in Chapter 1, the genomes of humans and bacterial species are globally underwound (i.e., negatively supercoiled) (Bates and Maxwell 2005, Linka, Porter et al. 2007, Deweese and Osheroff 2009). Despite this, regions of DNA that are downstream from replication forks, transcription complexes, and other DNA tracking machinery can become increasingly overwound (i.e., positively supercoiled) (Linka, Porter et al. 2007, Deweese and Osheroff 2009, Baxter, Sen et al. 2011). These differences in supercoil handedness can have profound effects on nucleic acid processes. The process of maintaining a globally underwound topological state and removing potentially dangerous overwound topological structures thus requires specialized enzymes known as type II topoisomerases (Bates and Maxwell 2005, Deweese and Osheroff 2009). However, the essential catalytic functions of these very same enzymes generate the requisite, but potentially dangerous, structures known as cleavage complexes. Given that the formation of cleavage complexes may be more lethal with (+)SC over (-)SC, it is important to understand how type II topoisomerases can recognize DNA supercoil handedness when performing the DNA cleavage reaction.

Prior research has demonstrated that human type II topoisomerases and bacterial gyrase from *E. coli*, *B. anthracis*, and *M. tuberculosis* preferentially cleave (-)SC over (+)SC DNA (McClendon, Rodriguez et al. 2005, McClendon and Osheroff 2006, Ashley, Blower et al. 2017, Ashley, Dittmore et al. 2017). Bacterial topoisomerase IV from these same species does not

differentiate supercoil handedness during cleavage (Ashley, Dittmore et al. 2017). The work in this dissertation sought to understand the basis of the differential recognition of supercoil handedness by type II topoisomerases during the DNA cleavage reaction. Upon evaluating the individual steps of the forward cleavage reaction, the forward rate of cleavage appeared to be the determining factor as to differences in levels of cleavage. Human type II topoisomerases and gyrase maintain higher levels of cleavage with (-)SC DNA because these enzymes cleave underwound substrates faster. These differences in rates of cleavage may have implications when placed into the context of biological systems. The human type II topoisomerases and bacterial gyrase relax (+)SC DNA faster and maintain lower levels of cleavage complexes with overwound substrates. Additionally, their ability to discriminate supercoil handedness in the presence of drugs is also reflected in their short enzyme-DNA complex lifetimes when formed on (+)SC DNA. As such, these enzymes can more safely act upon overwound substrates that form ahead of replication forks and transcription complexes. These data may support the idea that some type II topoisomerases are predisposed towards maintaining genomic integrity while regulating global levels of negative supercoiling.

One interesting avenue of further research would aim to understand how type II topoisomerases are able to cleave (+)SC DNA less yet relax overwound substrates faster. A possible explanation for this would be that cleavage of (+)SC DNA is not as thermodynamically favorable due to the directionality of the DNA supercoil. Based on handedness, (+)SC DNA could be harder to "open" during scission, and thus less cleavage would occur; relaxation would have a smaller "window of opportunity" for strand passage, and thus would need to be carried out more rapidly. In contrast to overwound substrates, (-)SC DNA may be more predisposed to be cleaved, and thus the cleavage complex would be more stable. The reasoning for this difference between

(+)SC and (-)SC DNA could be attributable to the different directions (i.e., crossover angles) that the DNA gates open. The crossover angle at which the (+)SC DNA gate opens may generate a physical force "vector" that acts against the direction of enzyme activity. Conversely, the (-)SC DNA gate may be more easily opened if the directionality of the force "vector" aligns with that of the type II enzyme. To better understand the physical forces of gate opening that may be at play, single-molecule experiments may be necessary to interrogate the behaviors of supercoil handedness during formation of the DNA gate while also quantifying physical forces. Studying the contributions of supercoil directionality may thus shed greater light towards reconciling the above questions.

Overall, this dissertation has described experiments performed using techniques of classical biochemistry. Although these methods have been critical to our broad understanding of each of the steps in the type II topoisomerase catalytic cycle, there are limitations to the scale of study and precision, namely, being able to study a few enzymes or drugs at a time or obtaining results of *in vitro* experiments that represent averages in ensemble experiments. With the application of computational biology and software programming, however, it has become possible to better interrogate enzyme function at single-nucleotide precision levels and with larger data sets. To this end, we are currently collaborating with Drs. Keir Neuman and Ian Morgan of the Neuman Lab at the National Institutes of Health to (1) identify the pBR322 DNA sequences that are cleaved by human and bacterial type II topoisomerases in the presence or absence of stabilizing drugs, (2) utilize enzyme kinetics to monitor changes in DNA cleavage site preference over the course of the reaction, (3) determine the contribution(s) of specific cleavage sites towards the stabilities of cleavage complexes, and (4) determine the contribution(s) of specific sequences to rates of initial DNA cleavage.

The applications of Next-Generation Sequencing (NGS) in the field of topoisomerases have gained traction in the last decade (Baranello, Kouzine et al. 2014, Yu, Davenport et al. 2017, Sutormin, Rubanova et al. 2019, McKie, Maxwell et al. 2020), as a way of studying large sets of type II topoisomerase cleavage data *in vivo*. Because DNA cleavage requires the formation of a covalently-bound enzyme-DNA complex, it has been possible to extract and identify the nucleic acid sequences during scission. Human and bacterial cellular *in vivo* experiments already have been successful in identifying the DNA sequences that are cleaved by type II enzymes. Here, we are applying NGS towards our pBR322 plasmid model with human and bacterial type II topoisomerases, in the presence or absence of drugs. This high-throughput approach would generate substantial volumes of data, across multiple species and enzyme types, and at single-nucleotide level resolution. It would be interesting to observe any, if at all, differences in preferred cleavage sites based on enzyme type or DNA supercoil handedness, and how sites of cleavage can potentially change over time. We anticipate that, as our protocol for NGS becomes more streamlined, it will become possible to obtain a more precise and dynamic cleavage landscape for type II topoisomerases.

References

Ahmad, M., W. Shen, W. Li, Y. Xue, S. Zou, D. Xu and W. Wang (2017). "Topoisomerase 3β is the major topoisomerase for mRNAs and linked to neurodevelopment and mental dysfunction." *Nucleic Acids Res.* **45**(5): 2704-2713.

Aldred, K. J., T. R. Blower, R. J. Kerns, J. M. Berger and N. Osheroff (2016). "Fluoroquinolone interactions with *Mycobacterium tuberculosis* gyrase: Enhancing drug activity against wild-type and resistant gyrase." *Proc. Natl. Acad. Sci. U.S.A.* **113**(7): E839-846.

Aldred, K. J., E. J. Breland, V. Vlckova, M. P. Strub, K. C. Neuman, R. J. Kerns and N. Osheroff (2014). "Role of the water-metal ion bridge in mediating interactions between quinolones and *Escherichia coli* topoisomerase IV." *Biochemistry* **53**(34): 5558-5567.

Aldred, K. J., R. J. Kerns and N. Osheroff (2014). "Mechanism of quinolone action and resistance." *Biochemistry* **53**(10): 1565-1574.

Aldred, K. J., S. A. McPherson, P. Wang, R. J. Kerns, D. E. Graves, C. L. Turnbough, Jr. and N. Osheroff (2012). "Drug interactions with *Bacillus anthracis* topoisomerase IV: biochemical basis for quinolone action and resistance." *Biochemistry* **51**(1): 370-381.

Anderson, V. E. and N. Osheroff (2001). "Type II topoisomerases as targets for quinolone antibacterials: turning Dr. Jekyll into Mr. Hyde." *Curr. Pharm. Des.* **7**(5): 337-353.

Andriole, V. T. (2005). "The quinolones: past, present, and future." *Clin. Infect. Dis.* **41 Suppl. 2**: S113-119.

Antoniou-Kourounioti, M., M. L. Mimmack, A. C. G. Porter and C. J. Farr (2019). "The impact of the C-terminal region on the interaction of topoisomerase IIα with mitotic chromatin." *Int. J. Mol. Sci.* **20**(5).

Aravind, L., D. D. Leipe and E. V. Koonin (1998). "Toprim - a conserved catalytic domain in type IA and II topoisomerases, DnaG-type primases, OLD family nucleases and RecR proteins." *Nucleic Acids Res.* **26**: 4205-4213.

Ashley, R. E., T. R. Blower, J. M. Berger and N. Osheroff (2017). "Recognition of DNA supercoil geometry by *Mycobacterium tuberculosis* gyrase." *Biochemistry* **56**(40): 5440-5448.

Ashley, R. E., A. Dittmore, S. A. McPherson, C. L. Turnbough, Jr., K. C. Neuman and N. Osheroff (2017). "Activities of gyrase and topoisomerase IV on positively supercoiled DNA." *Nucleic Acids Res.* **45**(16): 9611-9624.

Ashley, R. E., R. H. Lindsey, Jr., S. A. McPherson, C. L. Turnbough, Jr., R. J. Kerns and N. Osheroff (2017). "Interactions between quinolones and *Bacillus anthracis* gyrase and the basis of drug resistance." *Biochemistry* **56**(32): 4191-4200.

Ashley, R. E. and N. Osheroff (2019). "Regulation of DNA topology by topoisomerases: Mathematics at the molecular level." 411-433.

Austin, C. A., K. C. Lee, R. L. Swan, M. M. Khazeem, C. M. Manville, P. Cridland, A. Treumann, A. Porter, N. J. Morris and I. G. Cowell (2018). "TOP2B: the first thirty years." *Int. J. Mol. Sci.* **19**(9): 2765-2786.

Austin, C. A. and K. L. Marsh (1998). "Eukaryotic DNA topoisomerase IIβ." *Bioessays* **20**: 215-226.

Austin, C. A., J. H. Sng, S. Patel and L. M. Fisher (1993). "Novel HeLa topoisomerase II is the IIβ isoform: complete coding sequence and homology with other type II topoisomerases." *Biochim. Biophys. Acta* **1172**(3): 283-291.

Azarova, A. M., Y. L. Lyu, C. P. Lin, Y. C. Tsai, J. Y. Lau, J. C. Wang and L. F. Liu (2007). "Roles of DNA topoisomerase II isozymes in chemotherapy and secondary malignancies." *Proc. Natl. Acad. Sci. U.S.A.* **104**(26): 11014-11019.

Baguley, B. C. and L. R. Ferguson (1998). "Mutagenic properties of topoisomerase-targeted drugs." *Biochim. Biophys. Acta* **1400**(1-3): 213-222.

Bakshi, R. P., S. Galande and K. Muniyappa (2001). "Functional and regulatory characteristics of eukaryotic type II DNA topoisomerases." *Crit. Rev. Biochem. Mol. Biol.* **36**(1): 1-37.

Baldwin, E. L. and N. Osheroff (2005). "Etoposide, topoisomerase II and cancer." *Curr. Med. Chem. Anticancer Agents* **5**(4): 363-372.

Bandele, O. J. and N. Osheroff (2008). "The efficacy of topoisomerase II-targeted anticancer agents reflects the persistence of drug-induced cleavage complexes in cells." *Biochemistry* **47**(45): 11900-11908.

Baranello, L., F. Kouzine, D. Wojtowicz, K. Cui, T. M. Przytycka, K. Zhao and D. Levens (2014). "DNA break mapping reveals topoisomerase II activity genome-wide." *Int. J. Mol. Sci.* **15**(7): 13111-13122.

Barret, J. M., A. Kruczynski, S. Vispe, J. P. Annereau, V. Brel, Y. Guminski, J. G. Delcros, A. Lansiaux, N. Guilbaud, T. Imbert and C. Bailly (2008). "F14512, a potent antitumor agent targeting topoisomerase II vectored into cancer cells via the polyamine transport system." *Cancer Res* **68**(23): 9845-9853.

Bates, A. D. and A. Maxwell (2005). *DNA Topology*. New York, USA, Oxford University Press.

Bauer, D. L. V., R. Marie, K. H. Rasmussen, A. Kristensen and K. U. Mir (2012). "DNA catenation maintains structure of human metaphase chromosomes." *Nucleic Acids Research* **40**(22): 11428-11434.

Bauer, W. R., F. H. Crick and J. H. White (1980). "Supercoiled DNA." *Sci. Am.* **243**(1): 100-113.

Bax, B. D., P. F. Chan, D. S. Eggleston, A. Fosberry, D. R. Gentry, F. Gorrec, I. Giordano, M. M. Hann, A. Hennessy, M. Hibbs, J. Huang, E. Jones, J. Jones, K. K. Brown, C. J. Lewis, E. W. May, M. R. Saunders, O. Singh, C. E. Spitzfaden, C. Shen, A. Shillings, A. J. Theobald, A. Wohlkonig, N. D. Pearson and M. N. Gwynn (2010). "Type IIA topoisomerase inhibition by a new class of antibacterial agents." *Nature* **466**(7309): 935-940.

Bax, B. D., G. Murshudov, A. Maxwell and T. Germe (2019). "DNA topoisomerase inhibitors: trapping a DNA-cleaving machine in motion." *J. Mol. Biol.* **431**(18): 3427-3449.

Baxter, J. and J. F. Diffley (2008). "Topoisomerase II inactivation prevents the completion of DNA replication in budding yeast." *Mol Cell* **30**(6): 790-802.

Baxter, J., N. Sen, V. L. Martinez, M. E. De Carandini, J. B. Schvartzman, J. F. Diffley and L. Aragon (2011). "Positive supercoiling of mitotic DNA drives decatenation by topoisomerase II in eukaryotes." *Science* **331**(6022): 1328-1332.

Bergerat, A., B. de Massy, D. Gadelle, P. C. Varoutas, A. Nicolas and P. Forterre (1997). "An atypical topoisomerases II from Archaea with implications for meiotic recombination." *Nature* **386**: 414-417.

Bergerat, A., D. Gadelle and P. Forterre (1994). "Purification of a DNA topoisomerase II from the hyperthermophilic archaeon *Sulfolobus shibatae*. A thermostable enzyme with both bacterial and eucaryal features." *J. Biol. Chem.* **269**(44): 27663-27669.

Biedenbach, D. J., S. K. Bouchillon, M. Hackel, L. A. Miller, N. E. Scangarella-Oman, C. Jakielaszek and D. F. Sahm (2016). "*In vitro* activity of gepotidacin, a novel triazaacenaphthylene bacterial topoisomerase inhibitor, against a broad spectrum of bacterial pathogens." *Antimicrob. Agents Chemother.* **60**(3): 1918-1923.

Bollimpelli, V. S., P. S. Dholaniya and A. K. Kondapi (2017). "Topoisomerase IIβ and its role in different biological contexts." *Arch. Biochem. Biophys.* **633**: 78-84.

Brill, S. J., S. DiNardo, K. Voelkel-Meiman and R. Sternglanz (1987). "Need for DNA topoisomerase activity as a swivel for DNA replication for transcription of ribosomal RNA." *Nature* **326**(6111): 414-416.

Bromberg, K. D. and N. Osheroff (2001). "DNA Cleavage and Religation by Human Topoisomerase IIα at High Temperature." *Biochemistry* **40**: 8410-8418.

Buck, D. (2009). DNA topology. *Applications of knot theory (Proc. Sympos. Appl. Math., 2009)*. D. Buck and E. Flapan. Providence, American Mathematical Society. **66:** 47-79.

Champoux, J. J. and R. Dulbecco (1972). "An activity from mammalian cells that untwists superhelical DNA--a possible swivel for DNA replication (polyoma-ethidium bromide-mouse-embryo cells-dye binding assay)." *Proc. Natl. Acad. Sci. U.S.A.* **69**(1): 143-146.

Chang, C. C., Y. R. Wang, S. F. Chen, C. C. Wu and N. L. Chan (2013). "New insights into DNA-binding by type IIA topoisomerases." *Curr. Opin. Struct. Biol.* **23**(1): 125-133.

Chen, S. H., N.-L. Chan and T.-S. Hsieh (2013). "New mechanistic and functional insights into DNA topoisomerases." *Ann. Rev. Biochem.* **82**(1): 139-170.

Chen, W., J. Qiu and Y. M. Shen (2012). "Topoisomerase IIα, rather than IIβ, is a promising target in development of anti-cancer drugs." *Drug Discov. Ther.* **6**(5): 230-237.

Christensen, M. O., M. K. Larsen, H. U. Barthelmes, R. Hock, C. L. Andersen, E. Kjeldsen, B. R. Knudsen, O. Westergaard, F. Boege and C. Mielke (2002). "Dynamics of human DNA topoisomerases IIα and IIβ in living cells." *J. Cell Biol.* **157**(1): 31-44.

Confalonieri, F., C. Elie, M. Nadal, C. de La Tour, P. Forterre and M. Duguet (1993). "Reverse gyrase: a helicase-like domain and a type I topoisomerase in the same polypeptide." *Proc. Nat. Acad. Sci. U.S.A.* **90**(10): 4753-4757.

Corbett, K. D. and J. M. Berger (2003). "Structure of the topoisomerase VI-B subunit: implications for type II topoisomerase mechanism and evolution." *EMBO J.* **22**(1): 151-163.

Corbett, K. D. and J. M. Berger (2004). "Structure, molecular mechanisms, and evolutionary relationships in DNA topoisomerases." *Annu. Rev. Biophys. Biomol. Struct.* **33**: 95-118.

Corbett, K. D. and J. M. Berger (2005). " Structural dissection of ATP turnover in the prototypical GHL ATPase TopoVI." *Structure* **13**(6): 873-882.

Corbett, K. D., A. J. Schoeffler, N. D. Thomsen and J. M. Berger (2005). "The structural basis for substrate specificity in DNA topoisomerase IV." *J Mol Biol* **351**(3): 545-561.

Corbett, K. D., R. K. Shultzaberger and J. M. Berger (2004). "The C-terminal domain of DNA gyrase A adopts a DNA-bending beta-pinwheel fold." *Proc Natl Acad Sci U S A* **101**(19): 7293-7298.

Cowell, I. G., Z. Sondka, K. Smith, K. C. Lee, C. M. Manville, M. Sidorczuk-Lesthuruge, H. A. Rance, K. Padget, G. H. Jackson, N. Adachi and C. A. Austin (2012). "Model for MLL translocations in therapy-related leukemia involving topoisomerase IIβ-mediated DNA strand breaks and gene proximity." *Proc. Natl. Acad. Sci. U.S.A.* **109**(23): 8989-8994.

Crisona, N. J., T. R. Strick, D. Bensimon, V. Croquette and N. R. Cozzarelli (2000). "Preferential relaxation of positively supercoiled DNA by *E. coli* topoisomerase IV in single-molecule and ensemble measurements." *Genes Dev.* **14**(22): 2881-2892.

Dalvie, E. D., J. Gopas, A. Golan-Goldhirsh and N. Osheroff (2019). "6,6'-Dihydroxythiobinupharidine as a poison of human type II topoisomerases." *Bioorg. Med. Chem. Lett.* **29**(15): 1881-1885.

Dalvie, E. D. and N. Osheroff (2021). DNA Recognition/Processing | DNA Topoisomerases: Type II☆. *Encyclopedia of Biological Chemistry III (Third Edition)*. J. Jez. Oxford, Elsevier**:** 479-486.

Dalvie, E. D., J. C. Stacy, K. C. Neuman and N. Osheroff (2022). "Recognition of DNA supercoil handedness during catenation catalyzed by type II topoisomerases." *Biochemistry* **61**(19): 2148-2158.

Delgado, J. L., C. M. Hsieh, N. L. Chan and H. Hiasa (2018). "Topoisomerases as anticancer targets." *Biochem J* **475**(2): 373-398.

Dereuddre, S., C. Delaporte and A. Jacquemin-Sablon (1997). "Role of topoisomerase II beta in the resistance of 9-OH-ellipticine-resistant Chinese hamster fibroblasts to topoisomerase II inhibitors." *Cancer Res.* **57**(19): 4301-4308.

Deweese, J. E., A. B. Burgin and N. Osheroff (2008). "Using 3'-bridging phosphorothiolates to isolate the forward DNA cleavage reaction of human topoisomerase IIα." *Biochemistry* **47**(13): 4129-4140.

Deweese, J. E., F. P. Guengerich, A. B. Burgin and N. Osheroff (2009). "Metal ion interactions in the DNA cleavage/ligation active site of human topoisomerase IIα." *Biochemistry* **48**(38): 8940-8947.

Deweese, J. E., M. A. Osheroff and N. Osheroff (2008). "DNA topology and topoisomerases: teaching a “knotty" subject." *Biochem. Mol. Biol. Educ.* **37**(1): 2-10.

Deweese, J. E., M. A. Osheroff and N. Osheroff (2009). "DNA topology and topoisomerases." *Biochemistry and Molecular Biology Education* **37**(1): 2-10.

Deweese, J. E. and N. Osheroff (2009). "The DNA cleavage reaction of topoisomerase II: Wolf in sheep's clothing." *Nucleic Acids Res.* **37**(3): 738-748.

Dickey, J. S. and N. Osheroff (2005). "Impact of the C-terminal domain of topoisomerase IIα on the DNA cleavage activity of the human enzyme." *Biochemistry* **44**(34): 11546-11154.

Dong, K. C. and J. M. Berger (2007). "Structural basis for gate-DNA recognition and bending by type IIA topoisomerases." *Nature* **450**(7173): 1201-1205.

Dong, S., S. A. McPherson, Y. Wang, M. Li, P. Wang, C. L. Turnbough, Jr. and D. G. Pritchard (2010). "Characterization of the enzymes encoded by the anthrose biosynthetic operon of Bacillus anthracis." *J Bacteriol* **192**(19): 5053-5062.

Dorman, C. J. and M. J. Dorman (2016). "DNA supercoiling is a fundamental regulatory principle
in the control of bacterial gene expression." *Biophys. Rev.* **8**(3): 209-220.

Dougherty, T. J., A. Nayar, J. V. Newman, S. Hopkins, G. G. Stone, M. Johnstone, A. B. Shapiro, M. Cronin, F. Reck and D. E. Ehmann (2014). "NBTI 5463 is a novel bacterial type II topoisomerase inhibitor with activity against gram-negative bacteria and *in vivo* efficacy." *Antimicrob. Agents Chemother.* **58**(5): 2657-2664.

Drlica, K., H. Hiasa, R. Kerns, M. Malik, A. Mustaev and X. Zhao (2009). "Quinolones: action and resistance updated." *Curr. Top. Med. Chem.* **9**(11): 981-998.

Drolet, M., S. Broccoli, F. Rallu, C. Hraiky, C. Fortin, E. Masse and I. Baalklini (2003). "The problem of hypernegative supercoiling and R-loop formation in transcription." *Front. Biosci.* **8**: 210-211.

Earnshaw, W. C., B. Halligan, C. A. Cooke, M. M. Heck and L. F. Liu (1985). "Topoisomerase II is a major component of mitotic chromosome scaffolds." *J. Cell Biol.* **100**: 1706-1715.

Ellis, R., S. Brown and M. Boggild (2015). "Therapy-related acute leukaemia with mitoxantrone: Four years on, what is the risk and can it be limited?" *Mult. Scler.* **21**(5): 642-645.

Espeli, O. and K. J. Marians (2004). "Untangling intracellular DNA topology." *Mol. Microbiol.* **52**(4): 925-931.

Ezoe, S. (2012). "Secondary leukemia associated with the anti-cancer agent, etoposide, a topoisomerase II inhibitor." *Int. J. Environ. Res. Public Health* **9**(7): 2444-2453.

Falaschi, A., G. Abdurashidova, O. Sandoval, S. Radulescu, G. Biamonti and S. Riva (2007). "Molecular and structural transactions at human DNA replication origins." *Cell Cycle* **6**(14): 1705-1712.

Felix, C. A. (2001). "Leukemias related to treatment with DNA topoisomerase II inhibitors." *Med. Pediatr. Oncol.* **36**(5): 525-535.

Felix, C. A., C. P. Kolaris and N. Osheroff (2006). "Topoisomerase II and the etiology of chromosomal translocations." *DNA Repair (Amst)* **5**(9-10): 1093-1108.

Finzi, L. and W. K. Olson (2016). "The emerging role of DNA supercoiling as a dynamic player in genomic structure and function." *Biophys. Rev.* **8**: 1-3.

Forterre, P. and D. Gadelle (2009). "Phylogenomics of DNA topoisomerases: their origin and putative roles in the emergence of modern organisms." *Nucleic Acids Res.* **37**(3): 679-692.

Forterre, P. and D. Gadelle (2009). "Phylogenomics of DNA topoisomerases: their origin and putative roles in the emergence of modern organisms." *Nucleic Acids Research* **37**(3): 679-692.

Forterre, P., S. Gribaldo, D. Gadelle and M. C. Serre (2007). "Origin and evolution of DNA topoisomerases." *Biochimie* **89**(4): 427-446.

Fortune, J. M. and N. Osheroff (2000). "Topoisomerase II as a target for anticancer drugs: When enzymes stop being nice." *Prog. Nucleic Acid Res. Mol .Biol.* **64**: 221-253.

Fortune, J. M., L. Velea, D. E. Graves, T. Utsugi, Y. Yamada and N. Osheroff (1999). "DNA topoisomerases as targets for the anticancer drug TAS-103: DNA interactions and topoisomerase catalytic inhibition." *Biochemistry* **38**(47): 15580-15586.

Gadelle, D., M. Krupovic, K. Raymann, C. Mayer and P. Forterre (2014). "DNA topoisomerase VIII: a novel subfamily of type IIB topoisomerases encoded by free or integrated plasmids in Archaea and Bacteria." *Nucleic Acids Res.* **42**(13): 8578-8591.

Gasser, S. M., T. Laroche, E. Boy de la Tour and U. K. Laemmli (1986). "Metaphase chromosome structure. Involvement of topoisomerase II." *J. Mol. Biol.* **188**(4): 613-629.

Gellert, M., K. Mizuuchi, M. H. O'Dea and H. A. Nash (1976). "DNA gyrase: an enzyme that introduces superhelical turns into DNA." *Proc. Natl. Acad. Sci. U.S.A.* **73**(11): 3872-3876.

Gentry, A. C. and N. Osheroff (2013). DNA topoisomerases: Type II. Encyc. Biol. Chem. a. L. M. D. Lennarz W.J. Waltham, MA, Academic Press. **2:** 163-168.

Gentry, A. C., S. L. Pitts, M. J. Jablonsky, C. Bailly, D. E. Graves and N. Osheroff (2011). "Interactions between the etoposide derivative F14512 and human type II topoisomerases: Implications for the C4 spermine moiety in promoting enzyme-mediated DNA cleavage." *Biochemistry* **50**(15): 3240-3249.

Gibson, E. G., R. E. Ashley, R. J. Kerns and N. Osheroff (2018). Bacterial Type II Topoisomerases and Target-Mediated Drug Resistance. *Antimicrobial Resistance in the 21st Century***:** 507-529.

Gibson, E. G., R. E. Ashley, R. J. Kerns and N. Osheroff (2018). Fluoroquinolone interactions with bacterial type II topoisomerases and target-mediated drug resistance. *Antimicrobial Resistance and Implications for the 21st Century*. K. Drlica, D. Shlaes and I. W. Fong. New York, Springer**:** 507-529.

Gibson, E. G., B. Bax, P. F. Chan and N. Osheroff (2019). "Mechanistic and structural basis for the actions of the antibacterial gepotidacin against *Staphylococcus aureus* gyrase." *ACS Infect. Dis.* **5**(4): 570-581.

Gibson, E. G., T. R. Blower, M. Cacho, B. Bax, J. M. Berger and N. Osheroff (2018). "Mechanism of action of *Mycobacterium tuberculosis* gyrase inhibitors: a novel class of gyrase poisons." *ACS Infect. Dis.* **4**(8): 1211-1222.

Goto-Ito, S., A. Yamagata, T. S. Takahashi, Y. Sato and S. Fukai (2017). "Structural basis of the interaction between Topoisomerase IIIβ and the TDRD3 auxiliary factor." *Sci. Rep.* **7**(42123).

Grue, P., A. Grasser, M. Sehested, P. B. Jensen, A. Uhse, T. Straub, W. Ness and F. Boege (1998). "Essential mitotic functions of DNA topoisomerase IIα are not adopted by topoisomerase IIβ in human H69 cells." *J. Biol. Chem.* **273**(50): 33660-33666.

Hande, K. R. (1998). "Clinical applications of anticancer drugs targeted to topoisomerase II." *Biochim. Biophys. Acta.* **1400**(1-3): 173-184.

Hande, K. R. (1998). "Etoposide: Four decades of development of a topoisomerase II inhibitor." *Eur. J. Cancer* **34**(10): 1514-1521.

Harmon, F. G., R. J. DiGate and S. C. Kowalczykowski (1999). "RecQ helicase and topoisomerase III comprise a novel DNA strand passage function: a conserved mechanism for control of DNA recombination." *Mol. Cell* **3**(5): 611-620.

Harrison, S. C. and A. K. Aggarwal (1990). "DNA recognition by proteins with the helix-turn-helix motif." *Annu. Rev. Biochem.* **59**: 933-969.

Hasan, S. K., A. N. Mays, T. Ottone, A. Ledda, G. La Nasa, C. Cattaneo, E. Borlenghi, L. Melillo, E. Montefusco, J. Cervera, C. Stephen, G. Satchi, A. Lennard, M. Libura, J. A. Byl, N.

Osheroff, S. Amadori, C. A. Felix, M. T. Voso, W. R. Sperr, J. Esteve, M. A. Sanz, D. Grimwade and F. Lo-Coco (2008). "Molecular analysis of t(15;17) genomic breakpoints in secondary acute promyelocytic leukemia arising after treatment of multiple sclerosis." *Blood* **112**(8): 3383-3390.

Heck, M. M. and W. C. Earnshaw (1986). "Topoisomerase II: A specific marker for cell proliferation." *J. Cell. Biol.* **103**(6 Pt 2): 2569-2581.

Heck, M. M., W. N. Hittelman and W. C. Earnshaw (1988). "Differential expression of DNA topoisomerases I and II during the eukaryotic cell cycle." *Proc. Natl. Acad. Sci. U.S.A.* **85**: 1086-1090.

Heintzman, D. R., L. V. Campos, J. A. W. Byl, N. Osheroff and J. M. Dewar (2019). "Topoisomerase II Is Crucial for Fork Convergence during Vertebrate Replication Termination." *Cell Rep* **29**(2): 422-436 e425.

Heintzman, D. R., L. V. Campos, J. A. W. Byl, N. Osheroff and J. M. Dewar (2019). "Topoisomerase II is crucial for fork convergence during vertebrate replication termination." *Cell Rep.* **29**(2): 422-436 e425.

Hiasa, H. (2018). "DNA topoisomerases as targets for antibacterial agents." *Methods Mol Biol* **1703**: 47-62.

Hiasa, H., R. J. DiGate and K. J. Marians (1994). "Decatenating activity of Escherichia coli DNA gyrase and topoisomerases I and III during oriC and pBR322 DNA replication in vitro." *J. Biol. Chem.* **269**(3): 2093-2099.

Hiasa, H. and K. J. Marians (1994). "Topoisomerase IV can support *oriC* DNA replication *in vitro*." *J. Biol. Chem.* **269**(23): 16371-16375.

Holm, C., T. Goto, J. C. Wang and D. Botstein (1985). "DNA topoisomerase II is required at the time of mitosis in yeast." *Cell* **41**(2): 553-563.

Hooper, D. C. (1998). "Clinical applications of quinolones." *Biochim. Biophys. Acta* **1400**: 45-61.

Hooper, D. C. (2001). "Mechanisms of action of antimicrobials: focus on fluoroquinolones." *Clin. Infect. Dis.* **32 Suppl. 1**: S9-S15.

Hooper, D. C. and G. A. Jacoby (2016). "Topoisomerase inhibitors: Fluoroquinolone mechanisms of action and resistance." *Cold Spring Harb. Perspect. Med.* **6**(9).

Howard, M. T., S. H. Neece, S. W. Matson and K. N. Kreuzer (1994). "Disruption of a topoisomerase-DNA cleavage complex by a DNA helicase." *Proc. Nat. Acad. Sci. U.S.A.* **91**(25): 12031-12035.

Hsiang, Y. H., H. Y. Wu and L. F. Liu (1988). "Proliferation-dependent regulation of DNA topoisomerase II in cultured human cells." *Cancer Res.* **48**(11): 3230-3235.

Hsu, Y. H., M. W. Chung and T. K. Li (2006). "Distribution of gyrase and topoisomerase IV on bacterial nucleoid: implications for nucleoid organization." *Nucleic Acids Res.* **34**: 3128-3138.

Isaacs, R. J., S. L. Davies, M. I. Sandri, C. Redwood, N. J. Wells and I. D. Hickson (1998). "Physiological regulation of eukaryotic topoisomerase II." *Biochim. Biophys. Acta* **1400**(1-3): 121-137.

Jang, Y., H. Son, S. W. Lee, W. Hwang, S. R. Jung, J. A. W. Byl, N. Osheroff and S. Lee (2019). "Selection of DNA cleavage sites by topoisomerase II results from enzyme-induced flexibility of DNA." *Cell. Chem. Biol.* **26**(4): 502-511 e503.

Joannides, M. and D. Grimwade (2010). "Molecular biology of therapy-related leukaemias." *Clin. Transl. Oncol.* **12**(1): 8-14.

Joannides, M., A. N. Mays, A. R. Mistry, S. H. Hasan, A. Reiter, J. L. Wiemels, C. A. Felix, F. L. Coco, N. Osheroff and E. Solomon (2011). "Molecular pathogenesis of secondary acute promyelocytic leukemia." *Mediterr. J. Hematol. Infect. Dis* . **3**(1).

Joannides, M., A. N. Mays, A. R. Mistry, S. K. Hasan, A. Reiter, J. L. Wiemels, C. A. Felix, F. L. Coco, N. Osheroff and E. Solomon (2011). "Molecular pathogenesis of secondary acute promyelocytic leukemia." *Mediterranean journal of hematology and infectious diseases* **3**(1).

Ju, B. G., V. V. Lunyak, V. Perissi, I. Garcia-Bassets, D. W. Rose, C. K. Glass and M. G. Rosenfeld (2006). "A topoisomerase IIβ-mediated dsDNA break required for regulated transcription." *Science* **312**(5781): 1798-1802.

Kampranis, S. C. and A. Maxwell (1996). "Conversion of DNA gyrase into a conventional type II topoisomerase." *Proc. Natl. Acad. Sci. U.S.A.* **93**(25): 14416-14421.

Kato, J., Y. Nishimura, R. Imamura, H. Niki, S. Hiraga and H. Suzuki (1990). "New topoisomerase essential for chromosome segregation in E. coli." *Cell* **63**(2): 393-404.

Kato, J., H. Suzuki and H. Ikeda (1992). "Purification and characterization of DNA topoisomerase IV in *Escherichia coli*." *J. Biol. Chem.* **267**(36): 25676-25684.

Ketron, A. C. and N. Osheroff (2014). DNA topology and topoisomerases. *Molecular Life Sciences: An Encyclopedic Reference*. E. Bell. New York, NY, Springer New York**:** 1-19.

Ketron, A. C. and N. Osheroff (2014). "Phytochemicals as anticancer and chemopreventive topoisomerase II poisons." *Phytochem. Rev.* **13**(1): 19-35.

Khodursky, A. B., B. J. Peter, M. B. Schmidt, J. DeRisi, D. Botstein, P. O. Brown and N. R. Cozzarelli (2000). "Analysis of topoisomerase function in bacterial replication fork movement: Use of DNA microarrays." *Proc. Nat. Acad. Sci. U.S.A.* **97**: 9419-9424.

Kikuchi, A. and K. Asai (1984). "Reverse gyrase - a topoisomerase which introduces positive superhelical turns into DNA." *Nature* **309**: 677-681.

Kim, R. A. and J. C. Wang (1989). "Function of DNA topoisomerases as replication swivels in Saccharomyces cerevisiae." *J Mol Biol* **208**(2): 257-267.

Kimura, K., M. Saijo, M. Ui and T. Enomoto (1994). "Growth state- and cell cycle-dependent fluctuation in the expression of two forms of DNA topoisomerase II and possible specific modification of the higher molecular weight form in the M phase." *J. Biol. Chem.* **269**: 1173-1176.

Kingma, P. S., C. A. Greider and N. Osheroff (1997). "Spontaneous DNA lesions poison human topoisomerase IIα and stimulate cleavage proximal to leukemic 11q23 chromosomal breakpoints." *Biochemistry*(36): 5934-5939.

Kornberg, A. and T. A. Baker (1992). *DNA replication*, Wh Freeman New York.

Koster, D. A., V. Croquette, C. Dekker, S. Shuman and N. H. Dekker (2005). "Friction and torque govern the relaxation of DNA supercoils by eukaryotic topoisomerase IB." *Nature* **434**: 671-674.

Kramlinger, V. M. and H. Hiasa (2006). "The "GyrA-box" is required for the ability of DNA gyrase to wrap DNA and catalyze the supercoiling reaction." *J. Biol. Chem.* **281**(6): 3738-3742.

Krogh, B. O. and S. Shuman (2002). "A poxvirus-like type IB topoisomerase family in bacteria." *Proc. Nat. Acad. Sci. U.S.A.* **99**(4): 1853-1858.

Kruczynski, A., I. Vandenberghe, A. Pillon, S. Pesnel, L. Goetsch, J. M. Barret, Y. Guminski, A. Le Pape, T. Imbert, C. Bailly and N. Guilbaud (2011). "Preclinical activity of F14512, designed to target tumors expressing an active polyamine transport system." *Invest New Drugs* **29**(1): 9-21.

Lanz, M. A. and D. Klostermeier (2012). "The GyrA-box determines the geometry of DNA bound to gyrase and couples DNA binding to the nucleotide cycle." *Nucleic Acids Res.* **40**(21): 10893-10903.

Lee, I., K. C. Dong and J. M. Berger (2013). "The role of DNA bending in type IIA topoisomerase function." *Nucleic Acids Res.* **41**(10): 5444-5456.

Lee, J. H. and J. M. Berger (2019). "Cell cycle-dependent control and roles of DNA topoisomerase II." *Genes (Basel)* **10**(11).

Lee, M. P., S. D. Brown, A. Chen and T.-S. Hsieh (1993). "DNA topoisomerase I is essential in *Drosophila melanogaster*." *Proc. Natl. Acad. Sci. U.S.A.* **90**(14): 6656-6660.

Lee, S., S. R. Jung, K. Heo, J. A. Byl, J. E. Deweese, N. Osheroff and S. Hohng (2012). "DNA cleavage and opening reactions of human topoisomerase IIα are regulated via Mg^{2+}-mediated dynamic bending of gate-DNA." *Proc. Natl. Acad. Sci. U.S.A.* **109**(8): 2925-2930.

Lesher, G. Y., E. J. Froelich, M. D. Gruett, J. H. Bailey and R. P. Brundage (1962). "1,8-naphthyridine derivatives. A new class of chemotherapeutic agents." *J. Med. Pharm. Chem.* **5**(5): 1063-1065.

Levine, C., H. Hiasa and K. J. Marians (1998). "DNA gyrase and topoisomerase IV: biochemical activities, physiological roles during chromosome replication, and drug sensitivities." *Biochim. Biophys. Acta.* **1400**(1-3): 29-43.

Li, Y., H. Hao, E. Tzatzalos, R. K. Lin, S. Doh, L. F. Liu, Y. L. Lyu and L. Cai (2014). "Topoisomerase IIbeta is required for proper retinal development and survival of postmitotic cells." *Biol. Open* **3**(2): 172-184.

Linder, J. A., E. S. Huang, M. A. Steinman, R. Gonzales and R. S. Stafford (2005). "Fluoroquinolone prescribing in the United States: 1995 to 2002." *Am. J. Med.* **118**(3): 259-268.

Lindsey, R. H., Jr., M. Pendleton, R. E. Ashley, S. L. Mercer, J. E. Deweese and N. Osheroff (2014). "Catalytic core of human topoisomerase IIα: insights into enzyme-DNA interactions and drug mechanism." *Biochemistry* **53**(41): 6595-65602.

Lindsley, J. E. and J. C. Wang (1993). "On the coupling between ATP usage and DNA transport by yeast DNA topoisomerase II." *J. Biol. Chem.* **268**(11): 8096-8104.

Linka, R. M., A. C. Porter, A. Volkov, C. Mielke, F. Boege and M. O. Christensen (2007). "C-terminal regions of topoisomerase IIα and IIβ determine isoform-specific functioning of the enzymes *in vivo*." *Nucleic Acids Res.* **35**(11): 3810-3822.

Liu, L. F. and J. C. Wang (1987). "Supercoiling of the DNA template during transcription." *Proc. Natl. Acad. Sci. U.S.A.* **84**(20): 7024-7027.

Liu, Z., R. W. Deibler, H. S. Chan and L. Zechiedrich (2009). "The why and how of DNA unlinking." *Nucleic Acids Res.* **37**(3): 661-671.

Lyu, Y. L., J. E. Kerrigan, C. P. Lin, A. M. Azarova, Y. C. Tsai, Y. Ban and L. F. Liu (2007). "Topoisomerase IIβ mediated DNA double-strand breaks: implications in doxorubicin cardiotoxicity and prevention by dexrazoxane." *Cancer Res.* **67**(18): 8839-8846.

Lyu, Y. L. and J. C. Wang (2003). "Aberrant lamination in the cerebral cortex of mouse embryos lacking DNA topoisomerase IIβ." *Proc. Natl. Acad. Sci. U.S.A.* **100**(12): 7123-7128.

Marians, K. J. (1987). "DNA gyrase-catalyzed decatenation of multiply linked DNA dimers." *J. Biol. Chem.* **262**(21): 10362-10368.

Markovits, J., Y. Pommier, D. Kerrigan, J. M. Covey, E. J. Tilchen and K. W. Kohn (1987). "Topoisomerase II-mediated DNA breaks and cytotoxicity in relation to cell proliferation and the cell cycle in NIH 3T3 fibroblasts and L1210 leukemia cells." *Cancer Res* **47**(8): 2050-2055.

Martínez-Garcia, P. M., M. García-Torres, F. Divina, J. Terrón-Bautista, I. Delgado-Sainz, F. Gómez-Vela and F. Cortes-Ledesma (2021). "Genome-wide prediction of topoisomerase IIβ binding by architectural factors and chromatin accessibility." *PLoS Comput. Biol.* **17**(1).

McClendon, A. K., J. S. Dickey and N. Osheroff (2006). "Ability of viral topoisomerase II to discern the handedness of supercoiled DNA: Bimodal recognition of DNA geometry by type II enzymes." *Biochemistry*(45): 11674-11680.

McClendon, A. K., A. C. Gentry, J. S. Dickey, M. Brinch, S. Bendsen, A. H. Andersen and N. Osheroff (2008). "Bimodal recognition of DNA geometry by human topoisomerase IIα: preferential relaxation of positively supercoiled DNA requires elements in the C-terminal domain." *Biochemistry*(47): 13169-13178.

McClendon, A. K. and N. Osheroff (2006). "The geometry of DNA supercoils modulates topoisomerase-mediated DNA cleavage and enzyme response to anticancer drugs." *Biochemistry*(45): 3040-3050.

McClendon, A. K. and N. Osheroff (2007). "DNA topoisomerase II, genotoxicity, and cancer." *Mutat. Res.* **623**(1-2): 83-97.

McClendon, A. K., A. C. Rodriguez and N. Osheroff (2005). "Human topoisomerase IIα rapidly relaxes positively supercoiled DNA: Implications for enzyme action ahead of replication forks." *J. Biol. Chem.* **280**(47): 39337-39345.

McKie, S. J., A. Maxwell and K. C. Neuman (2020). "Mapping DNA Topoisomerase Binding and Cleavage Genome Wide Using Next-Generation Sequencing Techniques." *Genes (Basel)* **11**(1).

McKie, S. J., K. C. Neuman and A. Maxwell (2021). "DNA topoisomerases: advances in understanding of cellular roles and multi-protein complexes via structure-function analysis." *Bioessays* **43**(4): 2000286.

Menna, P., E. Salvatorelli and G. Minotti (2008). "Cardiotoxicity of antitumor drugs." *Chem. Res. Toxicol.* **21**(5): 978-989.

Miao, Z. H., A. Player, U. Shankavaram, Y. H. Wang, D. B. Zimonjic, P. L. Lorenzi, Z. Y. Liao, H. Liu, T. Shimura, H. L. Zhang, L. H. Meng, Y. W. Zhang, E. S. Kawasaki, N. C. Popescu, M. I. Aladjem, D. J. Goldstein, J. N. Weinstein and Y. Pommier (2007). "Nonclassic functions of human topoisomerase I: genome-wide and pharmacologic analyses." *Cancer Res.* **67**(18): 8752-8761.

Mirkin, S. M., E. N. Zaitsev, I. G. Panyutin and V. I. Lyamichev (1984). "Native supercoiling of DNA: The effects of DNA gyrase and ω protein in *E. coli*." *Molecular and General Genetics MGG* **196**(3): 508-512.

Mirski, S. E., J. H. Gerlach and S. P. Cole (1999). "Sequence determinants of nuclear localization in the alpha and beta isoforms of human topoisomerase II." *Exp. Cell Res.* **251**(2): 329-339.

Mirski, S. E., J. H. Gerlach, H. J. Cummings, R. Zirngibl, P. A. Greer and S. P. Cole (1997). "Bipartite nuclear localization signals in the C terminus of human topoisomerase IIα." *Exp. Cell Res.* **237**(2): 452-455.

Morham, S. G., K. D. Kluckman, N. Voulomanos and O. Smithies (1996). "Targeted disruption of the mouse topoisomerase I gene by camptothecin selection." *Mol. Cell Biol.* **16**(12): 6804-6809.

Murai, J. (2017). "Targeting DNA repair and replication stress in the treatment of ovarian cancer." *Int. J. Clin. Oncol.* **22**(4): 619-628.

Nitiss, J. L. (1998). "Investigating the biological functions of DNA topoisomerases in eukaryotic cells." *Biochim. Biophys. Acta* **1400**(1-3): 63-81.

Nitiss, J. L. (2009). "DNA topoisomerase II and its growing repertoire of biological functions." *Nat. Rev. Cancer* **9**(5): 327-337.

Nitiss, J. L. (2009). "Targeting DNA topoisomerase II in cancer chemotherapy." *Nat. Rev. Cancer* **9**(5): 338-350.

Noble, C. G. and A. Maxwell (2002). "The role of GyrB in the DNA cleavage-religation reaction of DNA gyrase: a proposed two metal-ion mechanism." *J. Mol. Biol.* **318**(2): 361-371.

Nöllmann, M., N. J. Crisona and P. B. Arimondo (2007). "Thirty years of *Escherichia coli* DNA gyrase: From in vivo function to single-molecule mechanism." *Biochimie* **89**(4): 490-499.

O'Riordan, W., C. Tiffany, N. Scangarella-Oman, C. Perry, M. Hossain, T. Ashton and E. Dumont (2017). "Efficacy, safety, and tolerability of gepotidacin (GSK2140944) in the treatment of patients with suspected or confirmed Gram-positive acute bacterial skin and skin structure infections." *Antimicrob. Agents Chemother.* **61**(6): e02095-02016.

Osheroff, N. (1986). "Eukaryotic topoisomerase II. Characterization of enzyme turnover." *J. Biol. Chem.* **261**(21): 9944-9950.

Osheroff, N. (1987). "Role of the divalent cation in topoisomerase II mediated reactions." *Biochemistry* **26**(20): 6402-6406.

Osheroff, N. (1989). "Effect of antineoplastic agents on the DNA cleavage/religation reaction of eukaryotic topoisomerase II: inhibition of DNA religation by etoposide." *Biochemistry* **28**(15): 6157-6160.

Pendleton, M., R. H. Lindsey, Jr., C. A. Felix, D. Grimwade and N. Osheroff (2014). "Topoisomerase II and leukemia." *Ann. N.Y. Acad. Sci.* **1310**(1): 98-110.

Peng, H. and K. J. Marians (1993). "Escherichia coli topoisomerase IV. Purification, characterization, subunit structure, and subunit interactions." *J Biol Chem* **268**(32): 24481-24490.

Peter, B. J., C. Ullsperger, H. Hiasa, K. J. Marians and N. R. Cozzarelli (1998). "The structure of supercoiled intermediates in DNA replication." *Cell* **94**(6): 819-827.

Pommier, Y., E. Leo, H. Zhang and C. Marchand (2010). "DNA topoisomerases and their poisoning by anticancer and antibacterial drugs." *Chem. Biol.* **17**(5): 421-433.

Pommier, Y. and C. Marchand (2012). "Interfacial inhibitors: Targeting macromolecular complexes." *Nat. Rev. Drug. Discov.* **11**(1): 25-36.

Pommier, Y., Y. Sun, S.-y. N. Huang and J. L. Nitiss (2016). "Roles of eukaryotic topoisomerases in transcription, replication and genomic stability." *Nat. Rev. Mol. Cell Biol.* **17**(11): 703-721.

Pommier, Y., Y. Sun, S. N. Huang and J. L. Nitiss (2016). "Roles of eukaryotic topoisomerases in transcription, replication and genomic stability." *Nat. Rev. Mol. Cell Biol.* **17**(11): 703-721.

Postow, L., N. J. Crisona, Peter, C. D. Hardy and N. R. Cozzarelli (2001). "Topological challenges to DNA replication: Conformations at the fork." *Proc. Natl. Acad. Sci. U.S.A.* **98**(15): 8219-8226.

Puigvert, J. C., K. Sanjiv and T. Helleday (2016). "Targeting DNA repair, DNA metabolism and replication stress as anti-cancer strategies." *FEBS J.* **283**(2): 232-245.

Rashidi, A. and S. I. Fisher (2013). "Therapy-related acute promyelocytic leukemia: a systematic review." *Med. Oncol.* **30**(3): 625.

Roca, J. and J. C. Wang (1992). "The capture of a DNA double helix by an ATP-dependent protein clamp: A key step in DNA transport by type II DNA topoisomerases." *Cell* **71**(5): 833-840.

Sandhaus, S., P. P. Chapagain and Y. C. Tse-Dinh (2018). "Discovery of novel bacterial topoisomerase I inhibitors by use of *in silico* docking and *in vitro* assays." *Sci. Rep.* **8**(1437).

Schmidt, B. H., A. B. Burgin, J. E. Deweese, N. Osheroff and J. M. Berger (2010). "A novel and unified two-metal mechanism for DNA cleavage by type II and IA topoisomerases." *Nature* **465**(7298): 641-644.

Schmidt, B. H., N. Osheroff and J. M. Berger (2012). "Structure of a topoisomerase II-DNA-nucleotide complex reveals a new control mechanism for ATPase activity." *Nat. Struct. Mol. Biol.* **19**(11): 1147-1154.

Schvartzman, J. B. and A. Stasiak (2004). "A topological view of the replicon." *EMBO Rep.* **5**(3): 256-261.

Sen, N., J. Leonard, R. Torres, J. Garcia-Luis, G. Palou-Marin and L. Aragon (2016). "Physical Proximity of Sister Chromatids Promotes Top2-Dependent Intertwining." *Mol Cell* **64**(1): 134-147.

Seol, Y., A. C. Gentry, N. Osheroff and K. C. Neuman (2013). "Chiral discrimination and writhe-dependent relaxation mechanism of human topoisomerase IIα." *J. Biol. Chem.* **288**(19): 13695-13703.

Seol, Y. and K. C. Neuman (2016). "The dynamic interplay between DNA topoisomerases and DNA topology." *Biophys. Rev.* **8**(Suppl 1): 101-111.

Sissi, C. and M. Palumbo (2009). "Effects of magnesium and related divalent metal ions in topoisomerase structure and function." *Nucleic Acids Res.* **37**(3): 702-711.

Sissi, C. and M. Palumbo (2010). "In front of and behind the replication fork: bacterial type IIA topoisomerases." *Cell. Mol. Life. Sci.* **67**(12): 2001-2024.

Slesarev, A. I., K. O. Stetter, J. A. Lake, M. Gellert, R. Krah and S. A. Kozyavkin (1993). "DNA topoisomerase V is a relative of eukaryotic topoisomerase I from a hyperthermophilic prokaryote." *Nature* **364**: 735-737.

Stein, G. E. (1988). "The 4-quinolone antibiotics: Past, present, and future ." *Pharmacotherapy* **8**(6): 301-314.

Stivers, J. T., T. K. Harris and A. S. Mildvan (1997). "Vaccinia DNA topoisomerase I: evidence supporting a free rotation mechanism for DNA supercoil relaxation." *Biochemistry* **36**: 5212-5222.

Stoll, G., O. P. Pietilainen, B. Linder, J. Suvisaari, C. Brosi, W. Hennah, V. Leppa, M. Torniainen, S. Ripatti, S. Ala-Mello, O. Plottner, K. Rehnstrom, A. Tuulio-Henriksson, T. Varilo, J. Tallila, K. Kristiansson, M. Isohanni, J. Kaprio, J. G. Eriksson, O. T. Raitakari, T. Lehtimaki, M. R. Jarvelin, V. Salomaa, M. Hurles, H. Stefansson, L. Peltonen, P. F. Sullivan, T. Paunio, J. Lonnqvist, M. J. Daly, U. Fischer, N. B. Freimer and A. Palotie (2013). "Deletion of TOP3β, a component of FMRP-containing mRNPs, contributes to neurodevelopmental disorders." *Nat. Neurosci.* **16**(9): 1228-1237.

Stone, M. D., Z. Bryant, N. J. Crisona, S. B. Smith, A. Vologodskii, C. Bustamante and N. R. Cozzarelli (2003). "Chirality sensing by *Escherichia coli* topoisomerase IV and the mechanism of type II topoisomerases." *Proc. Natl. Acad. Sci. U.S.A.* **100**(15): 8654-8659.

Sugimoto-Shirasu, K., N. J. Stacey, J. Corsar, K. Roberts and M. C. McCann (2002). "DNA topoisomerase VI is essential for endoreduplication in *Arabidopsis*." *Curr. Biol.* **12**(20): 1782-1786.

Sutormin, D., N. Rubanova, M. Logacheva, D. Ghilarov and K. Severinov (2019). "Single-nucleotide-resolution mapping of DNA gyrase cleavage sites across the *Escherichia coli* genome." *Nucleic Acids Res.* **47**(3): 1373-1388.

Tadesse, S. and P. L. Graumann (2006). "Differential and dynamic localization of topoisomerases in *Bacillus subtilis*." *J. Bacteriol.* **188**: 3002-3011.

Tan, K., Q. Zhou, B. Cheng, Z. Zhang, A. Joachimiak and Y. C. Tse-Dinh (2015). "Structural basis for suppression of hypernegative DNA supercoiling by *E. coli* topoisomerase I." *Nucleic Acids Res.* **43**(22): 11031-11046.

Taneja, B., A. Patel, A. I. Slesarev and A. Mondragón (2006). "Structure of the N-terminal fragment of topoisomerase V reveals a new family of topoisomerases." *The EMBO Journal* **25**: 398-408.

Terekhova, K., K. H. Gunn, J. F. Marko and A. Mondragón (2012). "Bacterial topoisomerase I and topoisomerase III relax supercoiled DNA via distinct pathways." *Nucleic Acids Res.* **40**(20): 10432-10440.

Travers, A. and G. Muskhelishvili (2007). "A common topology for bacterial and eukaryotic transcription initiation?" *EMBO Rep.* **8**(2): 147-151.

Tretter, E. M., J. C. Lerman and J. M. Berger (2010). "A naturally chimeric type IIA topoisomerase in Aquifex aeolicus highlights an evolutionary path for the emergence of functional paralogs." *Proc Natl Acad Sci U S A* **107**(51): 22055-22059.

Tse-Dinh, Y. C. (1998). "Bacterial and archeal type I topoisomerases." *Biochim. Biophys. Acta* **1400**(1-3): 19-27.

Uemura, T., H. Ohkura, Y. Adachi, K. Morino, K. Shiozaki and M. Yanagida (1987). "DNA topoisomerase II is required for condensation and separation of mitotic chromosomes in *S. pombe*." *Cell* **50**(6): 917-925.

Ullsperger, C. and N. R. Cozzarelli (1996). "Contrasting enzymatic acitivites of topoisomerase IV and DNA gyrase from *Escherichia coli*." *J. Biol. Chem.* **271**: 31549-31555.

Uuskula-Reimand, L., H. Hou, P. Samavarchi-Tehrani, M. V. Rudan, M. Liang, A. Medina-Rivera, H. Mohammed, D. Schmidt, E. J. Young, J. Reimand, S. Hadjur, A. C. Gingras and M. D. Wilson (2016). "Topoisomerase II beta interacts with cohesin and CTCF at topological domain borders." *Genome Biol.* **17**(1): 182.

Vann, K. R., A. A. Oviatt and N. Osheroff (2021). "Topoisomerase II poisons: converting essential enzymes into molecular scissors." *Biochemistry* **60**(21): 1630-1641.

Velez-Cruz, R. and N. Osheroff (2004). DNA topoisomerases: type II. *Encyclopedia of Biological Chemistry*, Elsevier Inc.**:** 806-811.

Voet, D. and J. G. Voet (2004). *Biochemistry*. New York, Wiley and Sons.

Voet, D., J. G. Voet and C. W. Pratt (2002). *Fundamentals of biochemistry*, Wiley New York.

Vos, S. M., I. Lee and J. M. Berger (2013). "Distinct regions of the *Escherichia coli* ParC C-terminal domain are required for substrate discrimination by topoisomerase IV." *J. Mol. Biol.* **425**(17): 3029-3045.

Vos, S. M., E. M. Tretter, B. H. Schmidt and J. M. Berger (2011). "All tangled up: How cells direct, manage and exploit topoisomerase function." *Nat. Rev. Mol. Cell. Biol.* **12**(12): 827-841.

Wang, J. C. (1971). "Interaction between DNA and an Escherichia coli protein ω." *J. Mol. Biol.* **55**(3): 523-533.

Wang, J. C. (1996). "DNA topoisomerases." *Annu. Rev. Biochem.* **65**: 635-692.

Wang, J. C. (1998). "Moving one DNA double helix through another by a type II DNA topoisomerase: the story of a simple molecular machine." *Q. Rev. Biophys.* **31**(2): 107-144.

Wang, J. C. (2002). "Cellular roles of DNA topoisomerases: A molecular perspective." *Nat. Rev. Mol. Cell. Biol.* **3**(6): 430-440.

Wang, X., R. Reyes-Lamothe and D. J. Sherratt (2008). "Modulation of *Escherichia coli* sister chromosome cohesion by topoisomerase IV." *Genes Dev.* **22**(17): 2426-2433.

Watson, J. D. and F. H. Crick (1953). "Molecular structure of nucleic acids; A structure for deoxyribose nucleic acid." *Nature* **171**(4356): 737-738.

Watson, J. D. and F. H. Crick (1953A). "Genetical implications of the structure of deoxyribonucleic acid." *Nature* **171**(4361): 964-967.

Wendorff, T. J., B. H. Schmidt, P. Heslop, C. A. Austin and J. M. Berger (2012). "The structure of DNA-bound human topoisomerase IIα: Conformational mechanisms for coordinating inter-subunit interactions with DNA cleavage." *J. Mol. Biol.* **424**(3-4): 109-124.

White, J. H. and W. R. Bauer (1986). "Calculation of the twist and the writhe for representative models of DNA." *J. Mol. Biol.* **189**(2): 329-341.

White, J. H. and N. R. Cozzarelli (1984). "A simple topological method for describing stereoisomers of DNA catenanes and knots." *Proc. Natl. Acad. Sci. U.S.A.* **81**(11): 3322-3326.

Willmore, E., A. J. Frank, K. Padget, M. J. Tilby and C. A. Austin (1998). "Etoposide targets topoisomerase IIα and IIβ in leukemic cells: isoform-specific cleavable complexes visualized and quantified *in situ* by a novel immunofluorescence technique." *Mol. Pharmacol.* **54**(1): 78-85.

Wilstermann, A. M. and N. Osheroff (2001). "Positioning the 3'-DNA terminus for topoisomerase II-mediated religation." *J. Biol. Chem.* **276**(21): 17727-17731.

Woessner, R. D., M. R. Mattern, C. K. Mirabelli, R. K. Johnson and F. H. Drake (1991). "Proliferation- and cell cycle-dependent differences in expression of the 170 kilodalton and 180 kilodalton forms of topoisomerase II in NIH-3T3 cells." *Cell Growth Differ.* **2**(4): 209-214.

Worcel, A. and E. Burgi (1972). "On the structure of the folded chromosome of *Escherichia coli*." *J. Mol. Biol.* **72**(2): 127-147.

Worland, S. T. and J. C. Wang (1989). "Inducible overexpression, purification, and active site mapping of DNA topoisomerase II from the yeast *Saccharomyces cerevisiae*." *J. Biol. Chem.* **264**(8): 4412-4416.

Wu, C. C., T. K. Li, L. Farh, L. Y. Lin, T. S. Lin, Y. J. Yu, T. J. Yen, C. W. Chiang and N. L. Chan (2011). "Structural basis of type II topoisomerase inhibition by the anticancer drug etoposide." *Science* **333**(6041): 459-462.

Wyckoff, E. and T. S. Hsieh (1988). "Functional expression of a Drosophila gene in yeast: genetic complementation of DNA topoisomerase II." *Proc. Natl. Acad. Sci. U.S.A.* **85**(17): 6272-6276.

Xu, D., W. Shen, R. Guo, Y. Xue, W. Peng, J. Sima, J. Yang, A. Sharov, S. Srikantan, J. Yang, D. I. Fox, Y. Qian, J. L. Martindale, Y. Piao, J. Machamer, S. R. Joshi, S. Mohanty, A. C. Shaw, T. E. Lloyd, G. W. Brown, M. S. Ko, M. Gorospe, S. Zou and W. Wang (2013). "Top3β is an RNA topoisomerase that works with fragile X syndrome protein to promote synapse formation." *Nat. Neurosci.* **16**(9): 1238-1247.

Yang, X., W. Li, E. D. Prescott, S. J. Burden and J. C. Wang (2000). "DNA topoisomerase IIβ and neural development." *Science* **287**: 131-134.

Yu, X., J. W. Davenport, K. A. Urtishak, M. L. Carillo, S. J. Gosai, C. P. Kolaris, J. A. W. Byl, E. F. Rappaport, N. Osheroff, B. D. Gregory and C. A. Felix (2017). "Genome-wide TOP2A DNA cleavage is biased toward translocated and highly transcribed loci." *Genome Res.* **27**(7): 1238-1249.

Zawadzki, P., M. Stracy, K. Ginda, K. Zawadzka, C. Lesterlin, A. N. Kapanidis and D. J. Sherratt (2015). "The localization and action of topoisomerase IV in *Escherichia coli* chromosome segregation Is coordinated by the SMC complex, MukBEF." *Cell Rep.* **13**(11): 2587-2596.

Zawadzki, P., M. Stracy, K. Ginda, K. Zawadzka, C. Lesterlin, A. N. Kapanidis and D. J. Sherratt (2015). "The localization and action of topoisomerase IV in *Escherichia coli* chromosome segregation Is coordinated by the SMC complex, MukBEF." *Cell Rep.* **13**: 2587-2596.

Zechiedrich, E. L., K. Christiansen, A. H. Andersen, O. Westergaard and N. Osheroff (1989). "Double-stranded DNA cleavage/religation reaction of eukaryotic topoisomerase II: Evidence for a nicked DNA intermediate." *Biochemistry* **28**(15): 6229-6236.

Zechiedrich, E. L., A. B. Khodursky, S. Bachellier, R. Schneider, D. Chen, D. M. Lilley and N. R. Cozzarelli (2000). "Roles of topoisomerases in maintaining steady-state DNA supercoiling in *Escherichia coli*." *J. Biol. Chem.* **275**(11): 8103-8113.

Zhang, Y. L., C. Yu, S. Y. Ji, X. M. Li, Y. P. Zhang, D. Zhang, D. Zhou and H. Y. Fan (2013). "TOP2beta is essential for ovarian follicles that are hypersensitive to chemotherapeutic drugs." *Mol. Endocrinol.* **27**(10): 1678-1691.